# Exploiting the Mitochondrial Fox 03A/SIRT3 Complex in Cancer Therapy

## Thesis

# Exploiting the mitochondrial FoxO3A/SIRT3 complex in cancer therapy

**Valentina Celestini**

Degree of Doctor of Philosophy

The Open University, UK

Discipline of Life Sciences

Affiliated Research Center

Istituto di Ricerche Farmacologiche Mario Negri IRCCS

Milan, Italy

September 2018

# Abstract

As other many transcription factors, FoxO family members are involved in several cellular processes, including proliferation, apoptosis, stress resistance and metabolism. Their activity is finely regulated by phosphorylation, acetylation and ubiquitination events, which are modulated by multiple signalling pathways. Through the combination of specific post-translational modifications, composing a unique "molecular FoxO code", FoxO proteins modulate different physiological processes and pathological events, such as cancer.

Previously, a mitochondrial arm of the AMPK-FoxO3A axis, representing a mechanism sustaining the energy metabolism upon nutrient shortage, has been revealed in normal cells and tissues. Data collected during this project show that in metabolically stressed cancer cells, FoxO3A is recruited to the mitochondria through activation of MEK/ERK and AMPK pathways. These kinases phosphorylate Serine 12 and 30, respectively, on the FoxO3A N-terminal domain, which is required for FoxO3A recruitment to the mitochondrial surface. Upon translocation into the organelle, the N-terminal domain is cleaved by processing peptidases, and the released product reaches the mitochondrial matrix. Here, the cleaved form of FoxO3A binds to the mitochondrial DNA (mtDNA) and activates the transcription of the mitochondrial genes, to support mitochondrial metabolism and cell survival. Interestingly, it seems to be a cancer-specific mechanism. Moreover, in cancer cells treated with chemotherapeutic agents, accumulation of FoxO3A into the mitochondria promotes their survival in a MEK/ERK-dependent

manner. Importantly, mitochondrial FoxO3A is required for apoptosis induction by Metformin. Elucidation of FoxO3A mitochondrial versus nuclear functions in cancer cell homeostasis might help devise novel therapeutic strategies to disable FoxO3A pro-survival activity selectively.

To my uncle Emidio

"Nature composes some of her loveliest poems for the microscope and the telescope".

Theodore Roszak

# Acknowledgements

This thesis would not have been possible without the help and the presence of several persons who in one way or another contributed to the development of this project. It is a pleasure to convey my gratitude to all of them.

First, my gratitude to my Director of Studies Dr. Mineko Terao and to Dr. Enrico Garattini for giving me the possibility to carry out this PhD, for their valuable assistance in the preparation and completion of this study. I want to thank all the members of the Molecular Biology Lab, for welcoming me and for the constructive comments on these data.

Then, importantly, my gratitude to Prof. Cristiano Simone, for his invaluable guidance and continous encouragement. I am extremely grateful for his support on both an academic and a personal level. Additionally, I gratefully thank Cristiano to introduce me to my scientific family: Alessia, Valentina, Giovanna, Luciana, Martina and Candida. Each of them changed my life, and each of them knows how. Then Paola and Tugsan. Paola you are my labmate and my person. Tuggy, you taught me more than you know. Our time together it has been very precious for me.

Then, I am very thankful to Dr. Concetta Bubici, for the helpful discussion and suggestions through these years, acting as supervisor of my PhD.

Finally, I would especially like to thank my husband Sante who has been an understanding, patient and loving partner throughout this adventure. Lastly, but certainly not least, I would like to thank my family and all the special persons that gave me constant love and support both before and during my Ph.D.

## PREFACE

The work described in this thesis was performed at the Istituto di Ricerche Farmacologiche Mario Negri IRCCS, in Milan and in the University of Bari Aldo Moro, in Bari, Italy, from 2015 to 2018.

The work was performed under the supervision of the Dr. Mineko Terao (director of studies), Dr. Cristiano Simone and Dr. Concetta Bubici (external supervisors).

## DECLARATION

This thesis has not been submitted in whole or in part for a degree or diploma or other qualifications to any other university. Part of the data described in the thesis has been published as my original work on Cell Death & Disease, in 2018 (see "Published Material" section).

I performed by myself the experimental work described herein. Collaborations to perform specific parts of the project – *in vivo* experiments and radioactive kinase assay- are indicated in the "Material and Methods" chapter.

# Table of content

# List of figures

# List of tables

# List of abbreviations

| | |
|---|---|
| 2DG | 2-Deoxy-d-Glucose |
| 5-FU | 5-FluroUracile |
| aa | amino acid |
| ABCB1 | ATP Binding Cassette Subfamily B Member 1 |
| ACC2 | Acetyl-Coa Carboxylase 2 |
| AFX | Forkhead transcription factor |
| AICAR | 5-AminIimidazole-4-Carboxamide-1-b-d-Ribofuranoside |
| AIF | Apoptosis-Inducing Factor |
| AKT | AKT Serine/Threonine kinase 1 |
| AMP | Adenosine MonoPhosphate |
| AMPK | Adenosine MonoPhosphate e Kinase |
| ATG | AuTophagy related Gene |
| ATP | Adenosine Triphosphate |
| BCL2 | B-Cell Lymphoma 2 |
| Bcl6 | B-Cell Lymphoma 6 |
| BCR-ABL | Breakpoint Cluster Region-Abelson |
| Bim | Bcl-2-like protein 11 |
| BNIP | BCL2 Interacting Protein |
| BNIPL | BCL2 Interacting Protein Like |
| CAMKKβ | $Ca^{2+}$/calmodulin-dependent protein kinase β |
| CC | Compound C |
| CDDP | Cisplatin |
| CDK | Cyclin Dependent Kinase |
| cDNA | complementary DNA |
| ChIP | Chromatin immunoprecipitation |
| Cisplatin | Cis-diamminePlatinum dichloride |
| CK1 | Casein kinase-1 |
| cl. FoxO3A | cleaved FoxO3A |

| | |
|---|---|
| CLB | Cell Lysis Buffer |
| CML | Chronic Myeloid Leukemia |
| Co-IP | Co-ImmunoPrecipitation |
| COX | Cytochrome C Oxidase Subunit |
| CR | Calorie Restriction |
| CRC | Colorectal cancer |
| CRISPR | Clustered Regularly Interspaced Short Palindromic Repeats |
| C-term. | C-terminal domain |
| CTP-11 | Irinotecan |
| CYTB | Cytochrome B |
| CYTC | Cytochrome C |
| DAPI | 4',6-DiAmidino-2-PhenylIndole |
| DBD | DNA Binding Domain |
| DISPHOS | Disorder-EnhAnced Phosphorylation Sites Predictor |
| DMEM | Dulbecco's Modified Eagle Medium |
| DMSO | DiMethyl SulfOxide |
| DNA | DeoxyriboNucleic Acid |
| DR | Dietary Restriction |
| DYRK1A | Dual-specificity Tyrosine (Y)-phosphorylation-regulated kinase |
| EDTA | Ethylene diamine tetraacetic acid |
| EGF | Endothelial Growth Factor |
| EGFP | Enhanced Green Fluorescent Protein |
| EGFR | Endothelial Growth Factor Receptor |
| EGTA | Ethylene Glycol-bis(2-aminoethylether)-N,N,N′ |
| ER | Oestrogen receptor |
| ERK | Extracellular-signal-regulated kinases |
| ERRα | Oestrogen-related receptor alpha |
| ETC | Electron Transport Chain |
| FASL | Fas Ligand |
| FBS | Fetal Bovine Serum |
| FD | Forkhead Domain |

| | |
|---|---|
| FH | Fumarate Hydratase |
| FHRE | Forkhead Response Element |
| FKHR | Forkhead transcription factor FoxO1 |
| FKHRL1 | Forkhead transcription factor FoxO3A |
| fl. FoxO3A | full-length FoxO3A |
| Fox | Forkhead box |
| FoxM | Forkhead boxclass M |
| FoxO | Forkhead box class O |
| GABARAP | GABA type A receptor-associated protein |
| GABARAPL | GABA type A receptor associated protein like |
| GADD45α | growth-arrest and DNA-damage inducible protein |
| GLS | Glutaminase |
| GBM | Glioblastoma |
| GR | Glucose restriction |
| GR | Glucose Restriction |
| gRNA | guide RiboNucleic Acid |
| GST | Glutathione-S-Transferase |
| HCC | Hepatocellular Carcinoma |
| HER | Human epidermal growth factor receptor |
| HG | High Glucose |
| HIF | Hypoxia Inducible Factor |
| HSP60 | Heat Shock Protein 60 |
| IBc | Isolation Buffer |
| IDH | Isocitrate DeHydrogenase |
| IGF | Insulin/Insulin-like growth factor |
| IgG | Immunoglobulin G |
| IKKβ | Inhibitor of nuclear factor Kappa-B Kinase |
| IMS | InterMembrane Space |
| IPTG | Isopropyl β-D-1-thiogalactopyranoside |
| JNK | c-Jun N-terminal Kinase |
| K | Lysine |
| KO | Knock-Out |

| | |
|---|---|
| LDH | Lactate Dehydrogenase |
| LG | Low Glucose |
| MAP1LC3B | Microtubule-Associated Protein 1 Light Chain 3 Beta |
| MAPK | Mitogen activated protein kinase |
| MAP3K | mitogen-activated protein kinase |
| MCL1 | BCL2 Family Apoptosis Regulator |
| MDM2 | Murine Double Minute 2 |
| MEK | Mitogen-activated protein kinase |
| MET | Metformin |
| MFF | Mitochondrial Fission Factor |
| MIM | Mitochondrial Inner Membrane |
| MIP | Mitochondrial Intermediate Peptidase |
| MMP | Matrix MetalloProteinase |
| MOM | Mitochondrial Outer Membrane |
| MOMP | Mitochondrial Outer Membrane Permeabilization |
| MOPS | 3-(N-morpholino)propanesulfonic acid |
| MPP | Mitochondrial Processing Peptidase |
| MPT | Mitochondrial Permeability Transition |
| mRNA | messenger RiboNucleic Acid |
| MSA | Multiple Sequence Alignment |
| MST-1 | Macrophage Stimulating 1 |
| mtDNA | Mitochondrial DNA |
| mtFoxO3A | mitochondrial FoxO3A |
| mTOR | mechanistic Target Of Rapamycin kinase |
| mtRNAPol | mitochondrial RNA Polymerase |
| MTS | Mitochondrial Import Signal |
| NADH | Nicotinamide Adenine Dinucleotide |
| NAM | Nicotinamide |
| ND | Mitochondrially Encoded NADH:Ubiquinone Oxidoreductase Core Subunit |
| NEAA | Non Essential Amino Acid |
| NES | Nuclear Export Signal |

| | |
|---|---|
| NLS | Nuclear Localisation Signal |
| NRF | Nuclear respiratory factors |
| N-term. | N-terminal domain |
| nDNA | Nuclear DNA |
| OSCC | Oral Squamous Cell Carcinoma |
| OXPHOS | OXidative PHOSphorylation |
| p21 | cyclin-dependent kinase inhibitor 1 |
| p27 | cyclin-dependent kinase inhibitor 1B |
| p38α | Mitogen- activated protein kinase |
| pACC | phospho-Acetyl-CoA Carboxylase |
| PAM | Proto-Spacer Adjacent Motif |
| pAMPK | phospho-AMPK |
| PARP | Poly ADP ribose polymerase |
| PBS | Phosphate Buffered Saline |
| PCR | Polymerase chain reaction |
| PDH | Pyruvate Dehydrogenase |
| PDK1 | Pyruvate Dehydrogenase Kinase 1 |
| PEPCK | Phosphoenolpyruvate carboxykinase |
| pERK | phospho-ERK |
| PGC-1α | Peroxisome Proliferator-Activated Receptor-Γ Coactivator-1α |
| PI3K | Phosphatidyl-Inositol 3-Kinase |
| PIP2 | PhosphatidylInositol-4,5-biPhosphate |
| PIP3 | PhosphatidylInositol-3,4,5-triPhosphate |
| PK | Proteinase K |
| PKB | Protein Kinase B |
| PMSF | Phenylmethylsulfonyl fluoride |
| PTM | Post-translational modification |
| POLG1 | DNA polymerase γ |
| PPAR | Peroxisome proliferator-activated receptor |
| PR | Progesteron receptor |
| PTEN | Phosphatase And Tensin Homolog |

| | |
|---|---|
| PUMA | p53 upregulated modulator of apoptosis |
| RAS | Rat Sarcoma |
| RNA | RiboNucleic Acid |
| ROS | Reactive Oxygen Species |
| rRNA | ribosomial RiboNucleic Acid |
| RT-PCR | Real-Time PCR |
| SDH | Succinate DeHydrogenase |
| SDS-PAGE | Sodium dodecyl sulphate-polyacrylamide gel electrophoresis |
| SEM | Standard Error of Mean |
| SET9 | SET domain-containing protein 7/9 |
| SGK | Serum and Glucocorticoidregulated Kinase |
| siRNA | short interfering RNA |
| SIRT | Sirtuin |
| SKP2 | S-phase kinase-associated protein 2 |
| SNP | Single Nucleotide Polymorphisms |
| SOD2 | manganese-containing SuperOxide Dismutase |
| SREBP-1 | Sterol Regulatory Element-Binding Protein-1 |
| STAT5 | Signal transducer and activator of transcription 5 |
| STK11 | Serine/Threonine Kinase 11 |
| TAD | TransActivation Domain |
| TAK1/MAP3K7 | Transforming growth factor-β-Activated Kinase 1 |
| TCA | TriCarboxylic Acid |
| TEM | Transmission electron microscope |
| TFAM | Mitochondrial Transcription Factor A |
| TFBM1 | Mitochondrial Transcription Factor B1 |
| TFBM2 | Mitochondrial Transcription Factor B2 |
| TMRE | Tetramethylrhodamine Ethyl Ester Perchlorate |
| TOR | Protein kinase/target of rapamycin |
| TRADD | Tumour Necrosis Factor Receptor-Associated Death Domain |
| TRAIL | Tumour Necrosis Factor-Related Apoptosis Inducing Ligand |
| tRNA | transfer RiboNucleic Acid |
| UCP2 | Mitochondrial uncoupling protein |

| | |
|---|---|
| VP-16 | Etoposide |
| WT | Wild Type |
| ZMP | AICAR monophosphate |

# Chapter 1 - Introduction

# 1.1 Introduction

# 1.2 Cancer

Cancer is the second largest cause of mortality in the western world, after cardiovascular disease. In Europe, in 2017, 3.5 million people were diagnosed. Every year the number of diagnosed cancer cases is increasing, regardless of sex, type or country. Colorectal cancer (13,0%) and breast cancer (13,5%) are the most prevalent ones in the world today.

Cancer is a heterogeneous disease resulting from a multistep process, by which several genetic and epigenetic alterations lead normal cells to evolve progressively to a neoplastic state. The abnormal cell growth, resulting in the neoplasia, is the biological endpoint of the process. The fundamental alternations that cancers have to undergo to transform from normal to cancer cells are outlined as "hallmarks of cancer" (Hanahan and Weinberg, 2000; Hanahan and Weinberg, 2011). All the procedures of transformation of normal cells to cancer cells include the ability to sustain proliferative signalling, evading growth suppressors, resist cell death, enabling replicative immortality, inducing angiogenesis, activating invasion and metastasis, re-programme energy metabolism and avoid immune destruction. Behind these events, there is the characteristic neoplastic genome instability, which induces the genetic variability that allows the hallmarks acquisition. The loss of the "caretakers" genes, involved in detecting and repairing DNA damage (Roth et al., 2000), supports the genomic instability, allowing the pre-malignant cells to reach

the essential hallmarks of cancer (Hanahan and Weinberg, 2000). Finally, yet importantly, tumour-promoted inflammation is essential to sustain multiple hallmark abilities and tumour microenvironment, by producing growth factors to promote proliferative signalling, survival factors to escape from cell death, pro-angiogenic factors and extracellular matrix-modifying enzymes to facilitate angiogenesis, invasion and metastasis. Cells that acquire all the hallmarks generate a malignant neoplasia' or 'malign cancer'. However, cells that do not acquire invasive and metastatic abilities nor immortality feature generate 'benign cancers', which are mostly well differentiated and unable to proliferate as much as malignant tumours (Figure 1.1).

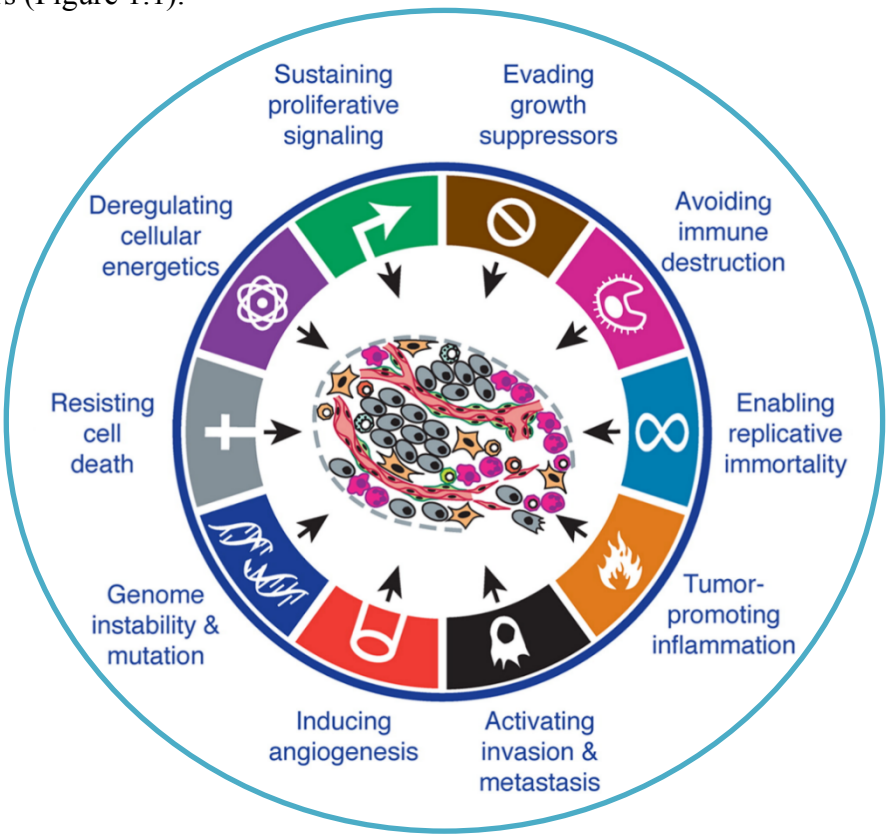


***Figure 1.1 -*** *Hallmarks of cancer.*

*The illustration encompasses the six hallmark capabilities originally proposed in 2000 Hanahan and Weinberg perspective (sustaining proliferative signalling,*

*evading growth suppressors, resisting cell death, enabling replicative immortality, inducing angiogenesis, and activating invasion and metastasis) and the new emerging characteristics and hallmarks described in 2011 (avoiding immune destruction, tumour-promoting inflammation, genome instability and mutation, deregulating cellular energetics). Image modified and adapted from Hanahan and Weinberg, 2011.*

### 1.2.1 Beyond Warburg effect

The energy metabolism reprogramming has been considered for decades as synonymon with the "Warburg effect" (Warburg O, 1956). This phenomenon, also known as "aerobic glycolysis", was described by the German biochemist Otto Heinrich Warburg as the impaired cell metabolism in the origin of cancer, due to mitochondrial respiration defects. Moreover, the theory proposed that the increased glycolytic flux as a compensatory mechanism of energy production required to maintain the viability of cancer cells. In the following decades, both biochemists and oncologists criticized Warburg theory to be too simplistic, not consistent with evidence of apparent normal respiratory function in some tumour cells.

Furthermore, Warburg did not consider the role of tumour-associated mutation. Therefore, the view of cancer as a metabolic disease was gradually replaced with the one of cancer as a genetic disease involving nuclear mutations in oncogenes and tumour suppressor genes (Hanahan and Weinberg, 2011). Nowadays, numerous experimental evidence is still keeping alive the resolve "the chicken and the egg" dilemma, about mitochondrial dysfunction and tumour formation. Specifically, two distinct hypotheses about mitochondrial role in

tumorigenesis keep the question still on the table: on the one hand the mitochondrial dysfunction considered as a primary cause of tumorigenesis, on the other as a "second hit" in the process of cancer metabolic transformation, consequence of accelerated glycolysis. Specifically this event may be caused by loss of tumour suppressors or activation of oncogenes.

The preference of aerobic glycolysis is currently recognised as one of the numerous ways by which malignant cells undergo metabolic reprogramming to survive and proliferate during tumour initiation, progression and metastasis (Koppenol et al., 2011). These pathways, such as mitochondrial metabolism, oxidative phosphorylation or redox balance, are usually pre-existing in normal cells and they are still functional in malignant ones. Among reprogrammed activities, there are mechanisms that allow tumour cells to take up abundant nutrients to produce ATP (Adenosine triphosphate), generate biosynthetic precursors and macromolecules, tolerate malignancy-associated stress (redox stress and hypoxia), allow cancer cells to tolerate nutrient depletion by catabolizing cellular or extra-cellular macromolecules through autophagy, macropinocytosis, or lipid scavenging (Commisso et al., 2013). The induction of these activities is regulated by signalling pathways commonly perturbed in cancer cells. Notably, even though the broad genetic heterogeneity of tumours, malignant cells share the induction of pathways related to anabolism, catabolism, and redox balance (Cantor and Sabatini, 2012). The resulting alterations in metabolite levels, in turn, induce post-translational modifications (PMTs) – such as acetylation, methylation, and thiol oxidation – that influence cellular signalling, epigenetics and gene expression. However, the acceptance of Warburg effect as the main consequence of genomic instability

selected during tumour progression (Kim et al., 2006), renewed the interest in the energy metabolism of cancer cells. Consequently, a new view of cancer cell homeostasis is emerging, related to the balance between newly acquired oncogenic and typical normal cell features (DeBerardinis and Chandel, 2016; Cairns et al., 2011). Importantly, the biological functions of normal cells are strongly required for the acquisition of malignant phenotype, and they are ensured by the proper preservation of key mitochondrial functions (Wallace, 2012; Weinberg and Chandel, 2015; Zong et al., 2016). Consistent with this view, proteins that have been classically considered as tumour suppressors are sometimes required to be functional for full malignant transformation. This is the case for the transcription factor FoxO3A which can be both friend and foe to cancer cells depending on the cellular context (Gomes et al., 2008; Zhang et al., 2011; Chiacchiera and Simone, 2010).

### 1.2.2 Altered energy-supplying pathways in cancer

The uncontrolled oncogene-driven proliferation of cancer cells causes hypoxia in tumours in the absence of an efficient local vascular bed (Eales et al., 2016). Moreover, mitochondria are not able to provide enough ATP for malignant cell survival. Thus tumour cells must up-regulate the glycolytic pathway. As in cancer cells p53 is often mutated, or its expression is impaired, the hypoxic condition is not lethal for them (Moll et al., 1998).

Furthermore, to restore an adequate supply of oxygen and nutrients, tumours need to induce the growth of the vascular network, in the process known as angiogenesis (Nishida et al., 2006). However, even after re-establishment of oxygen

supply, tumour cells prefer to perform glycolysis and to keep mitochondrial activity suppressed. This is a way, for example, for tumours to take advantage to support the invasion, since the improved production of lactate, because of the high rate of glycolysis, generates an acidic environment toxic for non-malignant cell populations (Gillies et al., 2007). Malignant cells can trigger the glycolytic pathway, mainly by inducing the Hypoxia-Inducible Factor-1 (HIF-1), an important regulator of genes involved in the control of angiogenesis, cell survival and invasion. HIF-1 can upregulate the enzymes stimulating glucose utilization. Remarkably, HIF-1 plays a very complex role in hypoxia, as it can induce apoptosis and, at the same time, prevent cell death, or even stimulate cell proliferation (Greijer et al., 2004). Moreover, hypoxia can increase the production of ROS in tumour cells, leading to cell damages, such as to mitochondrial DNA. Consequently, mitochondrial function is impaired and glycolytic pathway sustained (Wallace et al., 2012).

Dysfunction of mitochondria also leads to the activation of the glycolysis. For example, the nicotinamide adenine dinucleotide (NADH)-induced inactivation of the PI3K-phosphatase PTEN, causes the activation of AKT (Pelicano et al., 2006). This kinase can trigger post-transcriptional mechanisms related to the glycolytic pathway, such as the localisation of the glucose transporter to the cell surface or maintenance of hexokinase function in the absence of extrinsic factors (Elstrom et al. 2004). Furthermore, the impairment of mitochondrial respiration in tumour cells can lead to the accumulation of Krebs cycle substrates, such as succinate, lactate or pyruvate. This event allows the stabilization and activation of HIF-1 that, in turn, stimulates the glycolysis (Gottlieb et al., 2005; Lu et al., 2006)

and induces apoptosis through the stabilization of p53 (Greijer et al., 2004). Importantly, in tumour cells, HIF-1 also is a key modulator of the balance between glycolysis and oxidative phosphorylation. The energy utilization switch is directly controlled by the pyruvate dehydrogenase (PDH) and lactate dehydrogenase (LDH), both required for pyruvate utilization. HIF-1 modulates the pyruvate dehydrogenase kinase 1 (PDK1), which controls the activity of PDH and, consequently, the pyruvate oxidation. As a result, the Krebs cycle and mitochondrial respiration are severely impaired. Similarly, the HIF-mediated induction of the LDH expression diminishes the amount of pyruvate available for mitochondrial respiration (Kim et al., 2006; Semenza et al., 2007).

### 1.2.3 Mitochondrial basics

The ATP production for metabolic demands is the main but not the only mitochondrial activity affecting the cellular physiology. Other mitochondrial vital and lethal functions are essential for tumour cell homeostasis, growth and survival, in physiological and pathological conditions. As an example, mitochondria integrate many of the signals for initiating apoptosis. This awareness suggests that understanding the mitochondrial function in cancer might be helpful to design novel targeted approaches for cancer therapy.

Mitochondria can act as a buffer of intracellular calcium and iron homeostasis. Furthermore, they produce respiration reactive oxygen species (ROS) as a by-product of aerobic respiration. ROS are important regulators of various cellular signalling pathways (Yun & Finkel, 2014), but their excess might also damage the cell. Additionally, they are important for thermogenesis and the

synthesis/modulation of various metabolic intermediary pathways, including metabolism of amino acids, lipids, cholesterol and steroids.

Mitochondria are maternally inherited small cytoplasmic organelles, originated from symbiotic bacteria, characterized from a high dynamicity due to constant cycles of division and fusion (Wallace, 2012). The latter is very important to maintain the normal mitochondrial function, and it consists in the process of joining together neighbouring mitochondrial membranes. The mitochondrial fusion is required to recover the activities of depolarized membranes and ensure the proper distribution of metabolites and mitochondrial DNA (mtDNA). Moreover, to preserve the proper mitochondrial function, regular "fission" activity is also required, with the aim to redistribute correctly the mitochondrial DNA during cell division, as well as for mitochondrial transport during mitosis and meiosis process.

Each cell has a different number of mitochondria. To maintain the highest number of mitochondria, cells require a lot of energy, such as in the heart, brain, liver, muscles or kidneys (Alberts et al., 1994).The cells ability to increase in the mitochondrial population (proliferation), and to improve the functional capabilities of pre-existing mitochondria (differentiation), is defined as "mitochondrial biogenesis".

Furthermore, upon stress stimuli, mitochondrial turnover can be accelerated through an autophagy process called "mitophagy". Moreover, mitochondria can adopt different shapes depending on the metabolic demands of the cell. The "mitochondrial dynamics" describes the mitochondrial morphology and distribution in the cell (Alberts et al., 1994).

Mitochondria are composed of two highly specialized membranes, the outer (Mitochondrial Outer Membrane, MOM) and inner (Mitochondrial Inner Membrane, MIM): the MOM is a more porous membrane for the high content of Porin, whereas the MIM is folded into numerous cristae. The space between the outer and the inner membrane is defined as Intermembrane Space (IMS). The space enclosed by the inner membrane is the core of the mitochondria, the matrix, in which harbours the mitochondrial DNA. The mtDNA is a 16.6 kB circle of double-stranded DNA, packaged into small clusters called nucleoids. The two mtDNA strands are named heavy (H) and light (L), for their buoyant density. Notably, mtDNA is not protected by histones, so it is more exposed to oxidative damage (Alexeyev et al., 2009). Moreover, mtDNA lacks repair mechanisms (Alexeyev et al., 2009). mtDNA is present in thousands of copies in each human cell, which are usually all identical at birth (homoplasmy). However, it is possible that an individual may harbour a mixture of mutated and wild-type mtDNA within each cell (heteroplasmy), which can lead to mitochondrial disorders resulting from mutation of mtDNA, mainly related to dysfunctions of the mitochondrial respiratory chain (Zeviar et al., 2014).

The mitochondrial DNA produces mitochondrial proteins, in concert with the nuclear DNA. Specifically, it encodes 37 genes, of which 24 are dedicated to tRNAs and rRNAs, and 13 encode respiratory chain polypeptides of respiratory Complexes I, III, IV, and V, and 24 nucleic acids necessary for intra-mitochondrial protein synthesis (Birch-Machin et al., 2006; Wallace et al., 2012). Interestingly, Complex II proteins are encoded by nuclear genes. Briefly, oxidative phosphorylation is driven by pyruvate produced from the metabolism of carbohydrates and fatty acids,

which are imported into the mitochondrial matrix to produce acetyl-CoA that is used to produce substrates for the oxidative phosphorylation (OXPHOS). Among them, there is NADH, which generates electrons that are pumped from the mitochondrial matrix across the inner membrane through respiratory complexes III, IV, and I and then returned to the matrix down their electrochemical gradient, allowing the complex V to synthesize ATP (Figure 1.2).

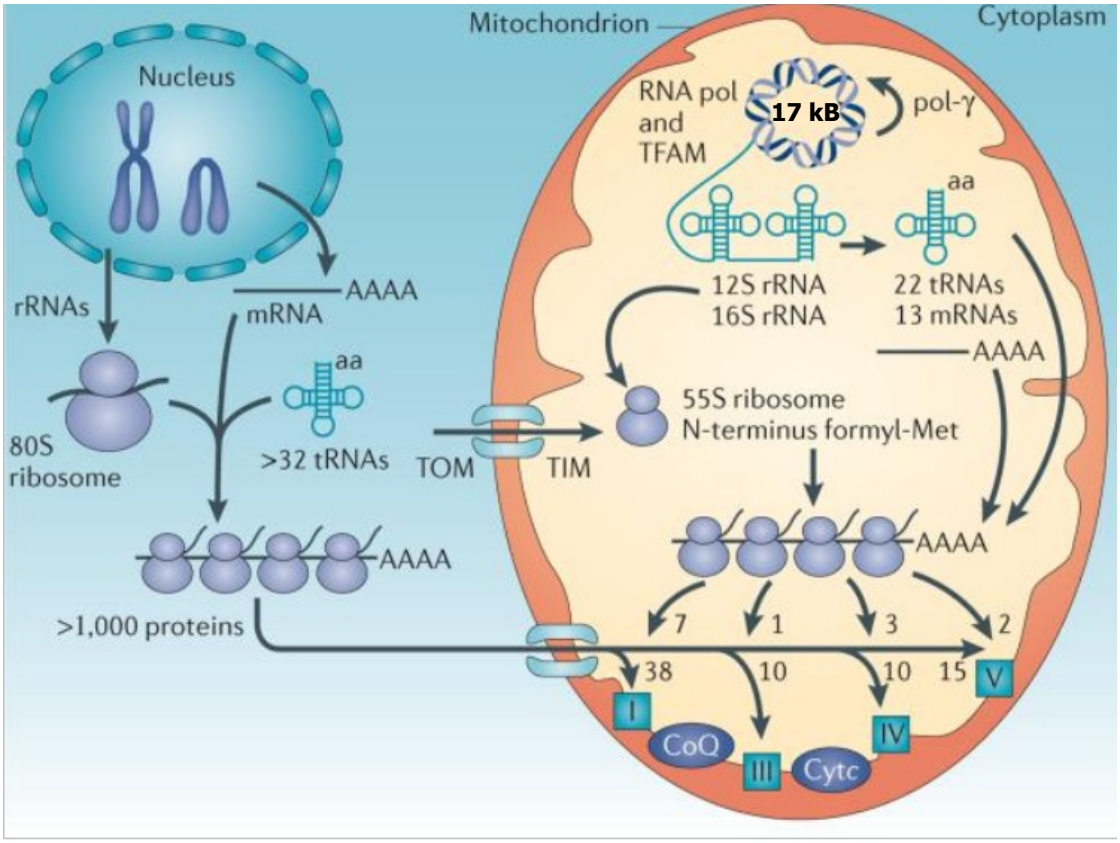


***Figure 1.2*** *– Scheme of mitochondrial biogenesis.*

*The mtDNA is packaged in the nucleoid and is replicated by DNA polymerase-γ (pol-γ). It is transcribed by mitochondrial RNA polymerase from both strands. The mtDNA encodes 22 tRNAs, and 12S and 16S rRNAs and 13 proteins: seven of complex I; (ND1, ND2, ND3, ND4, ND4L, ND5 and ND6), cytochrome b of*

*complex III; three of complex IV (cytochrome oxidase I (COI), COII and COIII); and two of complex V (ATP6 and ATP8). All of the remaining mitochondrial proteins, including OXPHOS subunits and all four subunits of complex II, are encoded by nuclear DNA (nDNA). Then, nDNA-encoded subunits proteins are imported into the mitochondrion by transport through the outer (TOM) and inner (TIM) membrane complexes. Modified and adapted from Wallace, 2012.*

Notably, the major part of the mitochondrial respiratory chain polypeptides, as well as the components of the import machinery, are encoded by nuclear genes and translated in the cytoplasm with a mitochondrial targeting sequence that directs them through the mitochondrial translocation machinery. Also, the proteins for the maintaining of the mitochondrial genome are nuclear-encoded. Among them, there are the mitochondrial DNA polymerase γ (POLG1) (Van Goethem et al., 2001), the mitochondrial transcription factor A (TFAM) and the mitochondrial transcription factors B1 and B2 (TFBM1 and TFBM2) (Larsson et al., 1998; Falkenberg et al., 2002), crucial factors for mitochondrial biogenesis during development and differentiation (Larsson et al., 1998).

If on one hand mitochondria are indispensable for cell survival, on the other hand, mitochondria are key regulators of cell death, mainly apoptosis. In mammalian cells, apoptosis is controlled by a wide range of extra- and intra-cellular signals, such as chemotherapy, growth factors or cytokines. Apoptosis can be initiated by two different ways: an "intrinsic" and an "extrinsic" pathways, converging in the apoptosis execution phase. The first one is activated by internal signals, such as DNA damage caused by chemotherapeutic agents, while the

extrinsic pathway is “switched on” by external signals. Mitochondria are essential regulators of the intrinsic pathway of apoptosis, by effector mechanisms by regulating the translocation of pro-apoptotic proteins from the mitochondrial intermembrane space to the cytosol (Zanzami et al., 1996).

Interestingly, mitochondria are involved in non-apoptotic cell death, such as the regulated necrosis mechanism named “necroptosis”. It has been described that necroptosis involves mitochondrial permeability transition (MPT), to lead the release of the apoptosis-inducing factor AIF. Furthermore, in the final step of programmed necrosis, the rapid mitochondrial dysfunction leads to ROS production failure in intracellular ATP production (Galluzzi and Kroemer, 2008).

### 1.2.4 Mitochondrial functions in cancer

Recent advances in cancer understanding suggest that not all the major hallmarks of cancer are linked to impaired mitochondrial function, as hypothesized by Otto Warburg. In some malignant tumours, there is the accumulation of morphologically normal respiration-proficient mitochondria (Lang et al., 2015). Indeed, although aberrant tumour cell growth is frequently associated with alterations of biochemical metabolism, mitochondrial function is not always impaired (Wallace, 2012; Weinberg and Chandel, 2015; Zong et al., 2016).

Since the lacking of histones and the absence of self-repair mechanisms, mtDNA molecules are frequently exposed to damage from ROS produced by these organelles. Notably, ROS is one of the most important causes of mitochondrial DNA mutations. The accumulation of constant oxidative damage to mtDNA, and subsequent nuclear DNA (nDNA) influences cellular and organ functions, leading

to disease states and ageing (Zeviar et al., 2014). Somatic and germline mtDNA mutations have been described for various tumours, such as renal adenocarcinoma, colon cancer, head and neck tumours, astrocytic tumours, thyroid tumours, breast tumours, ovarian tumours, prostate and bladder cancer and neuroblastomas (Wallace et al., 2012; Brandon et al., 2006). This evidence suggest the possibility that mtDNA mutations might contribute to cancer aetiology. However, large studies conducted to examine the mutational status of the mitochondrial genome in tumours revealed that selective pressure in human cancers allows the cells to retain mitochondrial genome functions. A wide analysis of the mitochondrial genome mutational landscape has been performed in over 2000 human cancers, including more than 30 tumour types, in comparison with normal tissue from the same patients (Zong et al., 2016). This analysis identified many somatic substitutions (with C to T and A to G) with strong replicative strand bias, on the mtDNA heavy strand. Surprisingly, these results revealed the mitochondrial polymerase G errors as the major cause of mutations, overshadowing the role of mitochondrial ROS. Moreover, while missense mutations are selectively neutral toward homoplasmy, harmful and pathogenic mtDNA mutations that remain heteroplasmic are negatively selected (Ju et al., 2014; Stewart et al., 2015).

On the other hand, while there is a negative selection for pathogenic mitochondrial genome mutations, some cancers have mutations in nuclear-encoded Krebs cycle enzymes – such as the isocitrate dehydrogenase (IDH) 2, succinate dehydrogenase (SDH) and fumarate hydratase (FH) - that lead to the oncogenic metabolites production (Gaude and Frezza, 2014). Interestingly, this kind of mutations induces tumour cells to perform reductive carboxylation to generate the

necessary Krebs cycle intermediates. As a result, the metabolism of these tumours is distinct from normal cells (Cardaci et al., 2015).

### 1.2.5 Targeting mitochondria for cancer therapy

The increasing understanding of the role of mitochondria in cancer cells represents a great opportunity to design novel approaches to targeted therapy for the treatment of various cancer (Fulda et al., 2010; Zong et al., 2016). One of the most challenging strategies explored for cancer therapy is to correct cancer-associated mitochondrial dysfunctions to re-establish cell death programmes by pharmacological agents that can facilitate mitochondrial membrane permeabilisation. Cancer cells bypass the mitochondrial apoptosis pathway by suppressing signals related to the process of rupture of MOM defined mitochondrial outer membrane permeabilisation (MOMP). Importantly, the loss of the MOM impermeability is the result of the process of dissipation of the mitochondrial membrane potential and osmotic swelling of the mitochondrial matrix that occur during the mitochondrial permeability transition (MPT). The MPT can be triggered by using various agents that can stimulate ROS generation, which represents a pro-apoptotic stimulus able to induce MPT, through the permeability transition pore complex (Fulda et al., 2010). Some of them are able to induce directly excess generation of ROS and antioxidant systems inhibition, such as the Menadione and Motexafin gadolinium, that have been successfully investigated in clinical study involving paediatric glioblastoma and hepatocellular carcinoma patients, respectively (Costantini et al., 2000; Magda and Miller, 2006). Other drugs elevate ROS levels by inhibiting the antioxidant systems (Maeda et al., 2004; Dragovich et

al., 2007), for example, by inhibiting the synthesis of reduced glutathione (e.g. buthionine sulphoximine) or by depleting its pool (e.g. Imexon). This approach demonstrated some efficacy in breast, prostate and lung cancer patients, alone or in combination with chemotherapy. Furthermore, agents able to increase superoxide levels by inhibiting the Superoxide dismutase (e.g. 2-methoxy oestradiol) showed selectively killing activity on human leukaemia cells (Huang et al., 2000).

The dependence of tumour cells on glycolysis for ATP generation can be exploited by anti-tumour strategies aimed to reverse their hyper-glycolytic state and lead them to cell death (Gill et al., 2016). Specifically, the attempt consists in the selective inhibition of the glycolytic pathway to sensitize tumour cells to anticancer agents. An example is represented by 2-deoxy-d-glucose (2DG), a calorie restriction mimetic that inhibits the glycolytic pathway by competitively inhibiting the synthesis of glucose-6-phosphate from glucose through the phosphoglucoisomerase. 2DG significantly intensifies the cytotoxicity of various anti-tumour drugs, by enhancing oxidative stress, such as in Cisplatin treatment of human head and neck cancer cells (Simons et al., 2007), as well as in Doxorubicin and Paclitaxel treatments in human osteosarcoma and non-small cell lung cancers (Maschek et al., 2004). Furthermore, in breast cancer cell lines, 2DG acts synergistically with DNA damaging chemotherapeutic agents and causes cell death (Zhang and Aft, 2009). In tumours characterized by impaired mitochondrial bioenergetics, a similar approach consists in the stimulation of mitochondrial activity to overcome the upregulation of the glycolytic pathway and restore ATP production mechanism used by non-malignant cells. This kind of strategy has been implemented, as an example, by inhibiting PDK1 by dichloroacetate, to readdress

the pyruvate metabolism and shift metabolism from glycolysis to glucose oxidation (Bonnet et al., 2007).

A similar approach takes advantage of the presence of nuclear-encoded Krebs cycle enzymes mutations in cancer cells. Tumours with defective mitochondrial functions show a different metabolism compared with most normal tissues, as an example, by up-regulating this pathway to satisfy energy requirement. To exploit this metabolic vulnerability is possible to inhibit the glucose uptake. To this aim, the activity of mutant IDH has been investigated as a potential therapeutic target in glioma cells and human leukaemia (Rohle et al., 2013; Wang et al., 2013). Similarly, in SDH-associated malignancies, the loss of SDH activity induces a block of Krebs cycle and drives proliferating cells to aerobic glycolysis. This event represents a very interesting metabolic vulnerability that can be a targeted therapy. SDH activity lack leads cells, on the one hand, to consume the extracellular pyruvate needed to sustain glycolytic flux and, on the other hand, to divert glucose-derived carbons into aspartate biosynthesis, thus sustaining cell growth (Cardaci et al., 2015).

The mitochondrial contribution to molecules biosynthesis is being investigated too. Glutamine metabolism, for example, is being explored since cancer cells usually increase its uptake and utilization. Glutamine metabolism requires the activity of the mitochondrial enzyme, glutaminase (GLS), for the production of glutamate. This enzyme, in cancer cells, is the predominant Krebs cycle fuel and it is involved in the production of intermediates for fat synthesis (Zong et al., 2016). Interestingly, GLS expression is induced by the proto-oncoprotein c-Myc (Gao et

al., 2009). Furthermore, it has been described that glutamine deprivation leads Myc-expressing cells to apoptosis (Yuneva et al., 2007). Consequently, as pharmacological inhibition of GLS suppresses tumour growth in renal cell carcinoma in mouse models, targeting glutaminase might be a good strategy to explore in suppressing Myc-driven cancer therapy (Shroff et al., 2015).

Recent reports suggest that cancer cells are highly susceptible to the inhibition of oxidative phosphorylation. The anti-diabetic drug known as Metformin, is an inhibitor of complex I of the electron transport chain, which is used by cells to produce energy. Recently metformin has been investigated for its anticancer activity (Evans et al., 2005; Chae et al., 2016; Wheaton et al., 2014). In xenograft models of Ras-driven colon cancer, Metformin impairs tumour growth by blocking tumour-intrinsic metabolism, since a tumour is dependent on oxidative phosphorylation to make ATP. At least two ways have been proposed for Metformin activity on tumour growth (Wheaton et al., 2014). The first one suggests that the slower rate of tumor growth represents the side-effect of the Metformin activity of reducing the blood amount of insulin, which, in turns, stimuluses cancer cells division. On the other side, it has been proposed that Metformin targets cancer cells by reducing the mitochondria-produced energy supply. Moreover, low glucose-sensitive cell lines are not able to up-regulate the OXPHOS in low glucose conditions. This impairment, which is the result of mtDNA mutations in Complex I genes or impaired glucose utilization, induces cell sensitivity to Metformin, and, in general, to OXPHOS inhibitors (Birsoy et al., 2014).

Additionally, inhibitors of mitochondrial translation can also act as sensitizers to cancer therapeutics and chemotherapy (Kuntz et al., 2017), especially in a tumour characterized by high level of mitochondrial biogenesis (Tan et al., 2017). The antibiotic Tigecycline –a mitochondrial protein translation inhibitor - has been shown as selectively acting against hepatocellular carcinoma (HCC) by inducing mitochondrial dysfunction and oxidative damage, via decreasing mitochondrial membrane potential, complex I and IV activities, mitochondrial respiration and ATP levels. Similar results have been observed in chronic myeloid leukaemia (CML), in which the combined treatment with the c-Abl-specific Tyrosine kinase inhibitors, Imatinib and Tigecycline, selectively destroy leukemic stem cells in a xeno-model of human CML.

## 1.3 Forkhead box protein family

Forkhead box (Fox) protein family has been described first in *Drosophila* (Weigel et al., 1989). This heterogenic protein family includes more than 100 transcription factors, which can be divided into 19 subclasses based on phylogenetic analysis. To classify the numerous member of Fox family, the term "Fox" is used as the root symbol, followed by a letter (from A to S) that indicates the subclass, and a number that identifies each protein. Fox proteins share a conserved DNA-binding domain, a sequence of 80 to 100 amino acids named Forkhead domain (FD). A "winged-helix" motif characterizes the Forkhead motif, due to the butterfly-like appearance of the loops in the protein structure of the domain, with three α helices and two large disordered loops (Clark et al., 1993). Fox transcription factors are involved in

a plethora of diverse functions, including development regulation, metabolism, tumorigenesis, and cognition. Their function is tightly regulated through the interaction with various binding partners, including co-activators, co-repressors and other transcription factors (Carlsson and Mahlapuu, 2002).

The FoxO proteins have been identified in many species, including nematode (*Caenorhabditis elegans*), Zebra fish (*Danio rerio*), fruitfly (*Drosophila melanogaster*), mouse and human (Arden, 2004; Arden, 2006). Mammalian FoxOs are orthologues of the transcription factor DAF-16, identified in C. elegans, involved in insulin signalling and longevity (Van der Horst and Burgering, 2007). The FoxO class is made of four members, FoxO1 (previously known as FKHR), FoxO3A (previously known as FKHRL1), FoxO4 (previously known as AFX) and FoxO6. Most of them are ubiquitously expressed, even though they can differ in tissues or organs. Additionally, it has been recently unravelled that the human FoxO3A pseudogene FoxO3B is a true human gene, which encodes a FoxO3A-related protein product (Santo and Paik, 2018).

FoxO proteins share high sequence homology. Their subcellular localisation defines their activity. Their structure consists of four common main domains (Figure 1.3): the Forkhead DNA binding domain (DBD), a nuclear localisation signal (NLS) downstream of the DBD, a nuclear export sequence (NES) and a C-terminal trans-activation domain (Greer and Brunet, 2005). To exert their role as transcription factors, FoxO proteins bind, through their DBD, to the consensus motif (Forkhead Response Element, FHRE), 5'-TTGTTTAC-3', within the target promoter sequence (Van der Horst and Burgering, 2007). Once they are bound to

DNA, the C-terminal trans-activation domain initiates gene transcription, working as a transcriptional activator or repressor, possibly depending on the range of associated co-factors that they recruit.

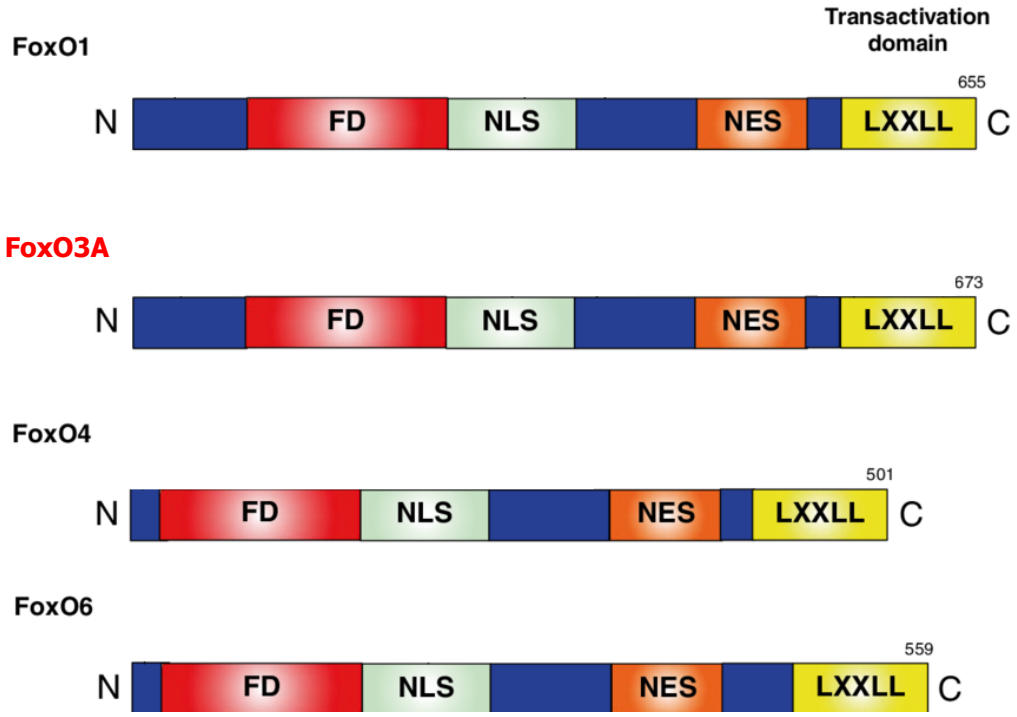


***Figure 1.3*** *–Domains contained in mammalian FoxO proteins.*

*The following are indicated: locations of the forkhead domain (FD), nuclear localisation sequence (NLS), nuclear export sequence (NES) and helical motif (LXXLL). Adapted from Sanchez et al. 2013.*

FoxO proteins are not equally expressed in all tissues, suggesting that individual proteins may have specificity in regards to cellular function (Fu and Tindall, 2008). As an example, the FoxO1 transcript is highly expressed in adipose tissues, while FoxO4 is expressed mostly in skeletal muscle. The formating transcript is abundant in brain, heart, kidney and spleen, while FoxO6 is predominantly found in the brain,

suggesting an important role for this FoxO to control cognitive and motor function (Figure 1.4)

| Types of FOXOs | Pathological Problems | Key roles of FOXOs |
|---|---|---|
| FoxO3a, FOXO proteins | Cancer | Transcriptional Activity of FOXO3a required to avert chronic myelogenous leukemia and B-chronic lymphocytic leukemia |
| | | FOXO proteins are involved in cell cycle regulation and proliferation process |
| | | Lack of functional FOXO proteins lead to prostate, breast and thymic tumors |
| FOXO1, FOXO3a | Alzheimer's disease and aging | FOXO protein translational activity prevention decreased the cell loss during neurodegeneration and oxidative stress |
| | | Amyloid caused phosphorylation of FOXO3a and FOXO1 |
| | | β-catenin had ability to modulate transcriptional activity of FOXO |
| FOXO1, FOXO3a | Diabetes mellitus | FOXO3a and FOXO1 linked with increased mortality and increased HbA1c |
| | | FOXO3a and FOXO1 associated with high risk of Stroke and diabetes |
| | | In several animal model of diabetes, FOXO3a activity loss may lead to disease complications |

***Figure 1.4-*** *Types of FoxO and their involvement in various diseases.*

*Image adapted from Farhan et al., 2017.*

### 1.3.1 FoxO target and functions

Through its transcription factor activity, FoxO proteins differentially affect cell fate in a downstream target-specific manner (Figure 1.5). Indeed, as their ability to bind a large number of gene promoters containing the DBD (Xuan and Zhang, 2005), they present a great diversity in function. In invertebrates, the homologous DAF-16 has been proven to increase lifespan and regulate nutrient sensing. These functions are conserved in Drosophila, where dFoxO is also involved in insulin signalling. In mammals, the members of the FoxO family play a role in stress resistance, proliferation/arrest, survival/death, metabolism and autophagy. FoxO proteins have been shown to get involved in tumour suppression, regulation of energy metabolism and development in some tissues. (Van de Horst A & Burgering BM, 2007). Interestingly, FoxO3A has also been described to regulate ovarian follicular development and fertility, glucose uptake after fasting and muscle regeneration (Castrillon et al., 2003; Sanchez et al. 2014).

One of the functions explored of FoxO is the regulation of cell cycle. In particular, FoxO is involved in the two important checkpoints for stress response, G1/S and G2/M. On the first point, it can block the G1 progression by repressing cyclin D1 and D2 either directly (Ramaswamy et al. 2002) or indirectly through Bcl6/STAT5 (Fernandez de Mattos et al. 2004). FoxO also promotes cell cycle arrest at the G1/S phase by up-regulating the CDK cyclin-dependent kinase inhibitors p21Cip1 (Seoane et al. 2004) and p27Kip1 (Medema et al. 2000). Furthermore, FoxO3A can act on p27Kip1 directly - by disrupting the cyclin D/CDK4 and Cyclin E/CDK2 complexes and causing an arrest at the G1 cellular checkpoint (Medema et al. 2000, Schmidt et al., 2002), or indirectly, through the

modulation activity exerted by c-Myc on FoxO3A (Bouchard et al., 2004). FoxO can also induce cell cycle arrest at the G2/M checkpoint by induction of growth-arrest and DNA-damage inducible protein GADD45α (Furukawa-Hibi et al. 2002, Tran et al. 2002), which is important in DNA-damage repair, maintaining genetic integrity, and promoting cell survival. Induced by FoxO, GADD45α interacts with the cdc25/Cyclin B complex and the CDKI p21, promoting the activation of the G2/M checkpoint, and the initiation of DNA repair mechanisms (Furukawa-Hibi et al. 2002). Moreover, by modulating GADD45α FoxO proteins participate to DNA conservation and repair, (Tran et al., 2002), to maintain the genomic integrity and reduce the accumulation of oncogenic mutations (Alekseyev et al. 2008).

FoxO proteins protect cells from ROS accumulation through the regulation of genes involved in cell detoxification and cell survival. Notably, FoxO3A is up-regulated in response to ROS accumulation. This event leads to an increase in the expression of its downstream transcriptional targets, such as the manganese superoxide dismutase (SOD2) and the Catalase (Kops et al. 2002).

FoxO proteins have various target genes in cell death pathways, which differentially express, through combinatory effects, ensure an efficient result. FoxO regulates the transcription of the tumour necrosis factor-related apoptosis inducing ligand, TRAIL (Modur et al., 2002), and of the tumour necrosis factor receptor-associated death domain, TRADD (Rokudai et al., 2002). Moreover, it has been widely explored that FoxO3A regulates the pro-apoptotic Bcl-2 family member Bcl-2-like protein 11 (Bim) expression (Dijkers et al., 2000a). Treatment of chronic myelogenous leukaemia (CML) cell lines driven by the BCR-ABL chimeric oncogene, with a BCR-ABL inhibitor, showed the activation of FoxO3A-dependent

Bim expression, resulting in apoptosis. (Essafi et al., 2005). FoxO3A has been widely shown to act as a tumour suppressor not only in leukaemia but also in breast and prostate cancers (Dansen and Burgering, 2008). Moreover, somatic deletion of FoxO1, FoxO3A, or FoxO4 in mice results in a cancer-prone phenotype, such as thymic lymphomas and haemangiomas (Paik et al., 2007).

Interestingly, the first identified FoxO member, DAF-16, which regulates the larva formation in *C.elegans*, is related to longevity (Kenyon et al., 1993). This function is evolutionally conserved. In recent years, the relationship between FoxO3A genotype and human longevity has been explored. Numerous single nucleotide polymorphisms (SNPs), located in intronic regions of the gene, are associated with longevity with statistical significance in different human populations (Willcox et al., 2008, Flachsbart et al., 2009, Anselmi et al., 2009).

FoxO proteins play a major role also in cellular differentiation. As an example, in mice models the absence of FoxO3A causes a deficiency in the ability of haematopoietic stem cells to repopulate the bone marrow, suggesting its possible role in promotion and maintenance of undifferentiated haematopoietic stem cells (Miyamoto et al., 2007).

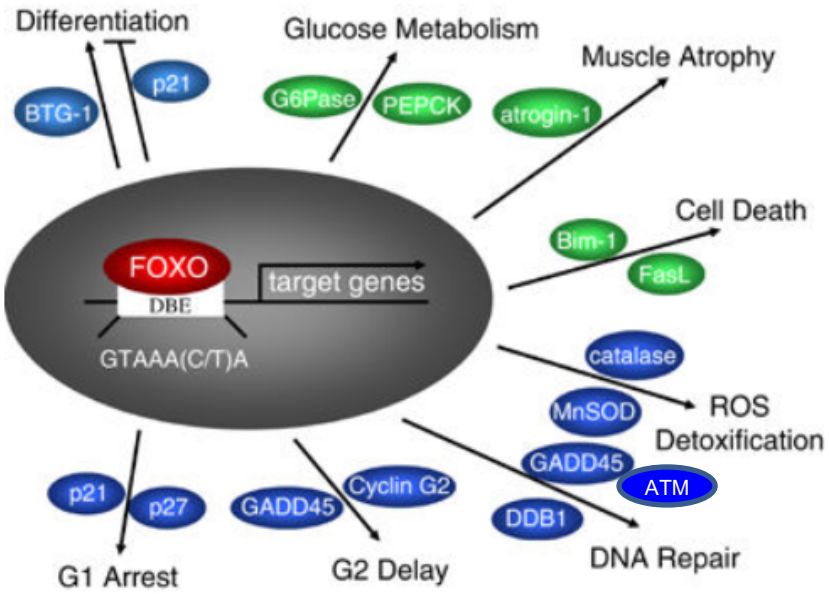


***Figure 1.5 -****FoxO target genes and cellular roles.*

*Adapted from Greer and Brunet, 2005.*

### 1.3.2 Regulation of FoxO

A complex cascade of post-translational modifications (PTMs), including phosphorylation, acetylation and ubiquitination, regulates FoxOs' transcriptional activity and protein-protein interactions (Figure 1.6). These modifications, known as "FoxO code" (Calnan and Brunet, 2008), are the result of the integration of cellular stimuli acting on FoxO. Notably, they determine the cellular localisation and the activity of FoxO proteins, since nuclear FoxOs can perform their typical transcriptional regulator activity, while cytoplasmic FoxOs are inactive and undergo proteasomal degradation. As a result, PMTs on FoxO influence the cell fate.

**Phosphorylation**

| Enzyme | FoxO1 | FoxO3 | FoxO4 | FoxO6 | Effect |
|---|---|---|---|---|---|
| Akt/SGK | T24<br>S256<br>S319 | T32,<br>S253<br>S315 | T28<br>S193<br>S258 | T26<br>S184 | - |
| CK1 | S322<br>S325 | S318,<br>S321 | S261<br>S264 | | - |
| DYRK1 | S329 | S325 | S268 | | - |
| CDK2 | S249 | | | | - |
| IKKβ | | S644 | | | - |
| AMPK | | *T179*<br>*S399*<br>S413<br>*S555*<br>*S588*<br>*S626* | | | + |
| JNK | | | T447<br>T451 | | + |
| MST1 | S207 | | | | + |
| PP2A | | | | | -/+ |

**Acetylation**

| Enzyme | FoxO1 | FoxO3 | FoxO4 | FoxO6 | Effect |
|---|---|---|---|---|---|
| CBP/<br>P300 | **K242**<br>**K245**<br>**K262** | *K242*<br>*K245*<br>*K259* | *K186*<br>*K189*<br>*K407* | *K173*<br>*K176*<br>*K190* | - |
| PCAF | *K294* | K290 | *K237* | *K229* | - |
| ?<br>Oxidative<br>Stress | *K274*<br>*K559* | K271<br>K569 | *K215* | *K202* | |
| SIRT1 | *K274*<br>*K294* | K271<br>K290 | *K215*<br>*K237* | *K202*<br>*K229* | -/+ ? |

**Ubiquitination**

| Enzyme | FoxO1 | FoxO3 | FoxO4 | FoxO6 | Effect |
|---|---|---|---|---|---|
| ? | | | K199<br>K211 | | Mono<br>+ |
| USP7/<br>HAUSP | | | K199<br>K211 | | - |
| Skp2 | ? | | | | Poly<br>- |

***Figure 1.6 -****Post-translational modifications of FoxO.*

*Effect: (−), Inhibition of FoxO; (+), activation of FoxO. Black, PTMs verified in cells; blue, expected site based on sequence alignment with other FoxO family members; green, PTMs verified in cells for the mouse FoxO; red, removal of PTMs. Italics—PTMs identified in vitro, not verified in cells. Adapted from Calnan and Brunet, 2008.*

### *Phosphorylation of FoxO3A*

Negative and positive regulation of FoxO3A involves principally phosphorylation events, mainly related to evolutionarily conserved signalling pathways, sensitive to metabolic and oxidative conditions of the cell. The main negative regulator of FoxO3A is represented by the insulin signalling pathway, constituted by phosphoinositide-3 kinase (PI3K) and the oncogenic protein kinase B (PKB), also known as the Serine/Threonine kinase 1AKT (Brunet et al. 1999,

Brownawell et al. 2001). Furthermore, two other main oncogenic kinases, like the inhibitor of NFκB signalling IKKβ and the mitogen-activated protein kinase MAP3K (also known as ERK, Extracellular-signal-regulated kinases) are also involved in the regulation FoxO3A nuclear localisation and activity (by phosphorylation), supporting the critical role of FoxO3A in cancer cells survival (Figure 1.7).

Activation of PI3K is induced by insulin-like growth factor (IGF-1) bound to its Tyrosine kinase-receptor IGF-1R. Activated PI3K phosphorylates the phosphatidylinositol-4,5-biphosphate (PIP2) membrane lipid to phosphatidylinositol-3,4,5-triphosphate (PIP3), offering the binding site on cell membrane for AKT, to localise it next to PDK1 (Phosphoinositide-Dependent protein Kinase 1). In this position, PDK1 can bind and activate AKT, leading to the phosphorylation of numerous substrates, including Threonine 32 and Serine 253 on FoxO3A (Greer and Brunet 2005). As a consequence, FoxO3A interacts with the chaperone proteins 14-3-3. This event blocks the FoxO3A nuclear import through interfering with its NLS region in the FHRE domain and shifts its localisation into the cytoplasm, leading to FoxO3A activity inhibition (Rena et al. 1999). Similar to AKT, Serum and Glucocorticoid-regulated Kinase (SGK) is also activated by PI3K and phosphorylates FoxO3A on the same residues of AKT (Brunet et al. 2001). IKKβ phosphorylates FoxO3A on S644 leading to its nuclear exclusion and promoting its degradation by an ubiquitin-proteasome-dependent pathway (Hu et al., 2004; Greer and Brunet 2005; Arden et al. 2004, Tezil et al. 2012).

The involvement of the RAS-ERK axis, one of the main actors in differentiation, proliferation and tumour progression in FoxO3A activity modulation, is performed by the direct interaction of ERK with the transcription factor and phosphorylation on its S294, S344 and S425. This post-translational modification results in FoxO3A stability suppression and nuclear exclusion (Yang et al., 2008). Moreover, the increase of FoxO3A cytoplasmic distribution improves its susceptibility to degradation via a murine double minute 2 (MDM2)-mediated ubiquitin-proteasome pathway, which serves as an E3 ligase. As a consequence, FoxO3A down-regulation promotes cell proliferation and tumorigenesis.

Notably, not all the phosphorylation events targeting FoxO3A lead to its negative regulation and cytoplasmic localisation. In fact, in response to oxidative stress, FoxO3A is phosphorylated by other kinases promoting its nuclear accumulation. As an example, the upstream activator of MAPK pathway, MST-1, can phosphorylate FoxO3A, disrupting the interaction with 14-3-3 and promoting its nuclear translocation (Lehtinen et al. 2006). Similarly, as a response to oxidative stress, the June-terminal kinase (JNK)-mediated phosphorylation results in FoxO3A nuclear localisation promotion and, consequently, its transcriptional activity (Eijkelenboom and Burgering, 2013). JNK can also modulate FoxO3A activity indirectly, by repressing the PI3K/Akt activity (Sunters et al. 2006, Ho et al. 2012). A similar pathway involves the MAPK p38, which promotes FoxO3A phosphorylation at S7 and its re-localisation to the nucleus, in response to chemotherapy treatment (Ho et al., 2012).

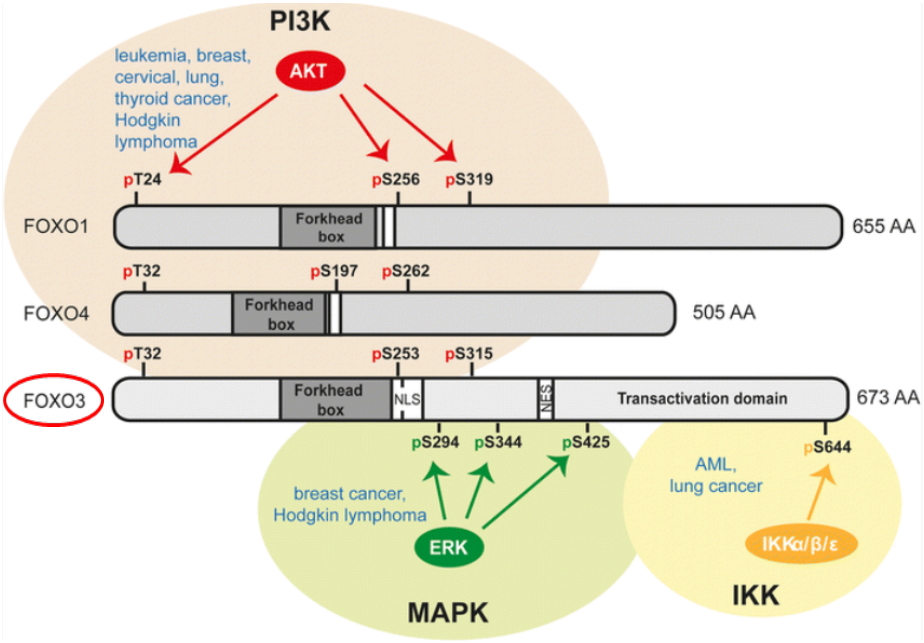


***Figure 1.7 -*** *Schematic representation of the major oncogenic signalling pathways linked with FoxO3A.*

*The phosphorylation mediated by AKT, ERK or IKK leads to FoxO3A inactivation and degradation, as described in several cancer types (as indicated). Image adapted from Coomans de Brachène and Demoulin, 2013.*

Similarly, in response to metabolic stress, the AMP-responsive kinase mediates FoxO3A phosphorylation and induces qualitative changes in the protein, influencing the shuttling between nucleus and cytoplasm and the transcriptional activity of the transcription factor (Greer et al. 2007b). AMPK is a central player in glucose and lipid metabolism, acting in response to nutrient and intracellular energy levels alterations. Interestingly, it phosphorylates FoxO3A on at least six specific sites, while experimental evidence suggesting that AMPK also acts on other sites (Greer et al. 2007b). Moreover, under metabolic stress, AMPK indirectly modulates FoxO3A transcriptional activity by activating the NAD+-dependent deacetylase,

Sirtuin1 (SIRT1, Canto et al. 2009, Brunet et al. 2004). Furthermore, AMPK can be triggered by mitochondrial ROS, through an alternative pathway that involves FoxO3A and its target genes such as SOD, catalase, and the peroxisome proliferator-activated receptor-γ coactivator-1α (PGC1α) (Colombo et al. 2009, Chiacchiera and Simone 2010). Remarkably, AMPK-phosphorylation is required for FoxO3A mitochondrial translocation, in normal cells (Peserico et al. 2013).

### *Acetylation/deacetylation of FoxO3A*

Acetylation/deacetylation events represent another important post-translational modification to regulate FoxO3A transcriptional activity, especially under oxidative stress (Figure 1.8). These events are evolutionarily conserved as in *C.elegans*, DAF-16 is positively regulated by acetylation (Tissenbaum and Guarente 2001, Motta et al. 2004). FoxO3A acetylation is performed by the acetyltransferases p300 and the cyclic-AMP responsive element binding (CREB)-protein, while the deacetylation is performed by NAD+-dependent deacetylases, like SIRT1 and SIRT3, which are parts of Sirtuin family (Brunet et al. 2004, Calnan and Brunet 2008, Kobayashi et al. 2005, Daitoku et al. 2014). Seven Sirtuins are known in humans, named as hSIRT1–7, mainly characterized by a NAD-dependent deacetylase activity (Schwer et al., 2002).

The acetylation/deacetylation status of FoxO3A results in the activation of different transcription programmes, such as apoptosis, through the strong activation of pro-apoptotic genes transcription, such as Bim, p21 and FASL6 (Brunet et al. 2004). Conversely, FoxO3A deacetylation by SIRT1 results in cell survival and FoxO3A-dependent apoptosis suppression, through the activation of downstream

targets involved in cell cycle arrest, DNA repair and antioxidant activity like GADD45α, SOD and p27 (Brunet et al. 2004). Therefore, SIRT1-mediated FoxO3A deacetylation can be considered as a cell-dependent cytoprotective mechanism (Greer and Brunet, 2005).

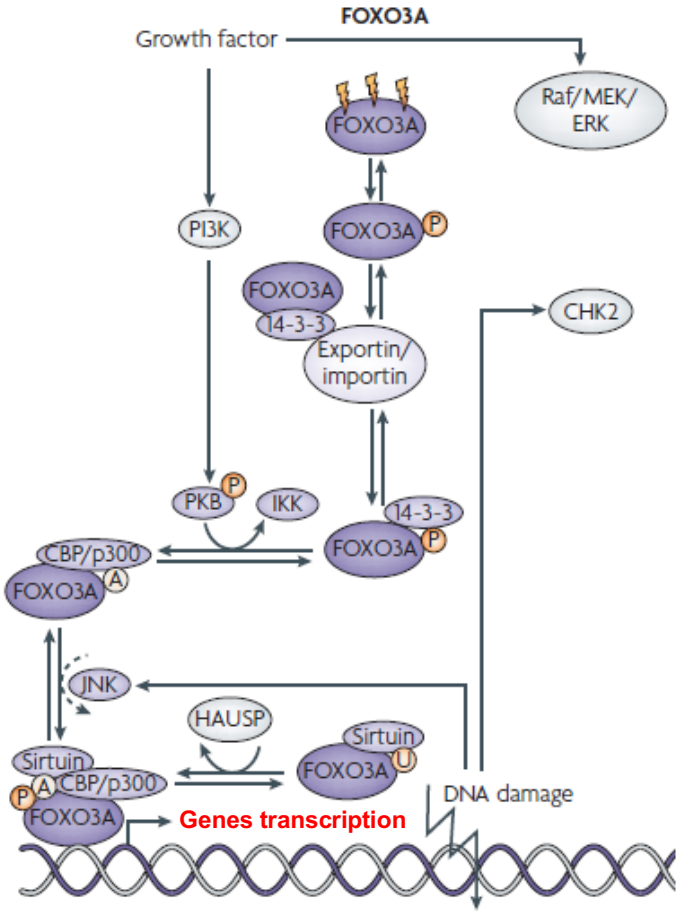


***Figure 1.8 -*** *Key regulators of post-translational modification of FoxO3A.*

*Stimulation with insulin or growth factors induces the phosphorylation of FoxO3A through PI3K pathway, leading to the association with 14-3-3 factors and nuclear export. The hypo-phosphorylated status of FoxO3A leads to Sirtuin recruitment and to the DNA binding promotion. Image adapted from Myatt et al., 2007.*

Besides SIRT1, even SIRT3, the main mitochondrial Sirtuin, can efficiently deacetylate FoxO3A (Kim et al., 2010). SIRT3 interacts directly with FoxO3A in mitochondria and nucleus. In the first case, the interaction promotes the transcription of oxidative stress response genes, such as catalase and SOD2 (Jacobs et al. 2008, Peserico et al. 2013, Tseng et al. 2013). Notably, the mitochondrial interaction between SIRT3 and FoxO3A will be discussed in the paragraph 1.3.3. In nucleus, SIRT3-FoxO3A interaction results in the nuclear localisation of FoxO3A and enhances the transcription of its nuclear target genes (Sundaresan et al. 2008). These events modulates FoxO3A ability to regulate cellular ROS accumulation. In mice, SIRT3-FoxO3A interaction ameliorates cardiac hypertrophy by ROS modulation, through FoxO3A nuclear localisation promotion and antioxidant genes transcription activation. (Sundaresan et al. 2008, Scher et al. 2007).

***Ubiquitination of FoxO3A***

FoxO3A protein levels and activity can be mediated among others by ubiquitin-dependent protein degradation (Tzivion et al., 2014). Two kinds of this PTM are possible: mono-ubiquitination (reversible) and poly-ubiquitination (not reversible), which results in the proteasome-mediated degradation (Figure 1.9). The poly-ubiquitination is performed in two steps: firstly, the target protein is covalently attached to the ubiquitin molecules, with the help of an ubiquitin-activating enzyme (E1-3). Then the 26S proteasome complex degrades the protein (Nakayama et al., 2006). The identified E3 ligases that mediate FoxO3A poly-ubiquitination is the S-phase kinase-associated protein 2 (SKP2) and MDM2, ubiquitin-ligases. MDM2 can both induce FoxO mono-ubiquitination as well as poly-ubiquitination. The

latter is related to AKT phosphorylation on Ser-253 of FoxO3A. On the other hand, ERK-phosphorylation induces FoxO3A mono-ubiquitination by MDM2 (Yang et al., 2008). IKK phosphorylation of FoxO3A induces its proteasome degradation. As IKK expression promotes cancer cell proliferation and tumorigenesis, FoxO3A-IKK phosphorylation might represent a promoting mechanism of tumorigenesis (Hu et al., 2004).

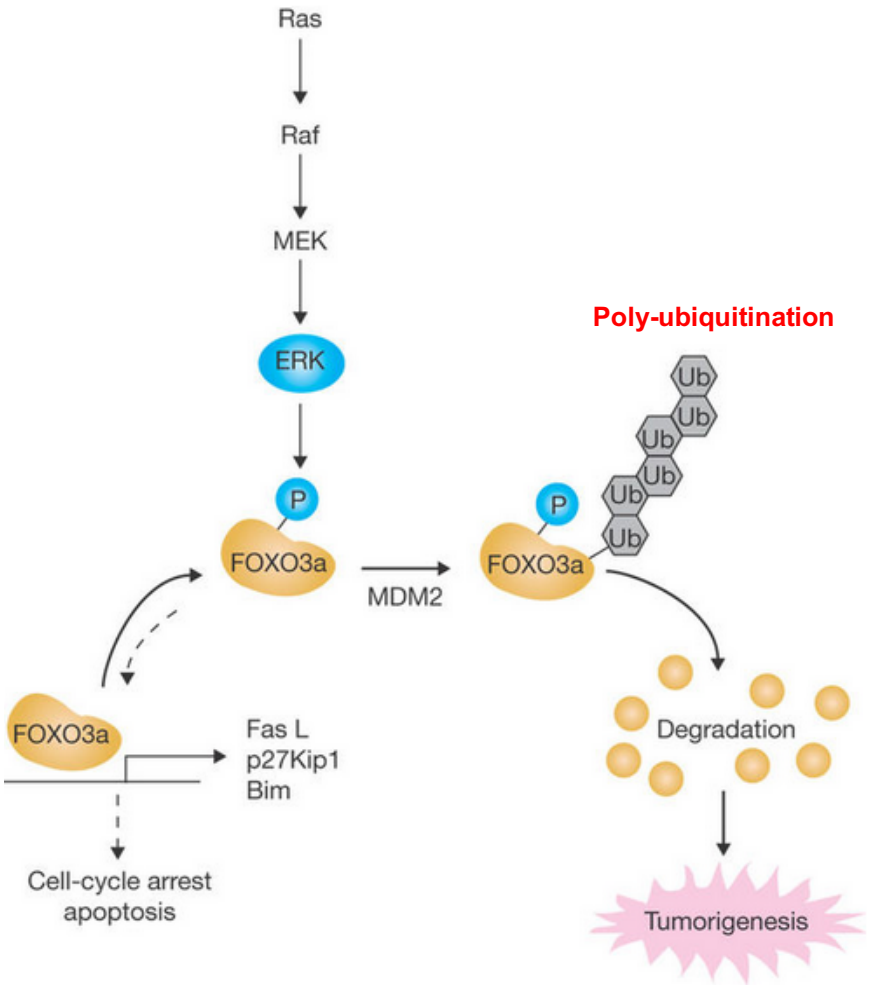


***Figure 1.9 -****ERK interaction and phosphorylation of FoxO3A.*

*The post-translational modification increases FoxO3A-MDM2 interaction and its degradation through a MDM2-dependent ubiquitin-proteasome pathway, promoting tumorigenesis. Adapted image from Yang et al., 2008.*

***Methylation of FoxO3A***

Lysine methylation of FoxO3A is not well-characterised. It has been reported that the methyl-transferase SET9 directly methylates FoxO3A, *in vitro* and cells, on the lysine 271. The methylation decreases the stability of FoxO3A. Howeverm it increasease FoxO3A transcriptional activity, upon stress stimuli (Calnan et al., 2012).

### 1.3.3 FoxO3A as tumour suppressor: a cancer therapy opportunity

To prevent the progression of cancer, surgery, radiotherapy, chemotherapy or their combinations are employed, depending on the stage and type of cancer. The aim of the chemotherapy focuses on promoting cancer cell death, preferably apoptosis, by changing the intracellular signalling pathways. Understanding how different therapeutic agents affect different cell types is instrumental to design more efficient and specific drugs. Worldwide, therapeutics in use is only 50% successful. In fact, varoius therapeutic resistance mechanisms interfere with the effect of drugs or/and desensitise the cells against cellular death signals. This phenomenon, known as chemo-resistance, can be acquired from cancer cells in the course of therapy or they can already be innate resistant genotypically. Currently, alongside the cytotoxic chemotherapies, targeted therapies that can modulate specific molecular oncogenic target (e.g. tumour suppressors), are taking holds, such as monoclonal antibodies and small molecules.

As briefly explained before, in mammals, FoxO proteins are involved in cell cycle arrest, DNA repair and apoptosis. The involvement in these function supports the idea of FoxOs as tumour suppressors. Indeed, loss of FoxO function decreases the ability to induce cell cycle arrest and to repair damaged DNA, subsequently leading to genomic instability and tumour development. Moreover, since apoptosis induction ability is compromised, in the absence of FoxOs, abnormal cells succeed to survive, resulting in tumour expansion. Simultaneous genetic deletion of five FoxOs alleles, correspondent to somatic FoxO1, FoxO3A, or FoxO4 in mice, resulted in a cancer-prone phenotype (Paik et al., 2007). The further deletion of all of the FoxOs alleles induces progressive cancers, late in life, such as thymic lymphomas and haemangiomas. Anyway, carcinoma has not been observed. Together, these data suggested FoxOs as putative tumour suppressors. However, genetic alterations inactivating FoxO loci in human cancers are quite rare. This evidence might explain why the tumour suppressor activity is visible only after inactivation of four to six alleles of FoxO. Furthermore, FoxO inactivation at protein and mRNA levels in cancer cells is efficiently performed via different oncogenic signalling pathways.

FoxO3A was one of the first FoxO factor recognised as a tumour suppressor in human breast cancer tissue samples, since its absence correlated with poor survival of patients (Hu et al., 2004). Additionally, low levels of FoxO3A protein expression are associated with poor prognosis in several types of cancers, including ovarian cancer, hepato-cellular carcinoma, gastric cancer, and lung adenocarcinoma (Fei et al., 2009; Jiang et al., 2013; Habashy et al., 2011; Yang et al., 2013; Yu et al., 2016; Liu et al., 2015).

During tumour development, inhibition of the transcriptional activity of FoxO3A promotes cell transformation, tumour progression and angiogenesis, while its over-expression inhibits a breast tumour (Greer & Brunet 2005; Potente et al., 2005; Hu et al., 2004). In many types of human cancers, down-regulation of FoxO3A results from post-translational regulation by on-kinases, such as AKT, IKKβ and ERK, as well as from the over-activation of upstream regulatory pathways, like the Phosphatase And Tensin Homolog, PTEN.

FoxO factors tumour suppressor activity have been investigated as therapeutic targets in various cancers, especially as mediators of the cytostatic and cytotoxic effects of chemotherapeutic agents. Different strategies have been implemented to activate FoxO3A. As an example, Paclitaxel - a chemotherapeutic agent used in the treatment of breast carcinoma- activates FoxO3A by reducing the activity of its upstream kinase AKT (Sunters et al., 2005). Therefore, the interaction between FoxO3A with the 14-3-3 protein is impaired (Tzivion et al., 2011), as well as the 14-3-3-mediated FoxO3A nuclear export. Paclitaxel can modulate FoxO3A activation also through JNK, resulting in FoxO3A-DNA binding promotion and activation of the transcriptional programme (Sunters et al., 2006; Eijkelenboom and Burgering, 2013). Doxorubicin treatment induces p38-mediated FoxO3A nuclear re-localisation (Ho et al., 2012) in MCF breast carcinoma cell line. On the other hand, in sensitive leukemic cells, doxorubicin leads FoxO3A to induce the expression of the multidrug resistance gene ABCB1 in K562 doxorubicin-sensitive leukemic cells (Hui et al., 2008). Additionally, Imatinib, a drug used for chronic myelogenous leukaemia (CML) and acute lymphocytic leukaemia, activates

FoxO3A (Essafi et al., 2005) and induces Bim-dependent apoptosis through inhibition of BCR-ABL in CML, as briefly mentioned in the paragraph 1.2.4.

Another strategy for targeting FoxO3A in cancer therapy is represented by the modulation of the FoxO3A-FOXM1 transcriptional axis (Figure 1.10). The Forkhead box protein M1 (FOXM1) is a proto-oncogene acting as a transcriptional activator, which is involved in cell proliferation by regulating the expression of cell cycle genes, like cyclin B1 and cyclin D1. Its up-regulation is frequent in several human cancers, including liver, breast, lung, prostate, uterus, colon, and pancreas. Furthermore, FoxO3A directly repress the activity of FOXM1 (Wilson et al., 2011; Yao et al., 2017). Various anticancer drugs like the "tinibs" agents (Lapatinib, Imatinib and Gefitinib), Paclitaxel, Cisplatin and Doxorubicin can be used to modulate FoxO3A-FOXM1 axis. Intriguingly, their cytostatic and cytotoxic effects are mediated through the activation of FoxO3A and/or the inhibition of FOXM1 (Yao et al., 2017; Farhan et al., 2017).

Lapatinib, Imatinib and Gefitinib interfere with the PI3K-AKT-FoxO3A-FOXM1 axis by blocking the auto-phosphorylation of receptor-Tyrosine kinases and downstream signalling. On the other hand, as briefly described above, the JNK-triggering ability of Paclitaxel leads to the nuclear accumulation of FoxO3A and, consequently, to the inhibition of FOXM1. Similarly, Doxorubicin, promotes the nuclear translocation of FoxO3A by phosphorylating of p38 MAP kinase. Moreover, at the same time, it can directly down-regulates FOXM1 expression, as well as Cisplatin and Epirubicin (Yao et al., 2017; Farhan et al., 2017). Furthermore, in cancer cells in which Sirtuins activity is up-regulated (i.e. SIRT4, SIRT5, SIRT6

and SIRT7), the combined treatment with Sirtuins inhibitors, such as Sirtinol, Salermide or EX527 and Doxorubicin or Epirubicin helps cells to overcome chemo-resistance, by mediating the deacetylation and inhibition of FoxO3A (Yao et al., 2017).

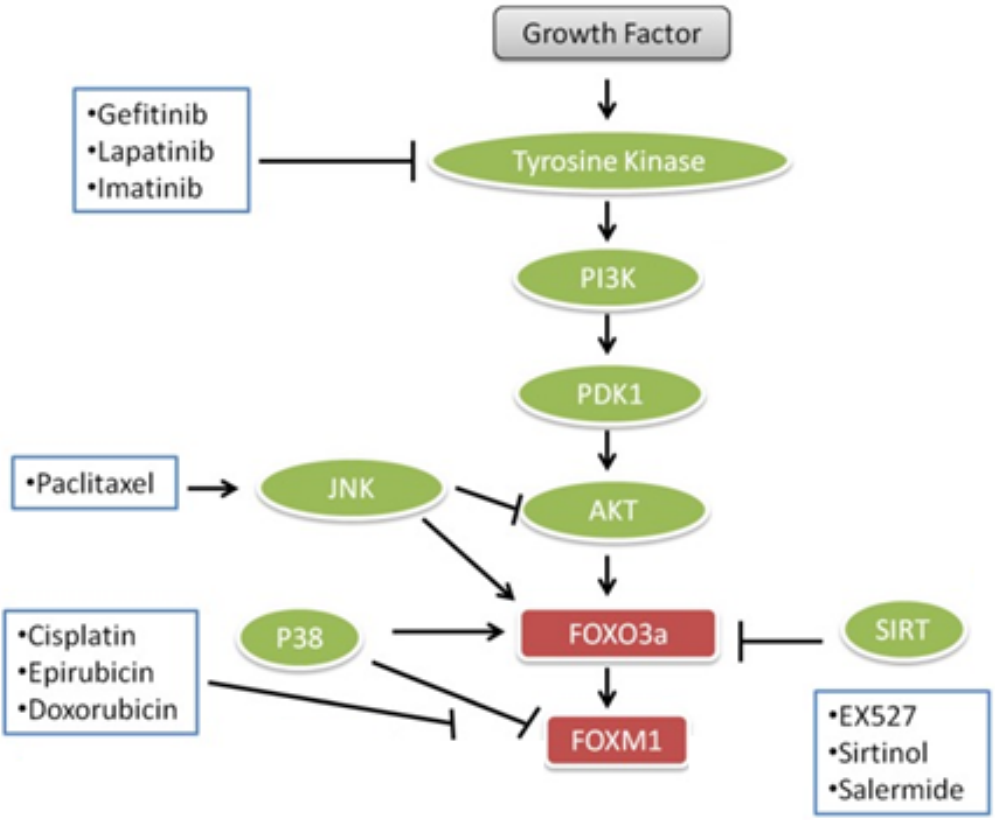


***Figure 1.10 -*** *Example of anticancer drugs interfering with FoxO3A pathway.*

*Image modified and adapted from Farhan et al., 2017.*

### 1.3.4 FoxO3A and chemo-resistance

Even if chemotherapy and radiotherapy are often successful in inducing cell death of tumours or reducing the tumour mass, many cancer patients develop resistance to cancer therapeutics, experience recurrence and die. A fascinating

therapeutic opportunity is represented by the combination of the FoxO3A tumour suppressor activity and other therapeutic agents, to sensitize resistant tumour cells.

In colorectal cancer (CRC) cells, FoxO3A is a mediator of the cytotoxic effect of Cisplatin. Inhibition of FoxO3A de-phosphorylation and nuclear translocation induced by Cisplatin in the PI3K/AKT/FoxO3A axis causes chemoresistance of CRC to the drug (Fernández de Mattos et al., 2008). Similarly, the PI3K/AKT/FoxO3A pathway activation plays an important role in 5-Fluorouracil (5-FU) resistance in CRC. The co-treatment of CRC cells with 5-FU and the PI3K/mTOR inhibitor, NVP-BEZ235, induces AKT survival pathway inhibition and the activation of FoxO3A-mediated transcription of genes target related to cell death (Wang et al., 2015). Additionally, the p38-FoxO3A axis can be targeted to overcome chemo-resistance of CRC cells to chemotherapeutics. *In vitro* co-treatment with a p38 inhibitor, SB202190 and Cisplatin induces FoxO3A activation and apoptosis mediated by FoxO3A-target genes. Moreover, *in vivo*, the same co-treatment results in tumour regression in xenograft mouse model (Germani et al., 2014). In ER-negative breast cancer, the activation of FoxO3A through the inhibition of the PDK-1/AKT pathway results in the sensitization of chemo-resistant cells to Tamoxifen (Weng et al., 2008).

Another opportunity of combined therapy involves the epidermal growth factor receptor/human epidermal growth factor receptor2 (EGFR/HER2) blocking agents, currently employed in clinical trials against breast, prostate, kidney, ovarian and lung cancers (Myatt et al., 2007). Especially, the inhibition of the EGFR family by monoclonal antibodies such as Trastuzumab or Cetuximab impairs the PI3K pathway and promotes FoxO3A activity (Real et al., 2005). Furthermore, the

reconstitution of active FoxO3A results in sensitisation of resistant cancer cells to EGFR/HER2 inhibitors like Lapatinib and Gefitinib (Myatt et al., 2007). Additionally, in osteosarcoma model, FoxO3A activation induces Bim and apoptosis in cells exposed to ionizing radiation (Yang et al., 2006). Thus, the combination of radiation with chemotherapy targeting FoxO3A may improve tumour cells sensibility to radiation therapy.

### 1.3.5 FoxO3A at the interface between cell death and survival

As briefly explained before, in cancer energy metabolism reprogramming, key mitochondrial functions are usually preserved in the majority of cancer cells and are required for the acquisition of a fully malignant phenotype. In this context, proteins usually considered as genuine tumour suppressors are sometimes required to be functional for full malignant phenotype acquisition depending on the cellular context, such as FoxO3A (Gomes et al., 2008; Zhang et al., 2011; Chiacchiera and Simone, 2010).

FoxO3A activity as tumour suppressors have been extensively explored and linked not only to its pro-apoptotic and anti-proliferative actions but also to its involvement in angiogenesis, resistance to oxidative stress and control of cell invasion (Figure 1.11). However, further experimental evidence suggested a dual role for FoxO3A at the crossroad between cell survival and death. Although its activity and expression are unaltered in different cancers, numerous studies performed in the last decade demonstrated that FoxO3A also has an unexpected function in the promotion of cancer and in modulating responses to cancer

treatment, through a variety of mechanisms (Storz et al., 2009; Scisci et al., 2013; Liang et al., 2013; Ahn et al., 2018).

Indeed, it has been recently proposed that FoxO3A can be involved in promotion of cancer cell survival, tumour expansion, and metastasis. As an example, in breast cancer, FoxO3A plays a pro-invasion role by regulating the expression matrix metalloproteinase (MMP), such as MMP-9 or MMP-13 (Storz et al., 2009; Scisci et al., 2013). In this context, any therapy under development to inactivate FoxO3A might be a candidate to block tumour expansion and metastasis (Storz et al., 2009; Scisci et al., 2013). Pro-oncogenic functions have been investigated in hepatocellular carcinoma (HCC) too, where FoxO3A activates serotonin-induced cell proliferation in serum-deprived HCC cells (Liang et al., 2013; Ahn et al., 2018). A more recent study showed the association between the over-expression of FoxO3A and aggressive phenotypes with a poor prognosis in patients with HCC.

Furthermore, the down-regulation of FoxO3A expression in HCC cell line inhibits cell proliferation and migration. Similarly, FoxO3A protein expression has been associated with progression and poor prognosis in glioblastoma (GBM) patients. Indeed, FoxO3A over-expression considerably promoted the colony formation and invasion ability in GBM cells, by activating of c-Myc, microtubule-associated protein 1 light chain 3 beta (MAP1LC3B) and Beclin1 (Qian et al., 2017). Consistently, FoxO3A knockdown strongly inhibited tumour progression. Other studies suggested that, at least in some types of cancer, like leukaemia, activation of FoxO3A is initially required for induction of apoptosis in response to chemotherapy, whereas its prolonged activity promotes drug-resistance by

increasing anti-oxidant defences and DNA damage repair (Hui et al., 2008). Furthermore, not surprisingly, FoxO3A has emerged as a major sensor for metabolic stress and chemotherapeutic drug response in cancer cells. As it will be exploited in section 1.3.2, in metabolically stressed cancer cells (colorectal, ovarian, prostate), activation of the FoxO3A-dependent transcriptional programme first leads to autophagy and cell cycle arrest as an attempt to retain energy and increase ATP levels to survive, but then triggers cell death under conditions of persistent stress (Chiacchiera and Simone, 2009).

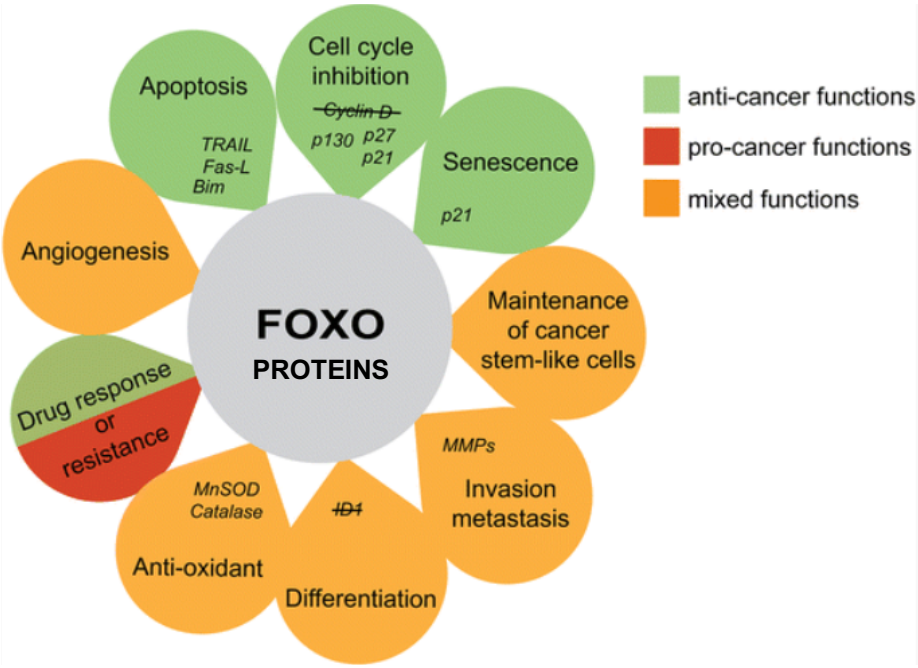


***Figure 1.11-*** *Dual role of FoxO protein in cancer.*

*FoxO plays a major role in a plethora of cellular functions (e.g. cell cycle arrest, apoptosis) aimed to the tumour development prevention and cancer cell death induced by various drugs (***green leafs***). By contrast, some FoxO3A functions appear as ambiguous (e.g., angiogenesis, oxidative stress resistance, differentiation, cancer stem cell maintenance and control of cell invasion and*

*metastasis,* orange **leafs***). The explicitly pro-tumour roles of FoxO, which as an example causes the resistance to certain treatments are indicated in the* **red** *leafs. Key target genes are indicated in* **smaller letters***, while the repressed ones are* crossed. Image adapted from *Coomans de Brachène and Demoulin, 2013.*

Taken together, these contradictory findings suggest that FoxO3A may have opposing roles in different tumour types, based on the extracellular stimuli or the specific cell type.

## 1.4 The AMPK-FoxO3A axis

As briefly mentioned above, the increase of the AMP/ATP ratio leads to the activation of the energy sensor pathway and consequently leads to the phosphorylation of FoxO3A by AMPK (Greer et al., 2007a-b). Experimentally, in mammalian cells, AMPK phosphorylates FoxO3A in response to stimuli associated with dietary restriction (DR) (Greer EL et al., 2007a-b).

### 1.4.1 AMPK activation

AMPK is a Serine/Threonine protein kinase complex, which forms a heterotrimer consisting of a catalytic α-subunit (α1 and α2), a scaffolding β-subunit (β1 and β2) and a regulatory γ-subunit (γ1, γ2 and γ3). AMPK is involved in various cell functions, such as cell growth regulation, reprogramming metabolism, autophagy and cell polarity modulation. Indeed, upon activation, AMPK "re-programmes" cell metabolism to turn on catabolic pathways, such as glycolysis and fatty acid oxidation, to generate ATP and inhibits ATP-consuming anabolic

processes not necessary for the immediate survival of the cell (Canto and Auwerx, 2010). Furthermore, to this aim, AMPK increases mitochondrial content and mitochondrial substrates as an energy source, by modulating the expression of the transcriptional coactivator PGC1-α, of the Oestrogen-related receptor alpha (ERRα), the nuclear respiratory factors 1-2 (NRF1, NRF2) and the Peroxisome proliferator-activated receptors (PPARs) (Reznick and Shulman, 2010). Therefore, as a cellular energy sensor, a variety of physiological and pathological conditions that deplete cellular energy levels, such as prolonged exercise, nutrient starvation, hypoxia, exposure to toxins that inhibit the mitochondrial respiratory chain and disease conditions, stimulate the AMPK signalling (Hardie et al., 2012; Mihaylova and Shaw et al., 2011). Specifically, in the presence of lowered intracellular ATP levels, AMP or ADP directly binds the γ-regulatory subunits, inducing a conformational change aimed to protect the phosphorylation of AMPK. The α-catalytic subunit contains the Thr172, which is phosphorylated by three known upstream kinases: the tumour suppressor Serine/Threonine kinase 11 (STK11, also known as LKB1), the MAPKKK family member transforming growth factor-β-activated kinase 1 (TAK1/MAP3K7), and the Ca2+/calmodulin-dependent protein kinase kinase β (CAMKKβ) kinase, which is triggered in response to calcium flux. Additionally, several pharmacological agents can activate AMPK (Figure 1.12). These drugs can act in two different ways: directly, by inducing activating conformation changes in the AMPK complex, without any significant change in cellular ATP, ADP or AMP levels, or indirectly, through the AMP or calcium accumulation modulation (Kim et al., 2016). The first group includes the AMPK activator 5-aminoimidazole-4-carboxamide riboside (AICAR). Upon

phosphorylation by adenosine kinase, AICAR monophosphate (ZMP) binds to the AMPKγ subunits. The group of indirect activators of AMPK includes Biguanides, Thiazolidinediones, Ginsenosides, α-Lipoic acid and Polyphenols (Kim et al., 2016). As an example, the polyphenol Resveratrol, which is abundant in the skin of red grapes, activates AMPK by increasing the AMP/ATP ratio as the result of the F1F0 mitochondrial ATPase inhibition. Similarly, quercetin, which is abundant in fruits, vegetables, grains and curcumin, from Curcuma longa, also is capable of activating AMPK by modulating AMP levels (Kim et al., 2016; Mihaylova and Shaw et al., 2011).

Metformin and other biguanides are classified as indirect activators of AMPK since they modulate ATP levels, through the inhibition of the Complex I of the respiratory chain. Metformin is a biguanide drug commonly used in the treatment of diabetes, which has been proven to have anticancer activity in diabetic patients (Evans et al., 2005; Chae et al., 2016).

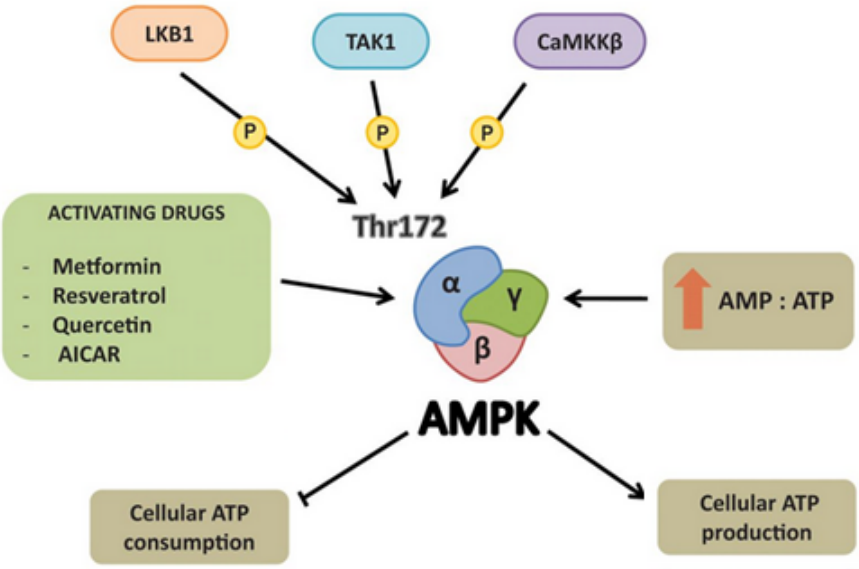


***Figure 1.12 -*** *The endogenous and exogenous stimuli activating AMPK.*

*Image modified and adapted from Andrade and Pires de Carvalho, 2014.*

Several phase II/III clinical trials are currently evaluating the efficacy of Metformin in association with chemotherapeutic agents as well as its chemoprevention activity as a single agent. However, the Metformin anticancer properties are still under debate, as briefly mentioned before (Paragraph 1.1.5). Of note, Metformin inhibits the activity of Complex I of the mitochondrial machinery responsible for oxidative phosphorylation, the same mechanism inducing AMPK activation in cultured cells (Wheaton et al., 2014).

***AMPK activation in dietary restriction (DR)***

The shortage of caloric intake nearly doubled the lifespan of rats (Mc Cay et al., 1989). Since that moment DR, meant as the reduction of food intake without inducing malnutrition, has been investigated with the aim to extend longevity and

lifespan. In various species, such as worms, flies and mice, a longevity effect correlated with DR (Masoro, 2005). Moreover, in mice, DR can reduce the incidence of major diseases (Fontana and Kline, 2007). In monkeys, DR can "halve" the incidence of neoplastic mass development compared with the control animals (Colman et al., 2009), while in humans, DR decreases the incidence of age-dependent diseases, including cancer (Michels and Ekbom, 2004).

AMPK plays a central role as a modulator of lifespan extension by DR (Cantó and Auwerx, 2011). AMPK activation increases lifespan in *C. elegans* and *D. melanogaster* through the mitochondrial metabolism remodelling in peripheral tissues. Similarly, Metformin treatment promotes healthy ageing in mice (Weir et al., 2017). In mammals subjected to DR, decreased levels of glucose and leptin activates AMP, in the brain but not in the liver (Greer et al., 2007b). AMPK-FoxO axis has been proposed as a mediator of lifespan- DR induced in C. elegans (Greer et al. 2007b).

### 1.4.2 AMPK-FoxO axis in cancer and longevity

So far, six mammalian FoxO3A residues are known to be phosphorylated by AMPK in vitro: T179, S399, S413, S555, S588, and S626 (Figure 1.13). Five of them are located in the transactivation domain (Greer et al., 2007b; Greer et al., 2009). Experimental evidence showed that the substitution of all six residues in FoxO3A with non-phosphorylatable amino acids, still partially retains (16%) the potential of AMPK to phosphorylate FoxO3A, strongly suggesting the existence of additional phosphorylation sites in the protein sequence.

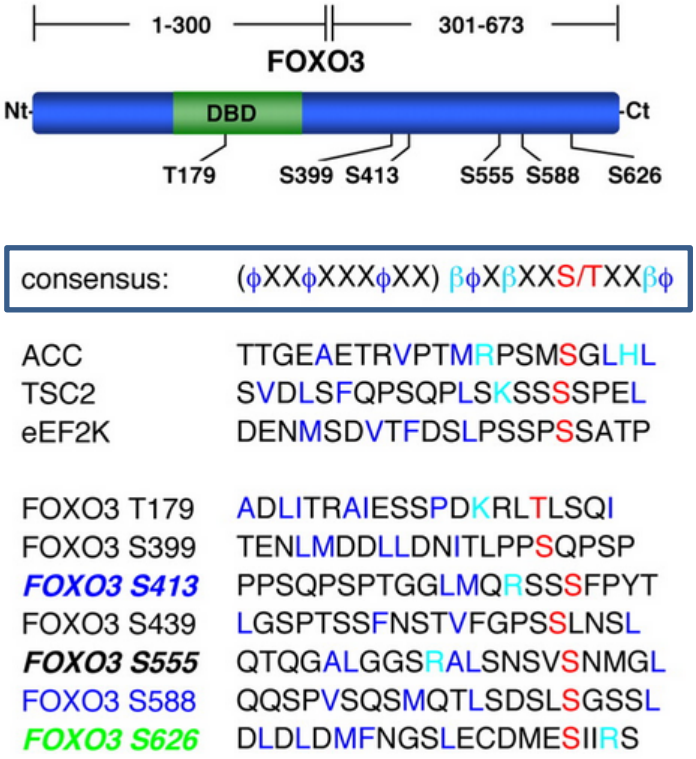


***Figure 1.13**–AMPK phosphor-sites in FoxO3A.*

*Alignments of the AMPK consensus phosphorylation motif with putative phosphorylation sites (in red) in human FoxO3A and sites in known substrates of AMPK. Boldface and italic: sites identified as being phosphorylated in vitro by AMPK by LC-MS/MS. Green: sites identified as being phosphorylated in cells by LC-MS/MS. Blue: sites phosphorylated in cells identified by using phosphospecific antibodies. Hydrophobic residues are indicated in dark blue. Basic ones in light blue. Image modified and adapted from Greer et al. 2007.*

Notably, the substitution of all six residues is not able to affect the ability of FoxO3A to shuttle between the nucleus and the cytoplasm, depending on nutrient condition. However, the nuclear transcriptional activity of FoxO3A is impaired (Greer et al., 2007b).

The AMPK-FoxO axis is required for dietary restriction-dependent health and lifespan extension (Greer et al., 2007b; Greer et al., 2009). As briefly mentioned before, in nematodes DR extends lifespan. This effect on longevity is blunted in AMPK defective nematodes and significantly reduced in FoxO mutant strains. Notably, FoxO involvement in DR-lifespan extension is not dependent on its transcriptional activity, since FoxO is not able to shuttle into the nuclei from the cytoplasm. On the other hand, the mutation of the insulin receptor extends lifespan in nematodes. DR further enhance lifespan (Greer et al., 2007b). The AMPK-FoxO axis plays a major role also in oxidative stress resistance in nematodes, which is strictly related to longevity and lifespan, through the modulation of its target gene SOD-3.

At least in human colorectal and ovarian cancers, AMPK/FoxO3A pathway is maintained as a functional metabolic switch capable of sensing variations in the AMP/ATP ratio. As an example, the decreased glycolysis caused by inhibition of the p38α/HIF1α pathway, activates FoxO3A transcriptional programme, in an AMPK-dependent way (Chiacchiera and Simone, 2009). Notably, pharmacological inhibition of p38α is a challenging strategy used in that kind of tumours, like CRC, in which p38α is required for cell proliferation and survival (Comes to et al., 2007; Chiacchiera et al., 2009). For example, in CRC, the combined use of the selective p38 inhibitor, SB202190, and a kinase inhibitor, Sorafenib, approved for the treatment of renal cell carcinoma and hepatocellular carcinoma enhances the anti-cancer activity of Sorafenib, by inducing apoptosis (Grossi et al., 2012). In CRC, p38α signalling pathway inhibition significantly impairs the intracellular levels of ATP and decreases the HIF1α protein stability and the expression of key enzymes

involved in aerobic glycolysis. The metabolic stress activates AMPK, which promotes the nuclear accumulation of FoxO3A and the sequential transcription of its target genes related to autophagy, cell metabolism, cell cycle arrest and cell death (Chiacchiera et al., 2009).

FoxO3A activation leads first to the transcription of genes related to the autophagic flux, such as the GABA type A receptor-associated protein (GABARAP), GABA type A receptor-associated protein-like 1 and 2 (GABARAPL1 and GABARAPL2), and MAP1LC3. The autophagic flux consists of sequential steps, controlled by the ATG proteins (ATG6, ATG7 and ATG12), which lead to the degradation of cytoplasmic amino acids and fatty acids, to sustain cell metabolism. To this aim, FoxO3A-target genes involved in metabolisms, such as PGC1α, the PhosphoEnolPyruvateìCarboxyKinase (PEPCK) and the mitochondrial Uncoupling Protein (UCP2) are induced to convert the fatty acids and amino acids produced by the autophagic flux in ATP. Subsequently, FoxO3A induces the up-regulation of the cyclin D transcriptional repressor, Bcl-6, and of the CDK inhibitors, p21 and p27, to block the G1/S transition, leading the cell to exit from the cell cycle and trigger cycle arrest. If metabolic stress conditions persist, cell undergoes cell death, mediated by the FoxO3A-dependent activation of the transcription of the Autophagy-related 6, 7 and 12 genes (ATG6, ATG7 and ATG12), and of BH3-only proteins, such as the p53 up-regulated modulator of apoptosis (PUMA), Bim, the BCL2 Interacting Protein 3 (BNIP3) and the BCL2 Interacting Protein 3 Like (BNIP3L).

AMPK-dependent activation of FoxO3A transcriptional programme in metabolic stress conditions causes tumour growth inhibition, both *in vitro* and *in vivo* (Chiacchiera and Simone, 2009), suggesting that the pharmacological manipulation of the AMPK-FoxO3A axis is a interesting approach for cancer treatment.

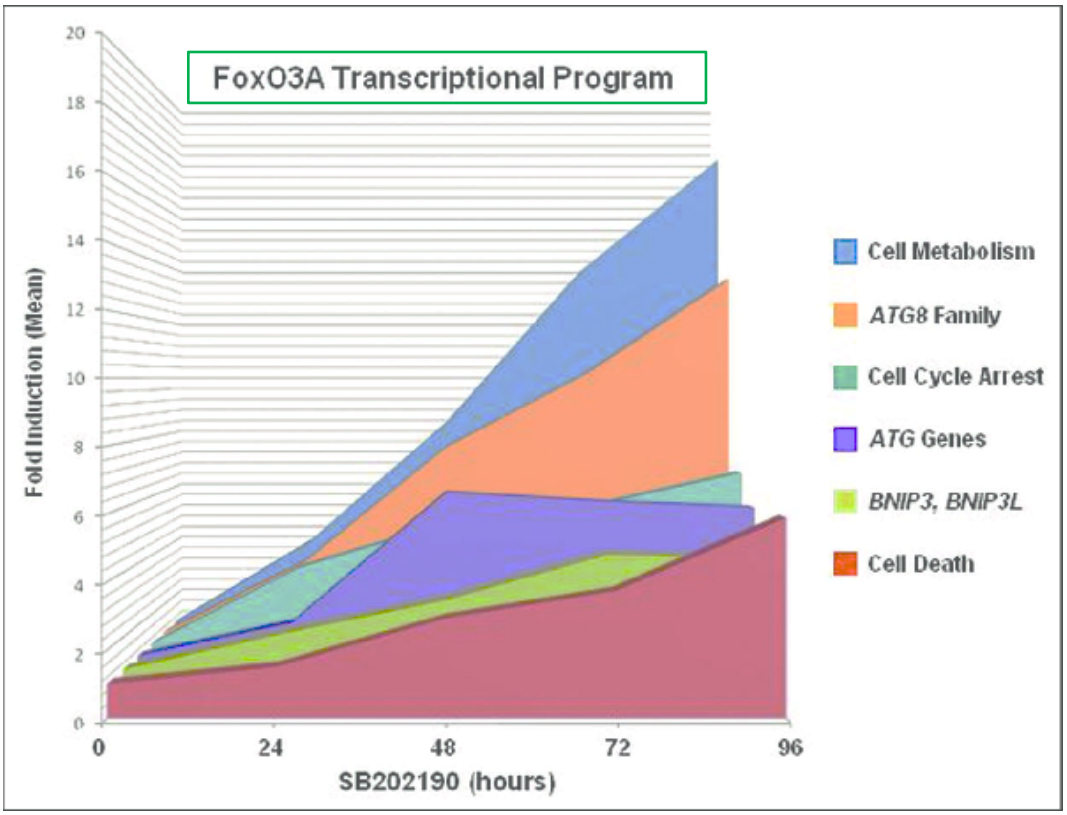


***Figure 1.14 -*** *AMPK-dependentFoxO3A transcriptional profile.*

*Gene transcription profile in response to p38α inhibition, SB202190-mediated. Adapted from Chiacchiera and Simone, 2009.*

### 1.4.3 The mitochondrial arm of AMPK-FoxO3A axis

Recently, a mitochondrial arm of AMPK-FoxO3A axis has been proposed (Figure 1.16). A growing body of evidence highlights the involvement of FoxO3A in

various mitochondrial functions, such as ROS detoxification, mitochondrial fission, biogenesis and morphology control (Ferber et al. 2012: Zhou et al., 2017). As an example, upon hypoxia, the increase of the mitochondrial ROS production required for the stabilisation of HIF-1α induces FoxO3A activation, which counteracts the hypoxia-dependent ROS increase and the accumulation of HIF-1α, through the modulation of c-Myc stability (Ferber et al., 2012).

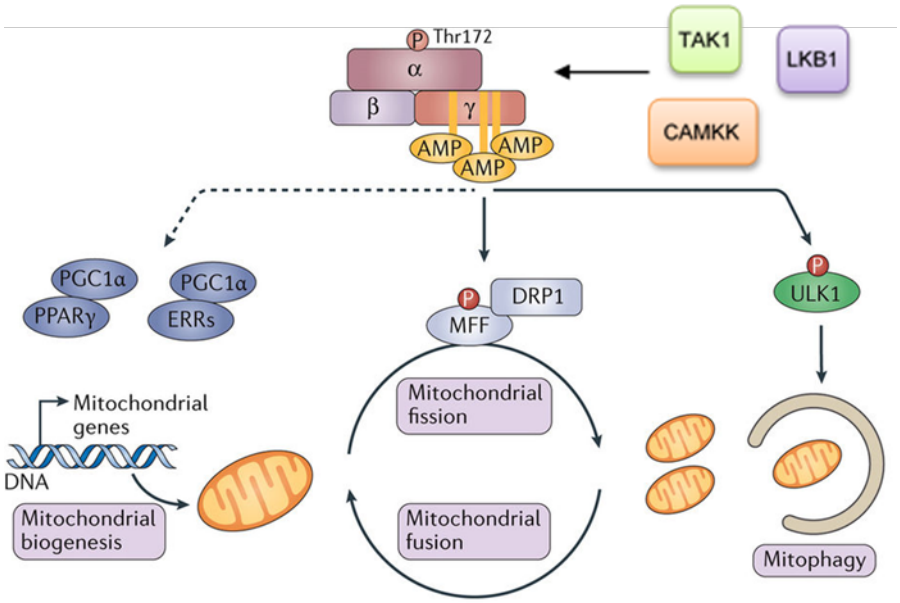


***Figure 1.15–****Mitochondrial target of AMPK.*

*AMPK phosphorylates mitochondrial fission factor (MFF) to regulate mitochondrial fission, which is required to degrade damaged mitochondria by mitophagy. During energy stress, AMPK also activates mitochondrial biogenesis genes through interaction with proliferator-activated receptor-γ PPARγ or oestrogen-related receptors (ERRs), though the co-activator 1α (PGC1α). Adapted from Herzig and Shaw, 2017.*

Recent studies have focused on the ability of AMPK to promote mitochondrial homeostasis, by regulating mitochondrial fission, mitophagy and transcriptional control of mitochondrial biogenesis, upon stress conditions (Herzig and Shaw, 2017). Furthermore, the presence of substrates of AMPK in the mitochondrial outer membrane, the mitochondrial fission factor (MFF) and the acetyl-CoA carboxylase 2 (ACC2), suggests that a pool of freely floating cytosolic AMPK can localise at least close to mitochondria in response to changes in energy status (Figure 1.15). In support of this hypothesis, it has recently been observed that a myristoylated form of AMPK is recruited to the mitochondria in response to mitochondrial damage, to mediate autophagy-dependent mitochondrial removal (Liang et al., 2015).

The mitochondrial AMPK-FoxO3A axis can modulate the balance between oxidative phosphorylation and glycolysis in response to metabolic stress (Peserico et al., 2013). Recently, a mitochondrial fraction of FoxO3A has been proposed (Jacob et al., 2008; Peserico et al., 2013; Caballero-Caballero et al., 2013). In mammalian cells -myotubes and fibroblasts -, FoxO3A can accumulate into the mitochondria upon glucose restriction (GR) (Peserico et al. 2013). This event requires AMPK activation, which is regulated by nutrient conditions, through the energy sensor pathway. Inside the organelles, FoxO3A physically interacts with mtRNA Polymerase and SIRT3, the main mitochondrial Sirtuin (Schwer et al., 2002).

SIRT3 is a soluble mitochondrial protein highly expressed in tissues rich in mitochondria, such as muscle and liver (Lombard et al., 2007). It is expressed as a full-length 44kDa protein that is targeted to the mitochondria by its N-terminal

localisation sequence (Schwer et al., 2002). The long form of SIRT3, located in the nucleus, has been considered as an inactive precursor for a long time. The importance of its nuclear form of SIRT3 is related to ROS detoxification activity (Sundaresan et al., 2008). The long form of SIRT3 is transported from the cytosol to the mitochondrial matrix, where the mitochondrial matrix processing peptidase (MPP) releases a cleaved 28kDa protein. In the mitochondria, SIRT3 regulates a plethora of functions (Alhazzazi et al. 2014, Haigis et al. 2010). It is primarily involved in the control of global mitochondrial protein acetylation (Lombard et al. 2007) in ATP production (Ahn et al. 2008), anti-oxidative response (Huang et al. 2010, Schwer and Verdin, 2008) cell death (Sundaresan et al., 2008; Allison et al., 2007; Verma et al.,2013) and human longevity (Park et al., 2013). Importantly, SIRT3 opposes the Warburg effect in cancer cells through HIF-1α destabilization (Finley et al., 2011). Interestingly, also for SIRT3, a dual role in tumour suppression and tumour promotion is still under intense debate (Alhazzazi et al., 2011; Chen et al., 2014). Indeed it seems to operate as both a tumour suppressive and oncogenic factors depending on the conditions. As an example, loss of SIRT3 induces a tumorigenic phenotype *in vivo* (Ferber et al., 2012), and SIRT3 KO mice spontaneously form oestrogen/progesterone receptors (ER/PR)-positive mammary tumours later in life (Ferber et al., 2012). Interestingly, SIRT3 levels are decreased in human breast cancer (Desouki et al., 2014), and this event is associated with poor prognosis in breast cancer patients. In contrast, SIRT3 is over-expressed in several human oral cancer cells, as an example in the Oral Squamous Cell Carcinoma (OSCC) where its down-regulation inhibits cancer cell growth and proliferation (Alhazzazi et al., 2011; Torrens-Mas et al., 2017).

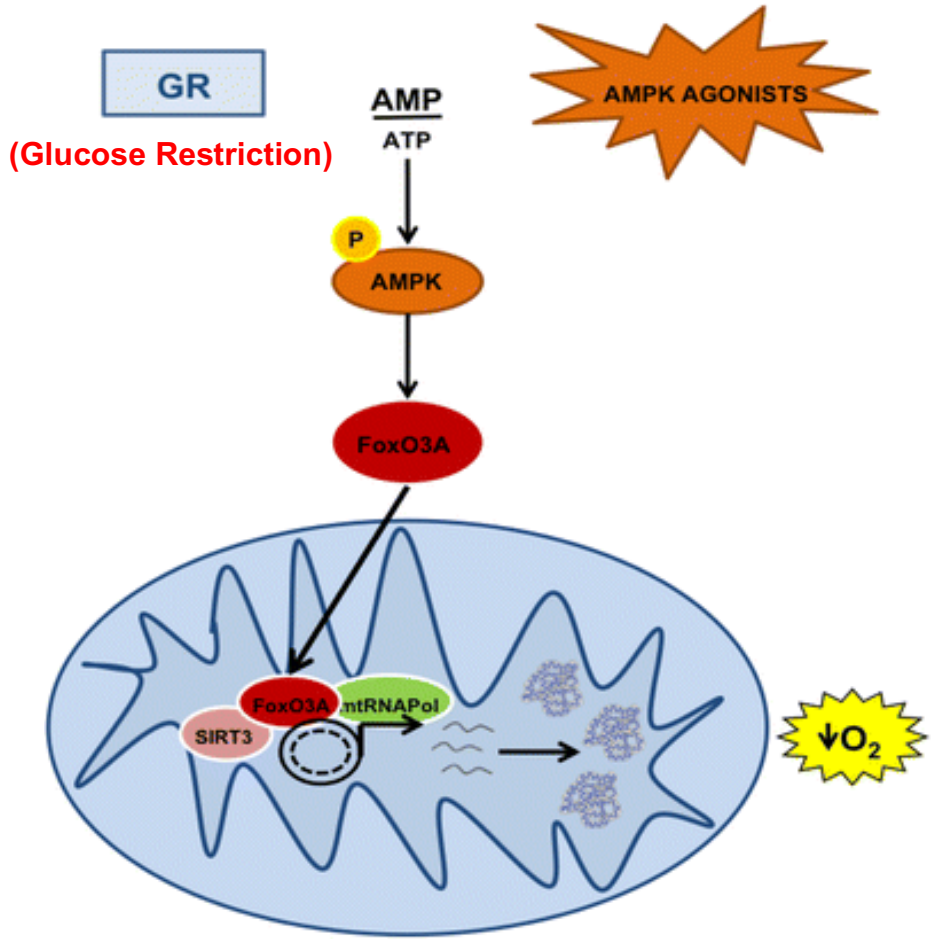


***Figure 1.16 -*** *The mitochondrial arm of AMPK-FoxO3A pathway.*

*The mitochondrial AMPK-FoxO3A-SIRT3 pathway induces mitochondrial transcription and respiration upon glucose restriction. Adapted from Peserico et al., 2013.*

Remarkably, the SIRT3-FoxO3A mitochondrial interaction allows the formation of a FoxO3A-SIRT3-mtRNAPol complex, which binds the mtDNA and activates the transcription of mitochondrial-encoded catalytic subunits of the OXPHOS machinery (Jacob et al., 2008; Peserico et al., 2013). Therefore, this event results in increased respiration and cell energy metabolism support. Importantly, accordingly to the proposed role of acetylation in the impairment of FoxO-chromatin interaction

in the nucleus, SIRT3 activity is required for FoxO3A recruitment on FHRE sites in the D-loop regulatory region and mtDNA binding. Notably, SIRT3 is not required for FoxO3A mitochondrial localisation (Figure 1.16).

# Chapter 2 - Aims

# 2 Aims

FoxO transcription factors are involved in several cellular processes, including proliferation, apoptosis, stress resistance and metabolism. Their activity is finely regulated through specific post-translational modifications functioning as a "molecular FoxO code". Recently, it has been described a novel mitochondrial arm of the AMPK-FoxO3A axis acting as a recovery mechanism to sustain energy metabolism upon nutrient shortage.

The research programme of my PhD is aimed to deepen the mechanisms underlying FoxO3A mitochondrial localisation and activity, through the identification of molecular mediators and partners involved. Considering the well-establish role of nuclear FoxO3A as a tumour suppressor, and its emerging function as a tumour cell migration and proliferation promoter, which is still under debate, the study is pointed to understand the role of mitochondrial FoxO3A in cancer cells and its possible contribution to nuclear FoxO3A activity. Data collected will be instrumental in devising novel pharmacological strategies aimed at manipulating cellular metabolism to counteract cancer.

# Chapter 3–Material and Methods

# 3 Material and methods

## 3.1 Experimental model and subject details

### 3.1.1 Cells culture and reagents

NIH3T3, MEFs, HEK293, HT29, IMR90, HeLa, LS174T, SW-480, Caco2, MDA-MB-468, BT474, OVCAR3, A549 and DU145 cells were obtained from the American Type Culture Collection (ATCC). EFM19 cells were obtained from the Leibniz-Institute DSMZ. NIH-3T3 and MEF: murine fibroblasts. HEK293: human kidney epithelial cells. IMR90: human lung normal. , LS174T, SW-480, Caco2, HT29, and HCT116: human colorectal cancer; MDA-MB-468, BT474 and EFM19: human breast cancer. OVCAR3: human ovarian carcinoma. A549: human lung adenocarcinoma. DU145: human prostate cancer.

HT29 Rho0 were kindly provided from Dr. Gaetano Villani's Lab (University of Bari – Department of medical sciences, neurosciences and sense organs). HCT116 FoxO3A$^{-/-}$ were generated for this project.

HCT116, HCT116 FoxO3A$^{-/-}$,NIH3T3, MEFs, HT29, HT29 Rho0, IMR90, HeLa, LS174T, MDA-MB-468, OVCAR3, A549 and SW-480 cells were cultured in DMEM high glucose (HG), without pyruvate (Gibco) with 10% FBS (Gibco) and 100 IU/ml penicillin-streptomycin (Gibco). BT474, EFM19 and Caco2 cells were maintained in the same conditions with 5% and 20% FBS, respectively. HEK293 cells were supplemented with 1% each of pyruvate and non-essential

amminoacids (NEAA, Sigma). DU145 cells were cultured in RPMI high glucose (HG), without pyruvate (Gibco) with 10% FBS (Gibco) and 100 IU/ml penicillin-streptomycin (Gibco). All media were prepared with 100 IU/ml penicillin and 100 µg/ml streptomycin, and cells were grown in a humidified incubator at 37°C and 5% $CO_2$ avoiding confluence at any time. All cell lines were glucose restricted by using DMEM containing 0.75 mM glucose (LG, low glucose). The final glucose concentration in the HG and LG medium should be considered as 40 and 15.75 mM, respectively (according to Li and Tollefson, 2011).

Compound C, PD98059, 2-Deoxy-D-glucose (2DG), Iodoacetic acid (IA), Metformin (MET), 5-Fluorouracile (5-FU), Cisplatin (cis-diammineplatinum dichloride, CDDP), Etoposide (VP-16), Irinotecan (CTP-11) and Nicotinamide (NAM) were purchased from SIGMA. Trametinib was from Selleckchem.

### 3.1.2 Animal husbandry

For *in vivo* studies reported in paragraph 4.7, C57/Bl6J male strain mice were bred on a 12-hour light/dark cycle and fed with standard diet. 8-10-week-old mice were divided in two experimental groups (fed/fasted) including at least five mice: free food access group (fed) and 18-hour fasted group. To minimize the effect of circadian variation on gene expression profile, mice were sacrificed at the beginning of the light cycle. Brain, kidney, lung, pancreas, colon, and liver were chopped into small pieces with a razor blade and then disaggregated using a Medimachine (Becton Dickinson). Cells were harvested and processed for total protein analysis and/or mitochondria isolation, as previously described (Frezza et al. 2007) and as briefly explained in the section 3.2.4.

For *in vivo* studies reported in the sections 4.2.5 and 4.3.3-5, female CD-1 athymic nude mice (6-8-week-old) were obtained from Charles River Laboratories. To develop xenograft tumours, $10x10^6$ HCT116 cells were injected subcutaneously into the flanks (0.2 ml per flank) of CD-1 mice. The volume of the tumours was measured every 2–3 days and calculated using the following formula:

$$volume\ (mm^3) = width^2\ *\ lenght *\ 0.5.$$

When the tumour volume reached 60 $mm^3$, mice were randomized into different treatment groups. Cisplatin (2 mg/kg) or 2-deoxygluocose (100 mg/kg) were given intra-peritoneally once every three days. Control groups received the vehicle only (normal saline). Mice were treated twice every 3 days. At the end of the treatment, mice were sacrificed and tumours explanted for immunoblot analysis. Animals were maintained in the animal colony at the University of Bari, following the institutional guidelines, in compliance with national, international laws, and policies. *In vivo* studies were performed in collaboration with Dr. Gadaleta and Dr. Scialpi of the Laboratory of "Medicina Interna Universitaria Frugoni", at the Department of Interdisciplinary Medicine of University of Bari Aldo Moro.

### 3.1.3 Bacterial strains

NEB5-alpha bacterial strains were grown in Luria-Bertani (LB) medium (Tryptone, Yeast extract and NaCl, Sigma) in the presence of Ampicillin (25 μg/ml, Sigma). Briefly, liquid LB was added to a 500 ml Erlenmeyer flask and the appropriate antibiotic to the correct concentration was added. With a sterile pipette tip, a single colony from each experimental agar plate was selected and the tip was

dropped into the Erlenmeyer flask and swirl. The culture was loosely covered with sterile aluminum foil and incubated at 37°C for 12-18 hours in a shaking incubator.

## 3.2 Methods Details

### 3.2.1 Cloning

The plasmids described in the manuscript were obtained, with specific primers, as previously described (Nakatani et al., 2003). Briefly, to prepare vector DNA for cloning, 2-5 μg vector DNA were digested by using restriction enzymes needed for the insert DNA. Then, gel purification of digested vector DNA was performed. To prepare insert DNA for cloning by using PCR, primers are been designed and obtained from CARLO ERBA Reagents S.r.l. Insert DNA was amplified from a template by PCR. Gel purification of insert DNA was performed. Ligation of insert and vector reaction was performed by using 1 mole of vector and 5 or more moles of insert, at 37°C for 30 minutes. Then, chemically competent cells (NEB 5-alpha Competent *E. coli*) were tarsformed with 1 μl ligation product by using heat-shock method. Briefly, after a short incubation in ice, a mixture of chemically competent bacteria and the ligation product is placed at 42°C for 90 seconds and then placed back in ice. Thus, the mixture is spread on LB agar plates with Ampicillin (25 μg/ml) and incubated at 37°C overnight. About 12-16 hours later colonies are picked. To screen for plasmids carrying the correct insert, colony PCR and consequent sequencing of the plasmid.was perfomed.

Site-directed mutagenesis was performed using the Q5® Site-Directed Mutagenesis Kit (New England Biolabs) according to the manufacturer's

instructions. Briefly, double-stranded plasmid DNA is exponentially amplified using standard primers and a master mix formulation of Q5 Hot Start High-Fidelity DNA Polymerase. The product is then incubated with an enzyme mix (containing a kinase, a ligase and DpnI) to allow the circularization of the PCR product and removal of the template DNA. Thus, chemically competent cells (NEB 5-alpha Competent *E. coli*) are transformed with the PCR product.

A list of the constructs generated and/or used in this thesis, as well as the list of site-directed mutagenesis primer sequences used are available in Appendix Tables 1 and 2.

### 3.2.2 Cell transfection and RNA interference

HCT116, HCT116 FoxO3A$^{-/-}$ and HEK293 cells were transiently transfected with mammalian expression plasmids using TransIT-LT1 Transfection Reagent (Mirus) according to the manufacturer's instruction.

For RNA interference, HCT116 cells were transfected with 50 nM validated Silencer® Select Pre-Designed siRNA (Thermo Fisher Scientific) directed against FoxO3A by using the HiPerfect reagent (QIAGEN) according to the manufacturer's instructions. On-TARGET-plus control siRNAs (Thermo Scientific) were used as a non-silencing negative control. siRNA sequences used in this study:

FoxO3A siRNA1: 5' CUCACUUCGGACUCACUUAtt 3',
5' UAAGUGAGUCCGAAGUGAGca 3'

FoxO3A siRNA2: 5' GCCUUGUCGAAUUCUGUCAtt 3',
5'UGACAGAAUUCGACAAGGCac 3'

### 3.2.3 Protein expression and purification

NEB5-alpha bacterial strains transformed with different pGEX-4T3-GST-FoxO3A constructs were grown in Luria Bertani medium in the presence of Ampicillin (25 μg/ml, Sigma). When bacteria reached the optical density of 0.6 (exponential growth phase), they were induced with 0.5 mM IPTG at 37°C, for 4 hours. Cells were then collected by centrifugation and pellets were lysed with B-PER lysis buffer (Thermo Fisher), according to the manufacturer's instructions. Then, the lysate was centrifuged at 15.000 x g for 5 min at 4°C. Recombinant protein expression was confirmed by SDS-PAGE. GST-fused proteins were purified by affinity chromatography using the GST Bulk Kit (GE Healthcare) according to the manufacturer's instructions. Briefly, Glutathione Sepharose slurry is resuspended and transferred to the appropriate tube. After slurry draining, the Glutathione Sepharose is washed by adding PBS. Thus, the sample is applied to the column and 2 washes with binding buffer are performed. Then, the protein is eluted by applying the elution buffer to the column. The obtained product were evaluated and quantified by SDS–PAGE.

### 3.2.4 Mitochondria isolation and treatment

Mitochondria-enriched fractions were obtained as previously described (Frezza et al., 2007). Briefly, cells were harvested and centrifuged at 600g at 4 °C for 10 min. Then, the pelleted cells were re-suspended in ice-cold IBc buffer (0.1M Tris–MOPS, 0.1M EGTA/Tris, 1 M sucrose) and homogenized by using a Teflon-glass pestle. The homogenate was centrifuged at 600 xg for 10 min at 4 °C and the supernatant was collected and centrifuged at 7,000 x g for 10 min at 4 °C. The pellet

was re-suspended in ice-cold IBc and centrifuged at 7,000 xg for 10 min at 4 °C. Eventually, the obtained mitochondria were treated with proteinase K 4 U/ml (Ambion) in order to degrade the outer mitochondrial membrane protein and/or TritonX-100 (0.25%) and analysed by immunoblotting. Notably, TritonX-100 tratment is performed as control of antibody specificity.

### 3.2.5 Proteinase K protection assay

Mitochondrial fractions, obtained as described in section 3.2.4, were re-suspended in an isotonic buffer (0.1M Tris–MOPS, 0.1M EGTA/Tris, 1 M sucrose) and incubated with various concentrations of proteinase K (1, 10 or 50 μg/ml, PK) for 20 minutes on ice, to minimize the enzymatic effect of PK.

Specifically, increasing concentrations of PK were used to degrade each layers of mitochondria. Memebrane degradation was followed by using specific mitochondrial markers. Digestion was stopped by adding 2 mM phenylmethylsulfonyl fluoride (PMSF) to the samples (Ryan et al., 2001). Mitochondrial proteins were analysed by immunoblot.

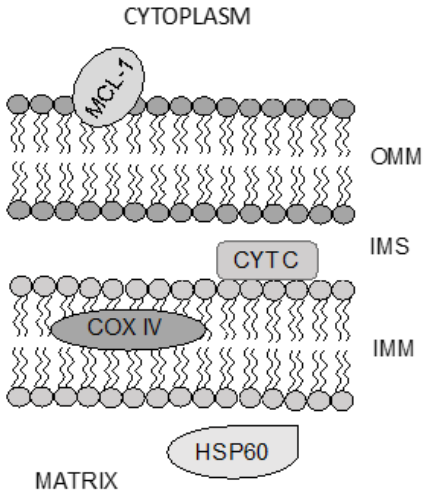


***Figure 2.1**–Proteinase K (PK) protection assay.*

*MCL1: outer membrane marker; CYTOCHROME C: inter-membrane space marker; COX4: inner membrane marker; VDAC1: inner membrane marker; HSP60: matrix marker.*

### 3.2.6 Mitochondrial swelling experiments

Mitochondrial fractions obtained as described in section 3.2.4 were re-suspended in a hypotonic buffer (10 mM MOPS-KOH) and incubated on ice for 15 min (Ryan et al., 2001). To obtain mitoplasts, part of the samples was incubated with proteinase K (25 µg/ml), on ice, for 20 min. To stop the protease activity, 2 mM PMSF was added. Mitochondria and mitoplasts were re-centrifuged at 7,000 xg for 10 min at 4 °C and analysed by SDS-PAGE.

### 3.2.7 Nuclear extraction

Nuclear extraction was performed using Nuclear Extraction Kit according to the manufacturer's instructions (#ab113474, Abcam, Cambridge, MA). Briefly, cells were grown to 70-80% confluency on a 100 mm culture plate. Then, the growth medium was removed and cells were washed twice with PBS. Then, 3 mL of fresh PBS were added to the plate and cells were scraped in a 15 mL tube and centrifuged for 5 minutes at 1000 rpm. Once discarded the supernatant, the pellet was resuspended in 100µL of 1X Pre-Extraction Buffer (per $10^6$) cells, and transferred to a micro-centrifuge vial. Then, the sample was incubated on ice for 10 min., vortexed vigorously for 10 seconds and centrifuged for 1 minute at 12,000 rpm. The supernant were recovered as cytoplasmic extract, while the pellet was recovered as nuclear one. The protein fractions were analysed by western blot.

### 3.2.8 Chromatin immunoprecipitation (ChIP)

To perform the Chromatin Immunoprecipitation of mitochondrial DNA, mitochondrial fractions obtained as described in section 3.2.4, were processed to eliminate genomic DNA contamination. Specifically, DNase I (Ambion, 4 U/100 mg wet mitochondria, 10 min, 4°C), was added to the mitochondrial fractions re-suspended in ice-cold IBc buffer (0.1M Tris–MOPS, 0.1M EGTA/Tris, 1 M sucrose) in the presence of 2.5 mM $MgCl_2$.The reaction was stopped by the adding of EDTA (final concentration 50 mM) into the mixture. Further ChIP analysis was performed as previously described (Peserico et al. 2013). Briefly, formaldehyde (Sigma) was added directly to mitochondrial fraction to a final concentration of 1%. Cross-linking was allowed to proceed for 15 min at room temperature and then stopped by the addition of glycine (Sigma) to a final concentration of 0.125 M. Cross-linked mitochondria were lysed in CLB buffer (10 mM Tris pH 8.0, 10 mM NaCl, 0.2 % NP40) plus protease inhibitors (Roche). Then, the mitochondrial fraction was enriched by differential micro-centrifugation. The chromatin solution was sonicated, cleared by centrifugation and the supernatant was divided into aliquots. 1% of the supernatant was taken as input. Four micrograms of antibody for each experimental group were used to immunoprecipitate chromatin-bound complexes. Immunoprecipitation was performed on a rotating platform overnight at 4°C with the indicated antibodies. IgG was used as unrelated antibodies. Immuno-complexes were pulled down using protein G (GE-healthcare). Following extensive washing, bound DNA was reverse cross-linked, purified using phenol:chloroform (Sigma) and analysed by quantitative real-time PCR.

ChIP assays on nuclear DNA were performed using the MAGnify Chromatin Immunoprecipitation System (Life Technologies) according to the manufacturer's instructions. Briefly, adherent cells (100 mm dish) were washed with PBS twice and then they were treated with with formaldehyde 37% (final concentration 1%) to generate protein-protein and protein-DNA crosslinks between molecules in close proximity within the chromatin complex. The cross-linking reaction was stopped by adding 1.25 M glycine. Then the sample was lysed by adding PBS twice and by performing centrifuge. Therefore, the cells were lysed, by adding Lysis Buffer with Protease Inhibitors to the cell pellet obtained from the previous step. Thus, the chromatin was released from the nuclei and sheared by sonication to reduce the average DNA fragment size to 200–500 bp for analysis by quantitative real-time PCR (qPCR) or 100–300 bp for analysis by massive parallel DNA sequencing. In order to immunoprecipitate and isolate the crosslinked protein of interest, specific ChIP-qualified antibodies conjugated to Dynabeads® Protein A/G were used. Specifically, 1 µg of indicated antibodies were used for each assay.IgG antibodies, used as ChIp-control, were included in the kit. The formaldehyde crosslinking was reversed by heat treatment, specifically by incubating the samples tubes and the input control tubes at 55°C for 15 minutes in a thermal cycler. Finally, the DNA associated with that protein was purified by adding DNA Purification Buffer to the sample and the, after sequential washing with DNA Washing Buffer, by eluting DNA by addinf DNA Elution Buffer. The obtained DNA DNA was analysed by quantitative real-time and PCR Primer sequences used are available in Appendix Table 5.

### 3.2.9 *In vitro* kinase assays

Purified AMPK (Millipore) and/or ERK (Active Motif) were incubated with various recombinant substrates (0.5 μg) in kinase reaction buffer [HEPES (32 mM) pH 7.4, dithiothreitol (650 μM), $Mg(CH_3COO)_2$ (10 mM), BriJ-35 (0,012%), non-radioactive ATP (50 μM)] and 0,9-1,8 μCi of [γ-32P]ATP (Perkin Elmer), at 30°C for 30 min. For AMPK, AMP (100 μM) was added to the reaction. Phosphorylation was detected by incorporation of radiolabeled [γ-32P] ATP. Radioactivity-Based Assays were performed in collaboration with Dr. Signorile and Dr. De Rasmo of the Department of Basic Medical Sciences, Neurosciences and Sense Organs, at the University of Bari Aldo Moro,

### 3.2.10 Immunoblotting

Protein extracts were obtained by treating cells or mitochondrial fractions with total lysis buffer (50 mM Tris-HCl pH 7.4, 250 mM NaCl, 5 mM EDTA, 0,1% TritonX-100, 1 mM DTT, 1 mM PMSF) supplemented with protease and phosphatase inhibitors (Roche). Protein concentration was determined using the Micro BCA Protein Assay Kit (Thermo Fisher), Briefly, Micro BCA Working Solution is prepared as instructed by the manufacturer. Then, 1 μl of protein lysate is diluted in 499 μl of diluent buffer and thus 500 μl of Micro BCA Working Solution is added to the tube. After 60 min incubation at 65°C, absorbance was read at 562 nm for each of the experimental samples. Protein concentrations were determined by using a Micro BCA-standard curve previously generated.

SDS gels consisted of a lower resolving gel and an upper stacking gel, were made using the acrylmide/bis stock solution. 25% percent ammonium persulphate

(APS) and Tetramethylethylenediamine (TEMED) were used as polymerisation catalysts. The percentage of the resolving gel used depended on the size of the protein of interest -Lower percentage gels are used in case of proteins of higher molecular weight and vice versa. To separate the proteins, 15-20 μg of protein lysate was added to an equal volume of 5X SDS loading buffer [4% (w/v) SDS, % (v/v) glycerol, 0.01% (w/v) bromophenol blue] and boiled for 5 minutes at 95ºC. Samples were then spin-down and the appropriate volume of sample was loaded into the gel wells. SDS-PAGE gels were run in running buffer (BIORAD) at 80V through the stacking gel and then 150V through the resolving gel. Once the proteins had been separated by SDS-PAGE, proteins were electrotransferred on nitrocellulose membranes (GE Healthcare) by using Trans-Blot TurboTransfer System (BIORAD) for 7-10 minutes. Accordingly on antibodies' requirement, membranes were then blocked in either 5% milk or 5% Bovine Serum albumin (BSA) in TBS plus 1% Tween (TBST) for 45 minutes at room temperature and then incubated with specific primary antibodies (see Appendix Table 3) for 16 hours at 4°C. Membranes were then washed every 10 minutes with 5 ml of TBST for 30 minutes at room temperature. They were then incubated with their respective peroxide-conjugated secondary antibody (anti-rabbit or anti-mouse – see Appendix Table 3) for one hour at room temperature. The membranes were then washed every 10 minutes with 5 ml of TBST for 30 minutes at room temperature.

The membranes were developed with the ECL-plus chemiluminescence reagent (GE Healthcare) in ChemiDoc™ Touch Imaging System (BIORAD), as manufacturer's instructions. The densitometric evaluation was performed by ImageJ software.

### 3.2.11 Microscopic quantification of viability and cell death

Cell viability and cell death of the reported cell lines were scored by counting, as previously described (Germani et al. 2014). Briefly, the supernatants (containing dead/floating cells) were collected, and the remaining adherent cells were detached by Trypsin/EDTA (SIGMA). Cell pellets were resuspended in 1X PBS and an aliquote (10 µl) was mixed with an equal volume of 0.01% Trypan blue solution for cell counting. Viable cells (unstained, Trypan blue negative cells) and dead cells (stained, Trypan blue positive cells) were counted with a phase contrast microscope. The percentages of viable and dead cells were calculated, as below:

$$Cell\ viability/control = \frac{(Average\ of\ viable\ cells)_{sample}}{(Average\ of\ viable\ cells)_{control}} * 100$$

$$Cell\ death/control = \frac{(Average\ of\ death\ cells)_{sample}}{(Average\ of\ death\ cells)_{control}} * 100$$

### 3.2.12 Immuno-gold labelling

The immuno-gold labelling assay was performed as previously described (Peserico et al. 2013). Briefly, cells were fixed with 4% formaldehyde and 0.005% glutaraldehyde, rinsed with PBS, incubated with the primary antibody overnight, and then with Nanogold conjugated Fab fragments of the secondary antibodies (Nanoprobes) for 2 hours. Nanogold particles were developed using the Goldenhance kit (Nanoprobes). TEM images were acquired from thin sections under a Philips Tecnai 10/12 electron microscope (Philips) using an ULTRA VIEW CCD digital camera (Soft Imaging Systems GmbH). Quantification of gold particles was carried out using the AnalySIS software (Soft Imaging Systems

GmbH). For each experimental condition, 20 cells were analysed. In each cell, 15 areas (mean[3]* $10^6$ $nm^2$) were randomly selected. Data presented in the Results section were obtained by scoring the percentage of FoxO3A-positive cells and counting the number of gold particles per single mitochondria. Immuno-gold labelling analyses were performed in collaboration with the Advanced Light and Electron Microscopy Facility of the Consorzio Mario Negri Sud (Santa Maria Imbaro, Chieti, Italy).

### 3.2.13 Real-time PCR

RNA extraction and real-time PCR were performed as previously described (Peserico et al. 2014). Briefly, total RNA was extracted with Trizol reagent (Invitrogen) following manufacturer's instructions. Samples were then treated with DNase-1 (Ambion) and 4 µg of total RNA was retro-transcribed using iScript™ cDNA Synthesis Kit (BIORAD) following manufacturer's instructions. cDNAs were used as template and gene expression was measured using RT-qPCR, which was performed using a QuantStudio3 Real-Time PCR System (Applied Biosystem), using the SYBR Green PCR Master Mix (BIORAD) according the the manufacturers instructions. As a control the established housekeeping genes were used to normalise gene expression between samples. The reaction mix contained 1,5 µl of sample and 7,5 µl of SYBR PCR Master Mix, primers and water were added to a final volume of 10 µl. All measurements were performed in triplicate. Relative quantification was performed by using the ΔΔCt method. Primer sequences used in this study are listed in Appendix Table 4.

### 3.2.14 Co-immunoprecipitation (Co-IP)

For co-IP, cells or mitochondria were lysed in IP lysis buffer (50 mM Tris HCl pH 7.4, 250 mM NaCl, 5 mM EDTA, 0,1% TritonX-100), supplemented with protease inhibitors (Pierce). Lysates were cleared by centrifugation and incubated overnight at 4°C with 1 µg of anti-FLAG, anti-FoxO3A, anti-SIRT3, anti-acetylLysine and/or IgG covalently bound to Protein G-Sepharose (GE Healtcare)/Protein A-Sepharose (GE Healtcare). Immunocomplexes were washed twice with IP lysis buffer, boiled in 5X SDS loading buffer [4% (w/v) SDS, % (v/v) glycerol, 0.01% (w/v) bromophenol blue] and boiled for 5 minutes at 95ºC. Samples were analysed by immunoblot as described in section 3.2.

### 3.2.15 Deacetylation assay

The deacetylation assay was performed as previously described (Hirschey et al. 2009). Briefly, the mitochondrial fraction isolated from HCT116 previously transfected with p3x-CMV14-FoxO3A-FLAG was immune-precipitated with anti-FLAG antibody and then incubated with GST-SIRT3 recombinant protein, in presence/absence of Sirtuin inhibitor Nicotinamide (NAM, 10 mM). Subsequently immunocomplexes were washed twice with IP lysis buffer (50 mM Tris HCl pH 7.4, 250 mM NaCl, 5 mM EDTA, 0,1% TritonX-100), boiled for 5 minutes at 95ºC. Samples were analysed by immunoblot as described in section 3.2.

### 3.2.16 Prediction analysis

Analysis of the N-terminal region of FoxO3A (corresponding to positions 1-148) was performed using the NetPhos (available at

http://www.cbs.dtu.dk/services/NetPhos) and DISPHOS 1.2 (available at http://www.dabi.temple.edu/disphos)prediction tools. The KinasePhos 2.0prediction server (available at http://kinasephos.mbc.nctu.edu.tw)was employed in consensus phosphorylation motifs investigation.

### 3.2.17 Citotoxicity assay

Citotoxicity assays were performed as previously described (Germani et al. 2014). Briefly, $1^{*}10^{5}$ cells were seeded in 60 mm dishes and after 24 hours they were treated with the indicated drugs. After 24 hours, media were discarded and cells were washed twice with 1X PBS. Therefore, 2 ml of Coomassie brilliant blue (Bradford) were added into each dish for 5 minutes. Eventually, cells were washed with ethanol 70% to remove the excess of Coomassie. Plates were dried at room temperature. Percent cell growth-inhibition at each concentration was quantified by densitometric evaluation using ImageJ software.

### 3.2.18 Mitochondrial membrane potential assay (TMRE staining) and immunofluorescence

Mitochondrial membrane potential assay was performed using tetramethylrhodamine ethyl ester perchlorate (TMRE, Sigma), according to the manufacturer's instructions. Nuclei were counterstained using DAPI (300 nM in PBS, Invitrogen).

HCT116 FoxO3A$^{-/-}$ cells were transiently transfected with eGFP-tagged mammalian expression plasmids. After transfection and treatment with the indicated drugs, cells were fixed with 4% paraformaldehyde, permeabilized with

1% TritonX-100, and then stained as described above. Nuclei were counterstained using DAPI (300 nM in PBS, Invitrogen).

Images were acquired using an Axio Observer Z1 microscope (Zeiss) in single-plan. For both TMRE staining and immunofluorescence, quantification of mitochondrial TMRE fluorescence in GFP+ cells was performed using ZEN imaging software (Zeiss). Moreover, for quantification of the staining, an area containing each staining signal was select and measured. Another set of measurements has been obtained from the same areas in a region outside the cell (background) and subtracted by the intensities previously measured. All the images contained in this manuscript have been obtained by using a 63X objective.

### 3.2.19 CRISPR/Cas9 genome editing system

The CRISPR/CAS9 reporter vector (GeneArt CRISPR Nuclease Vector Kit, Invitrogen) was used according to the manufacturer's instructions. Oligonucleotide sequences used to create the gRNA vector were designed to target the exon 2 of FoxO3A for "indel" mutation. The sequences are reported below:

*gRNA top strand oligo*: GTCTTCATCGTCCTCCTCCT

*gRNA bottom strand oligo*: AGGAGGAGGACGATGAAGAC

CHOPCHOP web tool was used for determining gRNAs off-targets. HCT116 cells were transfected using Lipofectamine 3000 (Thermo Fischer Scientific) according to the manufacturer's instruction. Isolation of clonal populations was performed with agarose-based cloning rings (Sigma). Cell clones were tested for site-specific deletions by PCR. Sequencing products were purified

using the Dye Ex 2.0 Spin Kit (QIAGEN) and sequenced on an ABI PRISM 310 Genetic Analyzer (Applied Biosystems). A scheme of gRNA location in FoxO3A locus, proto-spacer adjacent motifs (PAMs) and deleted region is reported in Figure 4.22.

### 3.2.20 Glucose restriction resistance assay

Glucose restriction resistance assays were performed on several cell lines. For each of them, a preliminary experiment was performed to determine the glucose restriction end-point. Specifically, $2.5 \times 10^4$ cells were plated for each cell line on a 12-well dish and switched 24 hours later to low glucose medium (0.75 mM glucose). Every 24 hours, the supernatants (containing dead/floating cells) were collected, and the remaining adherent cells were detached by Trypsin/EDTA (Sigma). Cell pellets were resuspended in 1X PBS and 10 µl were mixed with an equal volume of 0.01% trypan blue solution. Viable cells (unstained, trypan blue negative cells) and dead cells (stained, trypan blue positive cells) were counted with a phase contrast microscope. For each cell line, the glucose restriction end-point was established as the time point in which the amount of dead cells was at least 50% of the total. To investigate the correlation between glucose restriction resistance and FoxO3A protein levels, $2 \times 10^5$ cells were plated on 60-mm dishes and switched 24 hours later to low glucose medium (0.75 mM glucose). For each cell line, cells were harvested at the glucose restriction end-point preliminarily established as described above. Then, cell pellets were lysed and total proteins were analysed by immunoblot with a FoxO3A antibody. Densitometric evaluation of FoxO3A protein levels was performed by ImageJ software. The correlation index

between cell resistance (days) and FoxO3A protein levels was calculated by using Excel as:

$$Correl(X,Y) = \frac{\sum(x - x_m) * (y - y_m)}{\sqrt{\sum(x - x_m)^2} * \sqrt{\sum(y - y_m)^2}}$$

## 3.3 Quantification and statistical analysis

Results are expressed as mean ± SEM and n ≥ 3. Student's t test was used to define *p* values. A *p* value<0.05 was considered statistically significant. Multiple comparisons are accounted for via the Hochberg's method using PROC MULTTEST in SAS (Hochberg et al., 1988).

# Chapter 4 - Results

# 4 Results

## 4.1 The mitochondrial import and localisation of FoxO3A

Recently, it has been described a novel mitochondrial arm of the AMPK-FoxO3A axis in murine and human normal cells, and it is nutrient shortage-dependent (Peserico et al., 2013). Specifically, upon glucose restriction (GR) FoxO3A accumulates into the mitochondria in murine C2C12-derived myotubes and NIH-3T3 fibroblasts. In line with these findings, transmission electron microscope (TEM) analysis showed that specific immuno-gold signals revealed FoxO3A mitochondrial localisation also in metabolically stressed HeLa human cervix adenocarcinoma cells (Figure 4.1).

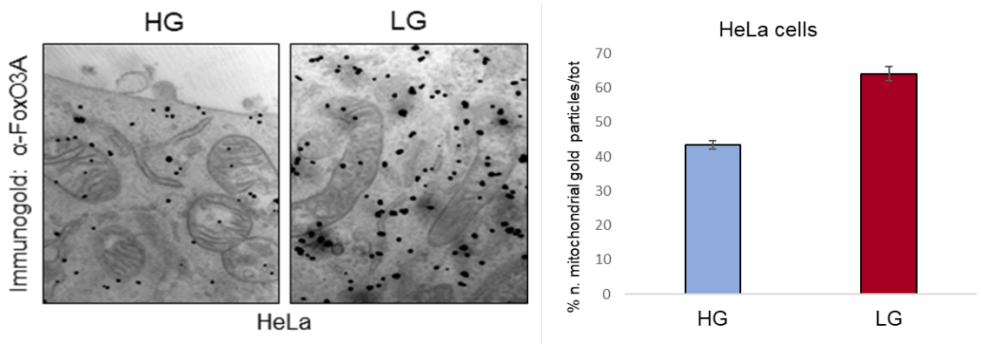


***Figure 4.1 -*** *FoxO3A accumulates into the mitochondria*

*Immuno-gold labelling of HeLa cells cultured in high glucose (HG) or switched to low glucose (LG, 0.75 mM glucose) for 24 h. On the left, black dots represent gold*

*particles recognizing FoxO3A immunocomplexes (Celestini et al., 2018). On the right, data were quantified by counting the number of gold particles per single mitochondria and scoring the total number of FoxO3A-positive particles.*

As the mitochondrial form of FoxO3A (mtFoxO3A) has been little explored (Jacob et al., 2008; Peserico et al., 2013; Caballero-Caballero et al., 2013), the mechanism underlying FoxO3A mitochondrial localisation is still not clear yet.

### 4.1.1 Characterization of the intra-mitochondrial form of FoxO3A

To characterise the mitochondrial translocation mechanism of FoxO3A, mitochondrial-enriched fractions have been isolated from several normal and cancer cell lines of different origin (Caco2, HT29, SW-480 and LS-174T: human colorectal cancer; HEK293: human kidney epithelial cells; BT474 and EFM19: human breast cancer; NIH-3T3 and MEF murine fibroblasts) for a deep molecular analysis. Since it has been reported that GR triggers FoxO3A accumulation into mitochondria of normal cells (Peserico et al. 2013), the selected cell lines were cultured in the presence of high (HG) or low (LG) glucose concentrations. Then, the mitochondrial fraction was processed by using a proteinase K (PK) protection assay to distinguish proteins localised at the outer membrane or inside the mitochondria. In LG conditions, anti-FoxO3A antibodies recognised two bands in the whole mitochondria fraction: one migrating at around 90kDa –the expected molecular weight of FoxO3A- and a second band migrating at around 70kDa. At the same time, the analysis of mitochondria treated with proteinase K detects only the 70kDa band into the organelles of all cell lines tested. These results indicate that FoxO3A antibodies recognised the full-length protein (resulting in the 90kDa band)

bound outside of the mitochondria and a shorter intra-mitochondrial form with the molecular weight of 70kDa (Figure 4.2). The obtained evidence was further confirmed by treating colorectal cancer cells (HCT116) with two diverse calorie restriction (CR) mimetics, 2-deoxyglucose (2DG) and iodoacetic acid (IA), that act by interfering with different limiting steps of the glycolytic cascade (Figure 4.3).

To ensure that these findings were not due to a cell culture artefact, mitochondria purified from different mouse tissues were analysed with anti-FoxO3A antibodies. Immunoblot images allowed to detect a migration pattern similar to the one obtained in human cancer cells (Figure 4.4a). Furthermore, to obtain an *in vivo* validation of these data, mitochondrial fractions purified from murine liver and kidney were treated with PK and analysed, demonstrating the presence of the FoxO3A full-length form on the outer mitochondrial membrane and the shorter 70kDa protein inside the organelles (Figure 4.4b). Notably, as it has been reported that FoxO3A co-localise into the mitochondria in complex with the NAD+¬-dependent deacetylase SIRT3 (Jacob et al., 2008; Peserico et al., 2013), its expression has been investigated in the same models, as a control (Figure 4.5).

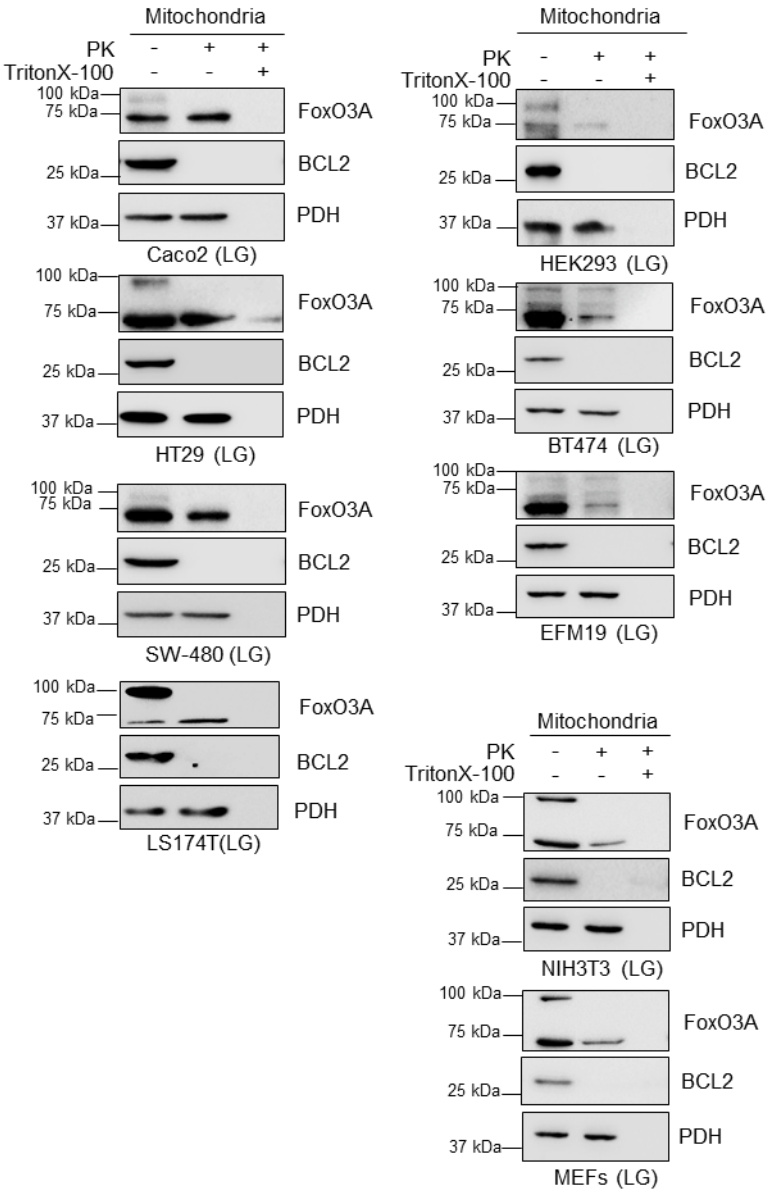


***Figure 4.2 -*** *FoxO3A accumulates into the mitochondria of glucose-restricted cells. Immunoblot analysis of mitochondrial fractions isolated from different cell lines (Caco2, HT29, SW-480 and LS-174T: human colorectal cancer; HEK293: human embryonic kidney epithelial cells; BT474 and EFM19: human breast cancer; NIH-3T3 and MEF murine fibroblasts) upon low glucose (LG, 0.75mM glucose) treatment. Mitochondrial fractions were treated with PK alone – in order to degrade the mitochondrial outer membrane proteins - or with PK and Triton X-100*

*to permeabilise mitochondria and degrade all mitochondrial proteins, as control of the antibody specificity. BCL2: outer membrane control; PDH: mitochondrial matrix control. The presented results are representative of at least three independent experiments (Celestini et al., 2018).*

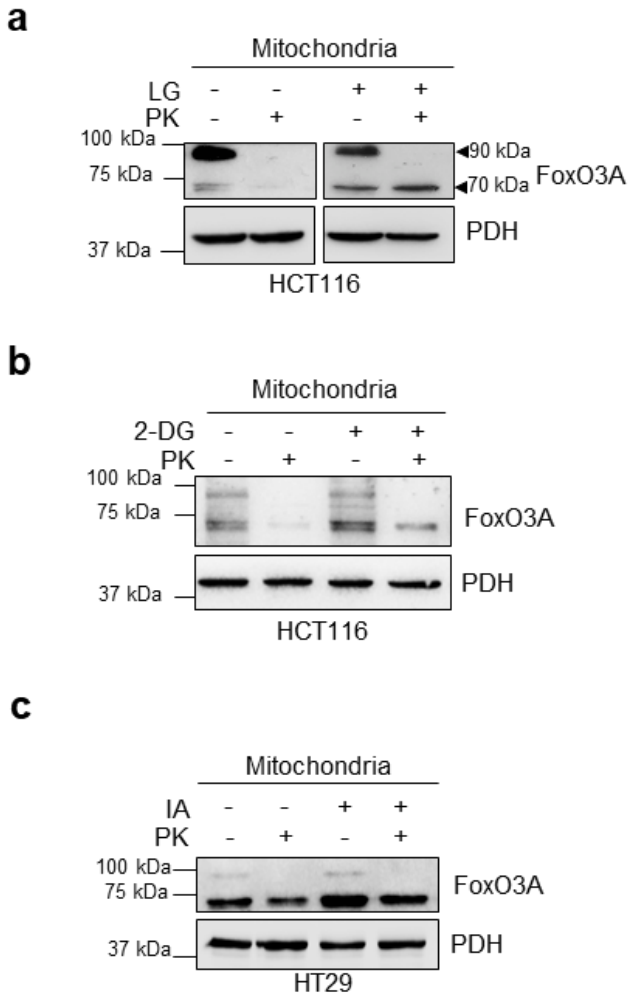


***Figure 4.3-*** *FoxO3Amitochondrial accumulation upon metabolic stress*

*Immunoblot analysis with the indicated antibodies of mitochondrial fractions isolated from HCT116 cells treated with (a) low glucose (LG, 0.75mM glucose) for 24 h, (b) 2-deoxy-glucose (2DG, 1 mM, 6 h) and (c) iodoacetic acid (IA, 0,5 mM, 5h), which are use as metabolic stress mimetics. Mitochondrial fractions were*

*treated with proteinase K (PK) to degrade outer mitochondrial membrane proteins. PDH: loading control. The presented results are representative of at least three independent experiments (Celestini et al., 2018)..*

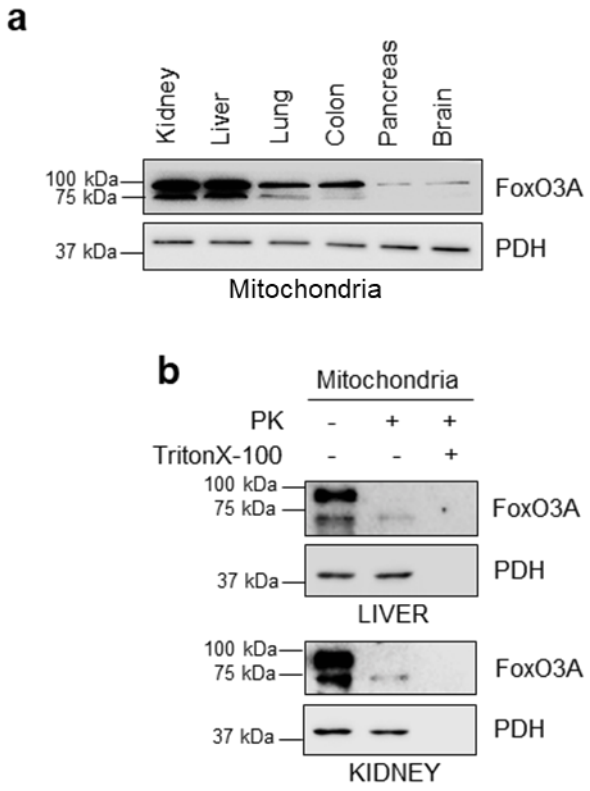


***Figure 4.4–****FoxO3Aaccumulates into murine mitochondria*

*(a) Immunoblot analysis of mitochondria purified from different murine organs with the indicated antibodies. PDH was used as a loading control. (b) Western blot analysis of mitochondria-enriched fractions isolated from murine kidney and liver. Mitochondrial samples were treated with PK alone – in order to degrade the mitochondrial outer membrane proteins - or with PK and Triton X-100 to permeabilise mitochondria and degrade all mitochondrial proteins, as control of the antibody specificity. PDH: mitochondrial matrix control. The presented results are representative of at least three independent experiments (Celestini et al., 2018).*

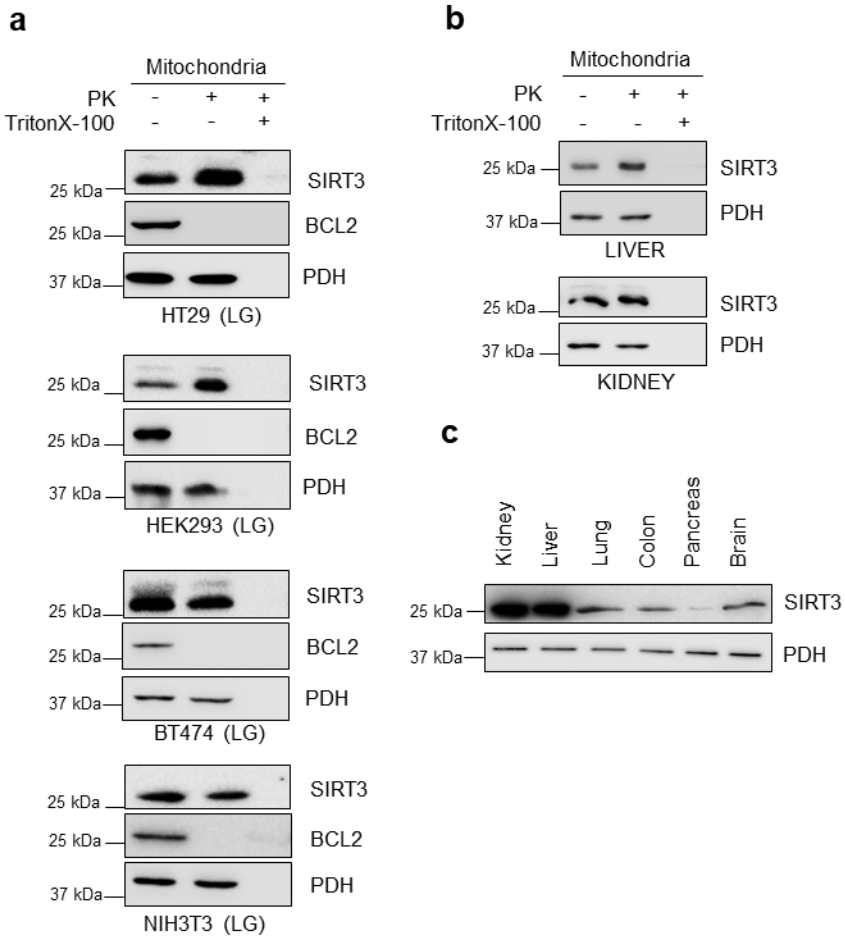


***Figure 4.5 –*** *SIRT3 accumulation into the mitochondria of different cell lines and in murine tissue.*

*(a) Immunoblot analysis of mitochondrial fractions isolated from different cell lines (HT29, human colorectal cancer; HEK293: human epithelial kidney; BT474, human breast cancer; NIH-3T3, murine fibroblasts) upon low glucose (LG, 0.75mM glucose) treatment. Mitochondrial fractions were treated with PK alone to degrade MOM proteins or with PK and Triton X-100 to permeabilise mitochondria and degrade all mitochondrial proteins, as control of antibody specificity. BCL2: outer membrane control; PDH: mitochondrial matrix control. (b) Western blot analysis of mitochondria-enriched fractions isolated from murine*

*kidney and liver and subjected to PK or combined PK and Triton X-100 treatment. PDH: mitochondrial matrix control. (c) Immunoblot analysis of different murine organs with the indicated antibodies. PDH was used as a loading control. The presented results are representative of at least three independent experiments.*

## 4.2 Requirements for the mitochondrial import and accumulation of FoxO3A

Experimental evidences described above supported for the first time the existence of a shorter, intra-mitochondrial form of FoxO3A, which may result from a processing mechanism similar to the one involving the canonical mitochondrial proteins. To exclude the possibility that the 70kDa band could represent another protein cross-reacting with FoxO3A antibodies, a plasmid DNA coding for FoxO3A FLAG-tagged at the C-terminal domain (Figure 4.6a) was transfected in glucose-restricted HCT116, and HEK-293 cells and the mitochondrial fraction obtained from transfected cells were analysed. In both cell lines, anti-FLAG antibodies revealed two bands, migrating at around 90kDa and 70kDa, which corresponded to exogenous FoxO3A in the purified mitochondrial fraction. Only the 70kDa band was detected after PK addition (Figure 4.6b).

It is well-established that mitochondrial nuclear-encoded proteins have a mitochondrial import signal (MTS) in their primary or secondary structure, required to direct them into the mitochondria. Several mitochondrial localisation signals have been described, and the 70% of them are localised in the N-terminal domain

of the protein. MTS allows proteins destinated to the mitochondrial matrix, to bind the surface of the organelle and translocate them across the mitochondrial membranes (OMM and IMM), through a general translocation apparatus. Upon mitochondrial import, MTS is proteolytically cleaved by the mitochondrial processing peptidase (MPP) and the released proteins folded in the matrix (Neupert and Herrmann, 2007, Chacinska et al., 2009). As experimental evidence demonstrates the ability of FoxO3A to bind mtDNA (Peserico et al., 2013), it is possible to speculate that mtFoxO3A can reach the mitochondrial matrix. However, as FoxO3A is not a canonical mitochondrial protein, a FoxO3A-mitochondrial targeting sequence has never been described before.

### 4.2.1 FoxO3A N-terminus cleavage upon mitochondrial translocation

Various preliminary *in silico* attempts aimed to identify putative cleavable N-terminal mitochondrial targeting signals in FoxO3A sequence failed (Fukasawa et al. 2015; Smith et al., 2016). Furthermore, the N-terminal of FoxO3A has been poorly characterised and defined, until today, as a "chromatin remodelling" domain of the protein (Calnan and Brunet, 2008). Therefore, to determine the presence of such an extension even in the FoxO3A structure, a new FoxO3A vector tagged both with HA - at the N-terminus - and with FLAG -at the C-terminus- (Figure 4.6a) was generated and transfected in glucose-restricted HCT116 cells. Results obtained showed the presence of both tags (HA and FLAG) at around 90kDa in purified mitochondria. Importantly, only one band running at around 70kDa was detected by anti-FLAG antibodies after PK treatment (Figure 4.6c), supporting the

hypothesis of a FoxO3A N-terminal domain cleavage event, occurring upon the mitochondrial translocation. These results corroborate those obtained with endogenous proteins, suggesting that exogenous full-length FLAG-tagged FoxO3A can localise at the outer mitochondrial membrane. Inside the mitochondria, it is present a shorter form that is still tagged at the C-terminus.

Moreover, genetic silencing using two siRNAs specific for FoxO3A showed that the 70kDa band detected inside the mitochondria is a shorter form of endogenous FoxO3A (Figure 4.7a). Therefore, a newly generated FLAG-tagged FoxO3A plasmid (Figure4.7b), deleted of the entire N-terminal domain (amino acids 1-148) was transfected in HCT116 cells, and the ability of this mutant to localise at the mitochondria was assessed. The collected data indicate that amino acids 1-148 are required for FoxO3A localisation and translocation into the mitochondria, functioning as an N-terminal mitochondrial import signal (Figure 4.7b). To get further confirmation, additional immunoblot analysis was performed on mitochondria isolated from metabolically stressed HCT116 and HEK-293 cells, using two distinct antibodies detecting the endogenous form of FoxO3A. The first, raised against the N-terminus recognised only a single band of around 90kDa in the whole mitochondria. The other targeting the C-terminal domain recognized both the 90kDa and the 70kDa bands in whole mitochondria and only the 70kDa inside the organelles (Figure 4.7c).

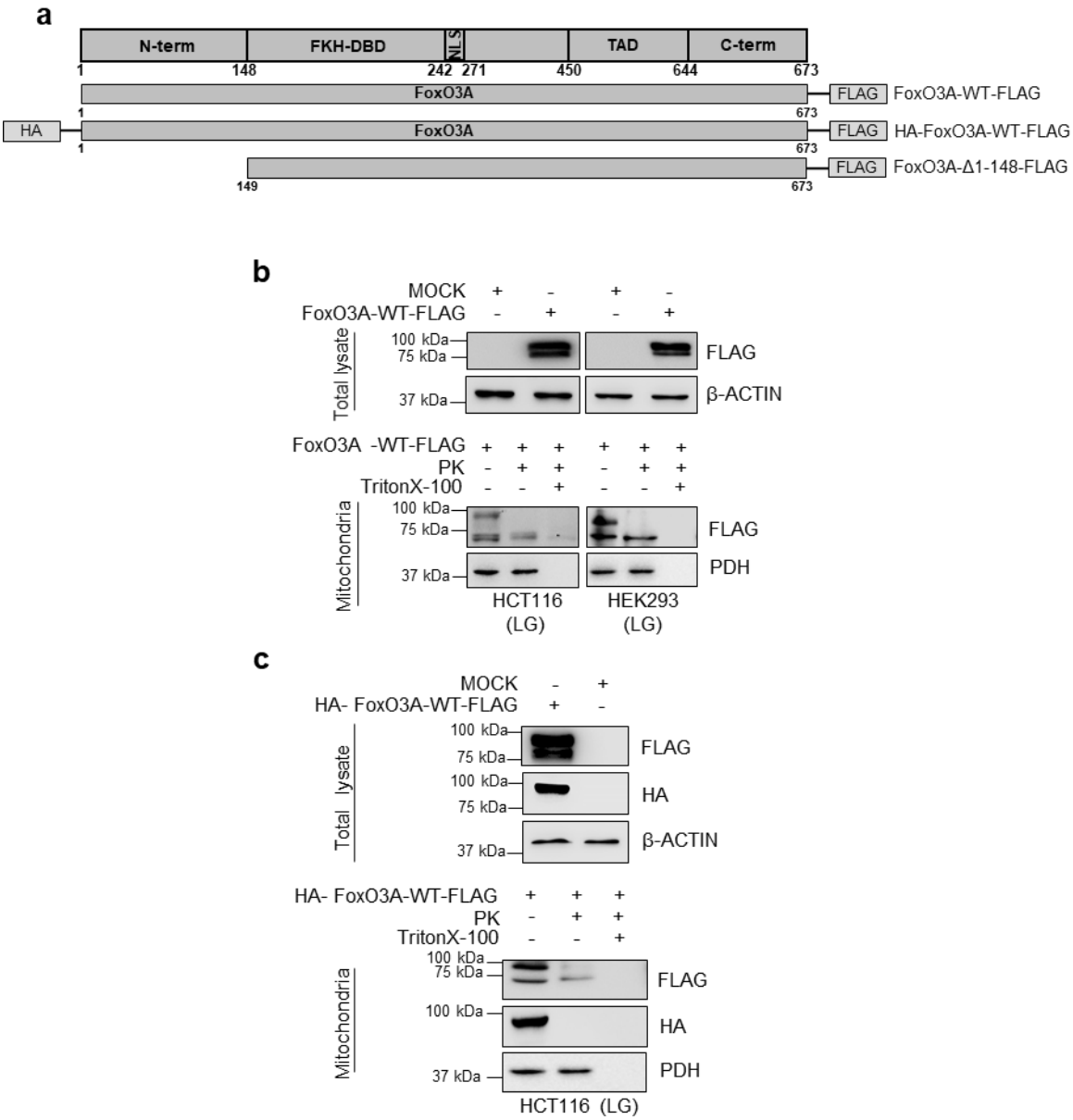


***Figure 4.6–*** *FoxO3Ais cleaved upon translocation into the mitochondria.*

*(a) Scheme of plasmids used. (b-c) Cells were transfected with (b) FoxO3A-FLAG and (c) HA-FoxO3A-FLAG for 48 h; upon LG (0.75mM glucose, 24 h), total and mitochondrial proteins were analysed by immunoblot with the indicated antibodies, upon PK treatment alone –to degrade the outer membrane proteins- or in combination with Triton X-100 to permeabilise mitochondria and degrade all*

*mitochondrial proteins, as control of the antibody specificity. β-ACTIN and PDH were used as total lysate and mitochondrial fraction controls, respectively. N-term. N-terminal domain, FKH-DBD forkhead DNA-binding domain, NLS nuclear localisation signal, TAD transactivation domain, C-term. C-terminal domain. The presented results are representative of at least three independent experiments (Celestini et al., 2018).*

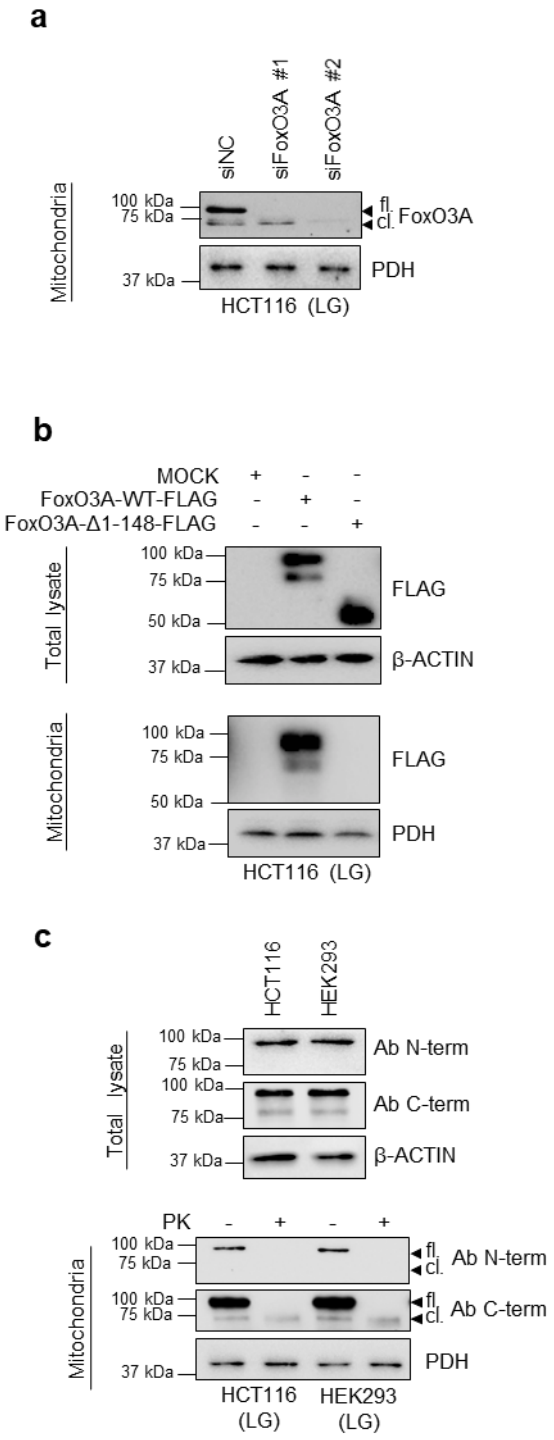


***Figure 4.7*** *– N-terminus of FoxO3A is required for its mitochondrial accumulation. (a) HCT116 cells were transfected with control (siNC) or FoxO3A-specific siRNAs for 48 h. Upon LG (0.75mM glucose, 24 h), FoxO3A mitochondrial levels were evaluated by immunoblot. PDH: loading control. (b) HCT116 cells transfected with*

*FoxO3A-WT-FLAG or FoxO3A-Δ1–148-FLAG. Upon LG (0.75mM glucose, 24 h), total and mitochondrial proteins were analysed by immunoblot with the indicated antibodies. β-ACTIN and PDH were used as total lysate and mitochondria controls, respectively. (c) Immunoblots performed with two different anti-FoxO3A antibodies in mitochondria isolated from HCT116 and HEK293 cells cultured in LG (24 h). Mitochondrial fractions were subjected to PK treatment to degrade outer membrane protines. β-ACTIN and PDH were used as total lysate and mitochondrial fraction controls, respectively (Celestini et al., 2018).*

### 4.2.2 Exploring the N-terminal domain of FoxO3A for the mitochondrial processing sequences

Upon import into mitochondria, the sequences of the most protein destined to the matrix are cleaved off by the heterodimer mitochondrial processing peptidases. Among them, mitochondrial processing peptidase (MPP) cleaves the majority of mitochondrial proteins, while the mitochondrial intermediate peptidase (MIP) processes only specific groups of precursor polypeptides. These proteases are structurally and functionally conserved across species, and their human homologues have been identified as potential players in mitochondrial diseases. Three mitochondrial protease recognition site motifs are reported:

"R-2 motif" [xRx**(↓)**x(S/x)], recognized by MPP

"R-3 motif" [xRx(Y/x)**(↓)**(S/A/x)x)], recognized by MIP

"R-10" motif [Rx**(↓)**(F/L/I)xx(T/S/G)xxxx], (Gakh et al.,2002; Mossmann et al., 2012), which are "merged" motifs recognizable by both MPP and MIP.

Although various in silico tools exist to predict these cleavage sites (Fukasawa et al. 2015), they failed in FoxO3A sequence analysis. Therefore, to extensively characterise the N-terminal region of FoxO3A, MPP and MIP consensus motif-like peptide probes were used to search exact matches in positions 1-148. Interestingly, in region 98-108 there is the sequence ARVLAPGGQD, which matches MPP and MIP consensus motifs R-2, R-3 and R-10. Of note, these motifs are partially overlapping in this region. This observation suggests that cleavage events mediated by mitochondrial processing peptidases may occur in region 98-108 of FoxO3A (Figure 4.8a). Thus, FLAG-tagged vector encoding for a mutant form of FoxO3A lacking residues 80-108 was generated (Figure 4.8b). The resulting protein was able to localise at the mitochondria, but was impaired in translocating into the mitochondria (Figure 4.8c).

Further proteinase K protection assays (see Figure 4.9a) confirmed that endogenous FoxO3A is translocated into the mitochondria and reaches the matrix in its cleaved form (Figure 4.9b, FoxO3A-cl.). These results were corroborated by immunoblot analysis of mitoplasts from swollen mitochondria treated with proteinase K (Figure 4.9c). Importantly, these data indicate that FoxO3A N-terminus, which is required for proper recruitment to the mitochondria, contains the key residues necessary for FoxO3A cleavage by mitochondrial peptidase and import into the mitochondrial matrix. Interestingly, alignment of the N-terminal region of FoxO3A with other human FoxO proteins, performed by using the CLUSTALW (1.83) tool -available on the Multiple Sequence Alignment server-, revealed that the region 98-108 is specific to FoxO3A since it is not conserved in other human FoxO proteins (Fig 4.10a). On the other hand, this region is

evolutionarily conserved across species, as revealed by phylogenetic analysis performed from *Caenorhabditis elegans* to *Homo sapiens*, through the T-Coffee tool-mediated multiple sequence alignment of the region including the mitochondrial processing peptidase consensus motifs R-2, R-3 and R-10 (aa: 98-108, Fig 4.10b).

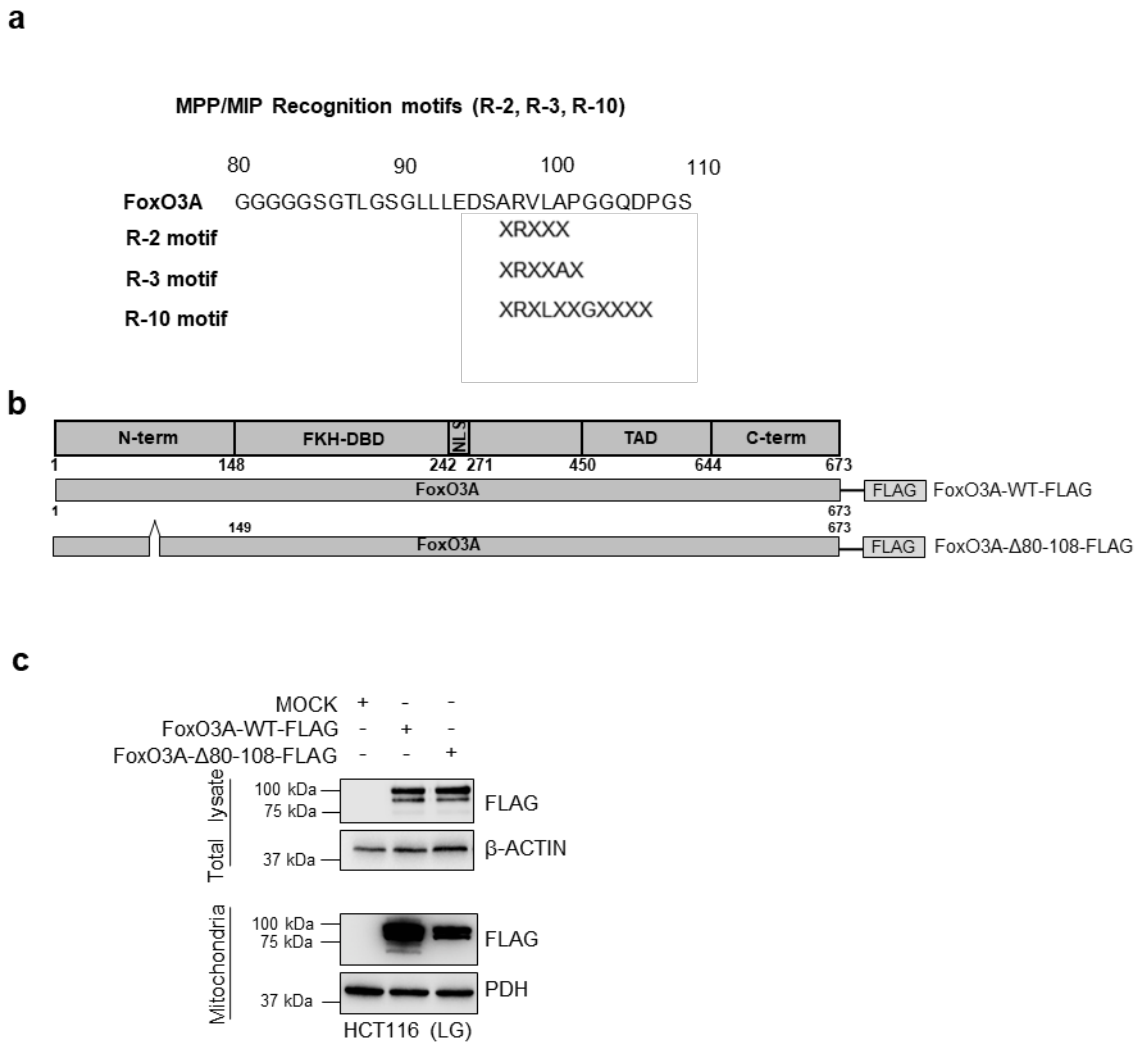


***Figure 4.8-*** *The cleavage region of FoxO3A.*

*(a) Alignment of FoxO3A N-terminal sequence and cleavable mitochondrial pre-sequences. R-2 (XRXXS) and R-3 (XRXXSX) motifs are cleavage sites recognized*

*by the mitochondrial processing peptidase (MPP). The R-10 motif (XRXLXXGXXXX) is sequentially cleaved by MPP and MIP (mitochondrial intermediate peptidase). (b-c) HCT116 cells were transfected with FoxO3A-FLAG and truncated FoxO3A (Δ80-108)-FLAG plasmids for 48 h. Total and mitochondrial proteins were analysed by immunoblot with the indicated antibodies. The cleaved FoxO3A mitochondrial band is not detectable into the mitochondria of cells transfected with FoxO3A (Δ80-108)-FLAG.β-ACTIN and PDH were used as total lysate and mitochondrial fraction controls, respectively. N-term. N-terminal domain, FKH-DBD forkhead DNA-binding domain, NLS nuclear localisation signal, TAD transactivation domain, C-term. C-terminal domain. fl.: full-length FoxO3A; cl.: cleaved FoxO3A. The presented results are representative of three or more independent experiments (Celestini et al., 2018).*

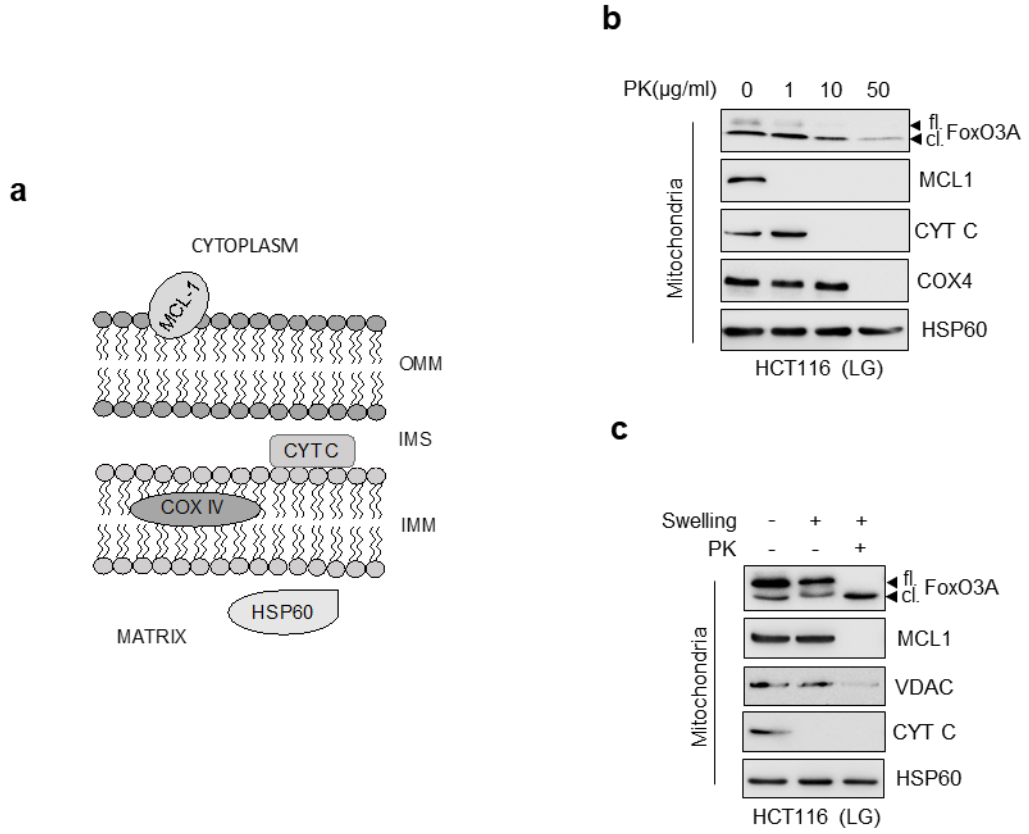


***Figure 4.9-*** *FoxO3A localise into the mitochondrial matrix.*

*(a) Proteinase K (PK) protection assay scheme, as described in section 3.2.5. (b) Immunoblot analysis with the indicated antibodies of mitochondrial fractions isolated from HCT116 cells, subjected to PK protection assay upon glucose restriction (LG, 0,75 mM glucose, 24h). (c) Immunoblot analysis with the indicated antibodies of mitoplasts obtained from HCT116 cells upon glucose restriction (LG, 24h). (B, C). MCL1: outer membrane marker; CYTOCHROME C: inter-membrane space marker; COX4: inner membrane marker; VDAC1: inner membrane marker; HSP60: matrix marker. fl.: full-length FoxO3A; cl.: cleaved FoxO3A. The presented results are representative of at least three independent experiments (Celestini et al., 2018).*

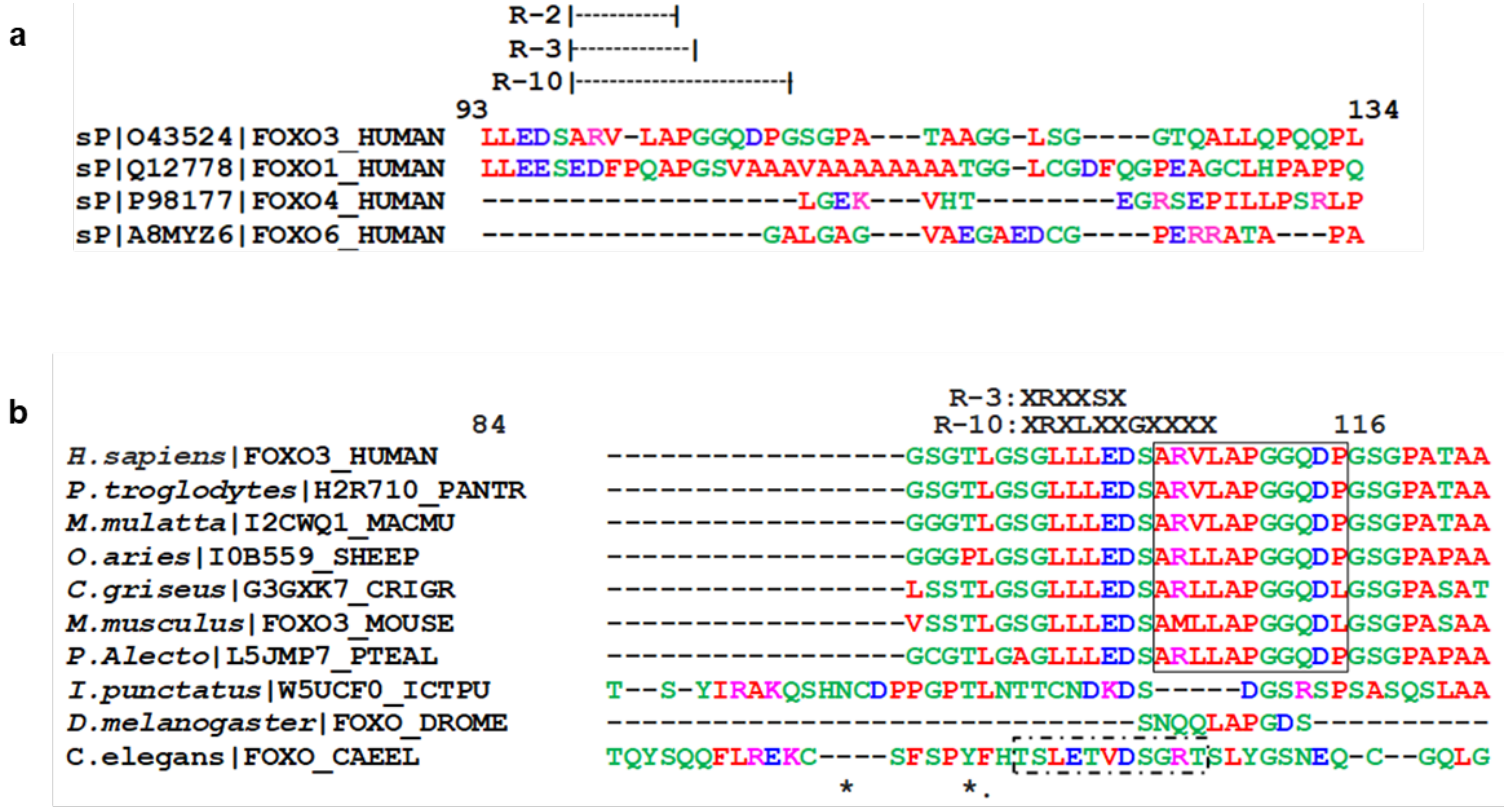


***Figure 4.10*** *– Analysis of the 98-108 region*

*(a) Alignment of the N-terminal region of human FoxO proteins annotated with specific UniProtKB/Swiss-Prot accession numbers and entry names (http://www.uniprot.org). (b) Multiple sequence alignment of the region the region encompassing residues 98-108, performed by using the T-Coffee tool available on the MSA (Multiple Sequence Alignment) server (http://www.ebi.ac.uk/Tools/msa/tcoffee/).*

### 4.2.3 Mitochondrial FoxO3A import requires Serine 12 and Serine 30 phosphorylation

So far, the N-terminal domain of FoxO3A – encompassing residues 1-148 – has been poorly characterised, except for Threonine 32, which is evolutionarily conserved and represents a well-known target of AKT, involved in FoxO3A subcellular compartments-shuttling (Brunet et al., 1999). Specifically, the AKT-dependent phosphorylation of FoxO3A on this amino acid, together with the modification of the Serine 253 and Serine 315, leads to FoxO3A nuclear exclusion, mediated by 14-3-3 proteins and, consequently, to FoxO3A transcriptional programme inhibition (Brunet et al., 1999).

With the support of various bioinformatics tools, the 1-148 region has been analysed in the search for novel amino acids (Serines, Threonines, Tyrosines) that could be potential targets for signalling pathways transducing extracellular stimuli. *In silico* analyses were performed by using NeTPhos 2.0 and DISPHOS 1.3. Specifically, NeTPhos server can predict Serine, Threonine or Tyrosine phosphorylation sites in eukaryotic proteins, by using ensembles of neural networks (Blom et al., 1999). Also, DISPHOS (Disorder-enhanced Phosphorylation Sites Predictor) performs the computational prediction of Serine, Threonine and Tyrosine phosphorylation sites in proteins, based on thousands of non-redundant experimentally confirmed protein phosphorylation sites, promising an accuracy around 80% (Iakoucheva et al., 2004). *In silico* analysis revealed the presence of only six residues that reached a significant threshold score (>0.6) with both tools, such as to be considered a high confident, positive prediction. These residues are

all Serines and are located at positions 12, 26, 30, 43, 48 and 55 of FoxO3A sequence (Table 4.1). Furthermore, although the involved kinases (or signalling pathways) have not been identified yet, these Serines have all been previously described to be phosphorylated *in vivo* by mass-spectrometry analysis of human samples of patients with different types of cancer (Pan et al., 2009; Kiyotsugu et al., 2014; Klammer et al., 2012; Mertins et al., 2014; Mertins et al., 2016; Olsen et al., 2010; Sharma et al., 2014).

| CONTEXT | POSITION | SCORE* | SCORE** |
|---|---|---|---|
| PAPL**S**PLEV | 12§ | 0.980 | 0.757 |
| FEPQ**S**RPRS | 26§ | 0.600 | 0.754 |
| SRPR**S**CTWP | 30§ | 0.970 | 0.775 |
| ELQA**S**PAKP | 43§ | 0.690 | 0.619 |
| PAKP**S**GETA | 48§ | 0.860 | 0.645 |
| TAAD**S**MIPE | 55§ | 0.940 | 0.778 |
| GRAG**S**AMAI | 75 | 0.483 | 0.810 |
| GGGG**S**GTLG | 85 | 0.027 | 0.625 |
| GTLG**S**GLLL | 90 | 0.006 | 0.359 |
| LLED**S**ARVL | 97 | 0.039 | 0.410 |
| QDPG**S**GPAT | 110 | 0.895 | 0.493 |
| AGGL**S**GGTQ | 120 | 0.137 | 0.324 |
| AAGG**S**GQPR | 144 | 0.013 | 0.416 |

***Table 4-1 -*** *Phosho-profile prediction di FoxO3A*

*****: *NetPhos 2.0 score (http://www.cbs.dtu.dk/services/NetPhos/).* ******: *Disphos score (http://www.dAbi.temple.edu/disphos/).* §: *All kinase orphan residues that show threshold score >0.6.*

As widely discussed in the Introduction chapter, phosphorylation events precisely regulate the transcriptional activity of FoxO3A and, importantly, its shuttling between cell compartments. Therefore, the prediction of six Serine phosphorylation sites in the N-terminus of FoxO3A is important for extending the characterisation of this domain to ascertain whether these residues could be involved in the signalling pathways inducing accumulation of FoxO3A into the mitochondria, under metabolic stress conditions. To test this hypothesis, all the indicated Serines have been mutagenised to non-phosphorylatable alanine residues (Figure 4.11a). Then, the indicated FoxO3A FLAG-tagged proteins have been expressed in glucose-restricted cancer cells, and the mitochondrial fractions isolated from them were analysed by immunoblot. Alanine substitution at positions 12 or 30 impaired the ability of full-length FoxO3A (90kDa form, FoxO3A-fl.) to be recruited at the outer membrane and then processed (70 kDa cleaved form, FoxO3A-cl.) to localise inside the mitochondria (Figure 4.11b-c).

Interestingly, the concomitant replacement of both Serines with Alanines (S12A/S30A) strongly decreases FoxO3A mitochondrial localisation (Figure 4.12a-b). Taken together this evidence suggests that S12 and S30 are both required by the signal transduction machinery to direct FoxO3A to mitochondria in metabolically stressed cancer cells. Furthermore, the transfection of a vector encoding for a FoxO3A mutant lacking the initial 30 residues (Figure 4.12c) of the N-terminal domain – encompassing both S12 and S30- showed that the deletion of this portion severely impaired the mitochondrial localisation of FoxO3A in metabolically stressed cancer cells, confirming the main role of the two Serines in FoxO3A mitochondrial translocation.

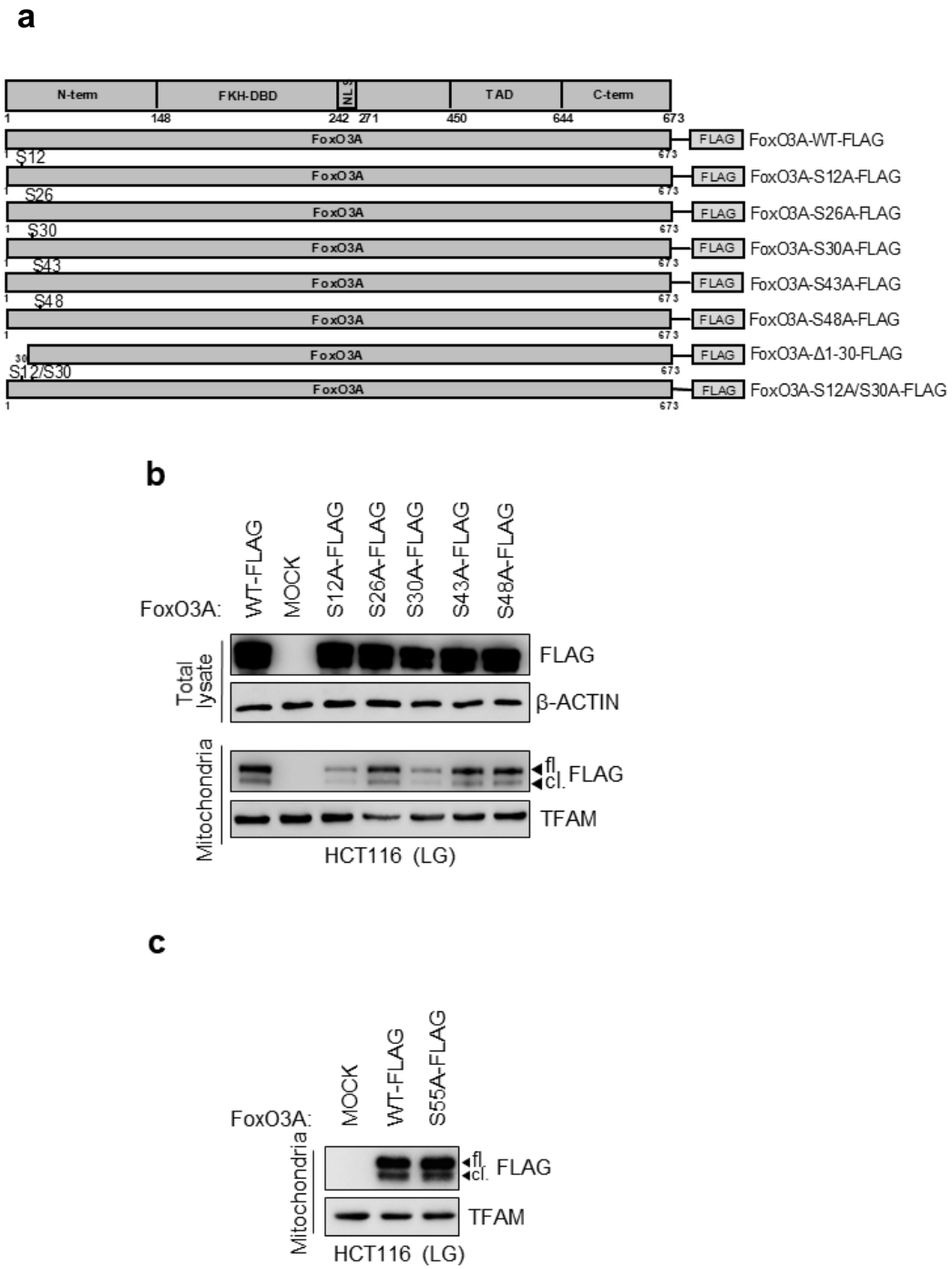


***Figure 4.11 -****PTMs required for FoxO3A mitochondrial accumulation.*

*(a) Scheme of FoxO3A-FLAG and mutated FoxO3A-FLAG plasmids obtained by site-directed mutagenesis. (b,c) HCT116 cells were transfected with the indicated FoxO3A-FLAG plasmids for 48 h and then subjected to a low glucose regimen for*

*24 hours (LG, 0,75 mM glucose, 24h). Total and mitochondrial proteins were analysed by immunoblot with the indicated antibodies. N-term. N-terminal domain, FKH-DBD forkhead DNA-binding domain, NLS nuclear localisation signal, TAD transactivation domain, C-term. C-terminal domain. The presented results are representative of three or more independent experiments (Celestini et al., 2018).*

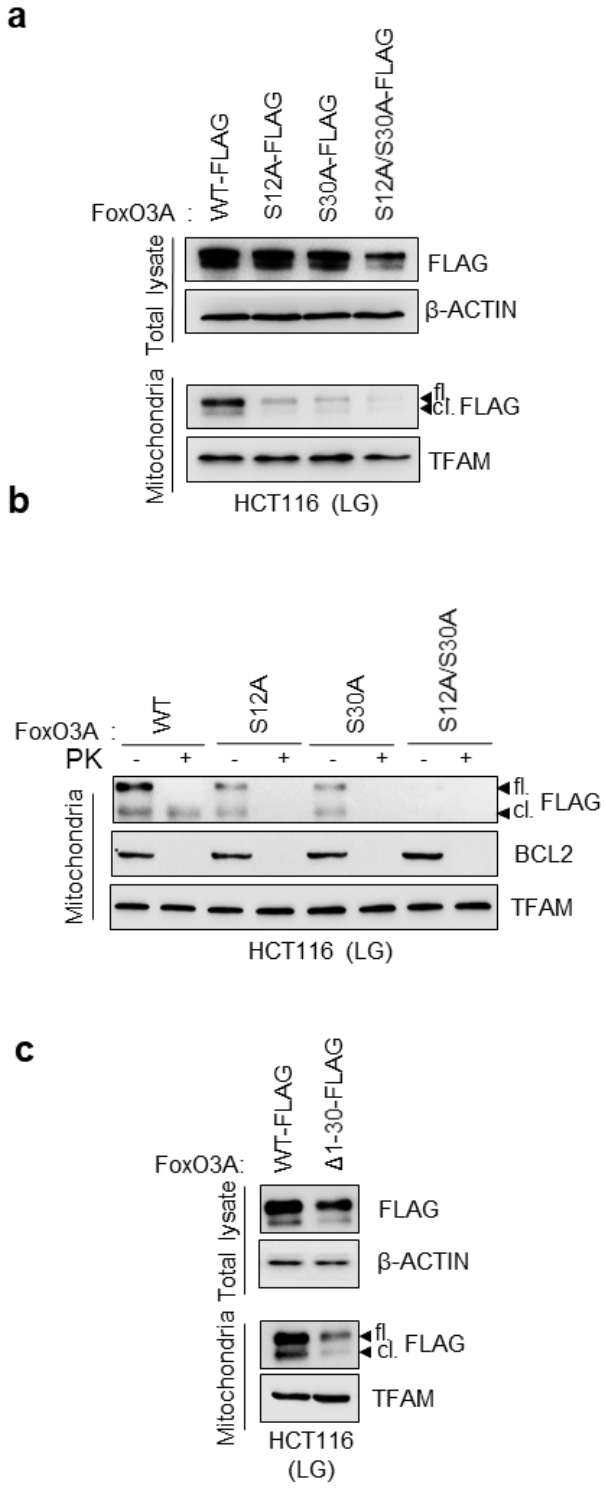


***Figure 4.12*** *–S12 and S30 are both required to direct FoxO3A to mitochondria in metabolically stressed cancer cells.*

*(a - c) HCT116 cells were transfected with the indicated FoxO3A-FLAG plasmids for 48 h and then subjected to a low glucose regimen for 24 hours (LG, 0,75 mM glucose, 24h). (a, c) Total and mitochondrial proteins were analysed by immunoblot with the indicated antibodies. β-ACTIN and TFAM were used as total lysate and mitochondrial fraction controls, respectively. (b) Mitochondrial fractions were subjected to PK treatment to degrade the outer membrane proteins. BCL-2 and TFAM were used as outer membrare and inner mitochondrial membranes markers, respectively. fl.: full-length FoxO3A; cl.: cleaved FoxO3A. The presented results are representative of three or more independent experiments (Celestini et al., 2018).*

### 4.2.4 Signalling involved in FoxO3A mitochondrial translocation

The finding of two major players for FoxO3A mitochondrial translocation required a more detailed investigation on the N-terminal domain of FoxO3A. The published evidence shows that genetic silencing of AMPK abolished FoxO3A accumulation into the mitochondria of normal cells under glucose shortage (Peserico et al., 2013). This suggests that AMPK could be a physiological kinase for N-terminus FoxO3A phosphorylation. In the literature, various approaches have been described - synthetic peptides, or mutational analyses of AMPK substrates- that elucidated the AMPK motif, in the effort to find novel substrates of AMPK (Gwinn et al., 2008; Marin et al., 2015). Mainly, as a highly selective kinase, AMPK prefers sites that have at least one basic side chain (usually R, but can be K or H), usually at the −3 or −4 positions, and hydrophobic residues at the −5 position and/or the +4 (usually L or M, but I, V or F in some cases). However, AMPK targets often

contain minor variants of the consensus sequence, such as the lack of the basic residues in the −4/-6 positions.

To determine whether AMPK is one of the kinases required for the phosphorylation of FoxO3A at S30, alignment has been performed between the AMPK phosphorylation sites sequence in the best-established *in vivo* substrates of the kinase and the amino acid sequence surrounding S30. The results of the comparative analyses revealed that the analysed region does carry AMPK signature sequence and, consequently, the S30 is likely an authentic substrate of AMPK (Table 4.2).

Furthermore, in the light of the previous *in silico* and *in vivo* results, KinasePhos 2.0, a web server aimed to the identification of protein kinase-specific phosphorylation sites, was questioned to predict which kinase might be required in the signalling pathway involving Ser12 (Wong et al., 2007). Specifically, this tool investigates uncharacterised protein sequences by exploiting known phosphorylation sites, categorised in the server by substrate sequences and their corresponding protein kinase classes. The KinasePhos analysis performed of N-terminus of FoxO3A suggested that S12 could be a part of an ERK consensus phosphorylation motif (Ser-Pro). Of note, experimental evidences showed that both AMPK and ERK kinases were phospho-activated in glucose-restricted HCT116 cells (Figure 4.13a) and that they can be localised at the mitochondria together with FoxO3A (Figure 4.13b). Importantly, pharmacological inhibition of the mitogen-activated protein kinase kinase (MEK)/ERK or the AMPK pathway by PD98059 or compound C (CC), respectively, significantly prevented FoxO3A localisation at

(FoxO3A-fl.) and accumulation into (FoxO3A-cl.) the mitochondria (Figure 4.14a-b). Moreover, consistent with previous reports (Peserico et al., 2013), activation of AMPK by AICAR significantly induced mitochondrial processing and import of FoxO3A, as shown by the levels of its cleaved form (FoxO3A-cl.) even in the presence of high glucose concentration in culture (Figure 4.14b).

| AMPK Substrate | -5 | -4 | -3 | -2 | -1 | 0 | +1 | +2 | +3 | +4 |
|---|---|---|---|---|---|---|---|---|---|---|
| FoxO3A | Q | S | R | P | R | **S30** | C | T | W | P |
| BI2L1 | P | S | L | Q | R | **S329** | V | S | V | A |
| ACC1 | M | T | H | V | A | **S1216** | V | S | D | V |
| ACC2 | I | R | S | S | M | **S80** | G | L | H | L |
| CRCT2/TORC2 | L | N | R | T | S | **S171** | D | S | A | L |
| RAPTOR | M | R | R | A | S | **S792** | Y | S | S | L |
| HORM. SENS. LIPASE | M | R | R | S | V | **S554** | E | A | A | L |
| LAP2 | K | N | I | V | R | **S913** | K | S | A | T |
| ARHG2 | L | A | K | S | V | **S151** | T | T | N | I |
| AT2B1 | K | P | E | S | R | **S1176** | S | I | H | N |
| P5I11 | L | M | K | K | H | **S14** | Q | T | D | L |
| TSC2 | L | S | K | S | S | **S1387** | S | P | E | L |

***Table 4-2. -*** *Signalling involved in FoxO3A mitochondrial translocation-*

*Protein alignment between N-terminus of FoxO3A and AMPK phosphorylation sites established in AMPK substrates. Grey boxes indicates similarity (polarity and/or hydropathy properties) among FoxO3A amminoacids surrounding S30 and the AMPK target sites residues.*

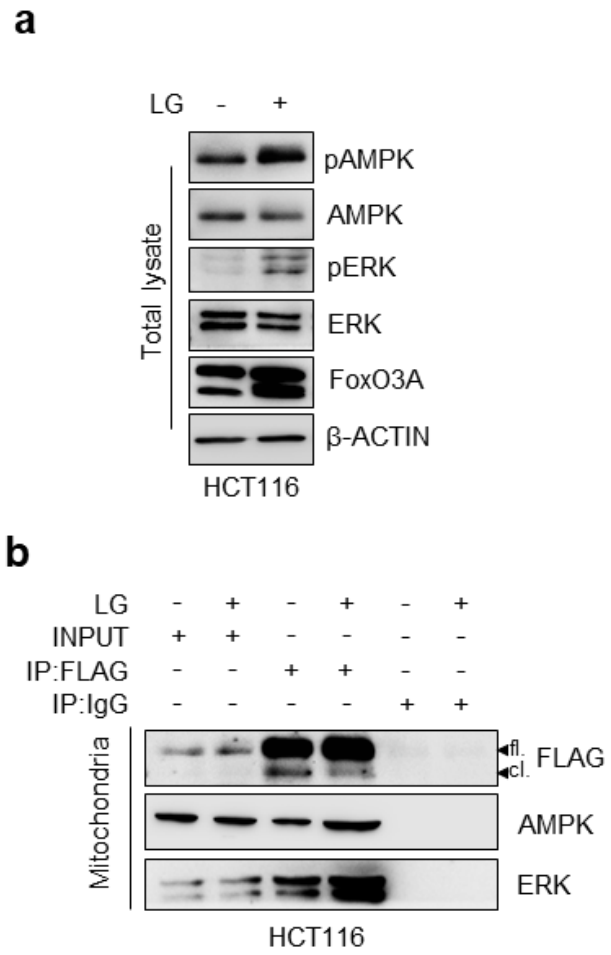


***Figure 4.13-*** *Signalling involved in FoxO3A mitochondrial translocation.*

*(a) Total proteins were extracted from HCT116 cells grown in standard (HG, 24 h) and low glucose conditions hours (LG, 0,75 mM glucose, 24h) and analysed by immunoblot with the indicated antibodies. β-ACTIN was used as a loading control. (b) Upon glucose restriction, HCT116 cells were transfected with FoxO3A-FLAG for 48 hours and mitochondrial fractions were isolated and analysed by co-immunoprecipitation. pAMPK: phospho-AMPK; pERK: phospho-ERK. fl: full-length FoxO3A; cl: cleaved FoxO3A. The presented results are representative of three or more independent experiments (Celestini et al., 2018).*

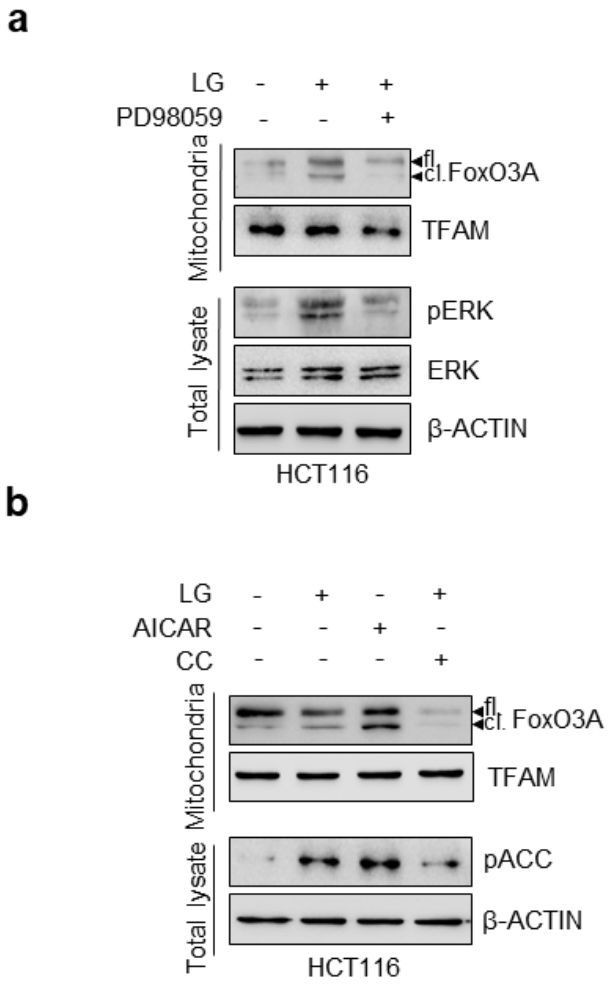


***Figure 4.14–****The pharmacological modulation of MEK/ERK and AMPK pathway influence FoxO3A mitochondrial translocation*

*(a) Pharmacological inhibition of MEK using PD98059 in HCT116 cells cultured in LG (24 h). (b) Pharmacological inhibition or activation of AMPK using compound C (CC, 5 μM) or AICAR (5 mM), respectively, in HCT116 cells cultured in LG (24 h). Total and mitochondrial proteins were analyzed by immunoblot. (a-b) PD98059, compound C and AICAR concentrations were defined accordingly on dose-response curve previously performed. β-ACTIN and TFAM were used as total lysate and mitochondrial fraction controls, respectively. pACC: phospho-ACC;*

*pERK: phospho-ERK; fl: full-length FoxO3A; cl: cleaved FoxO3A. The presented results are representative of three or more independent experiments (Celestini et al., 2018).*

Collectively, these data strongly propose that S12 and S30 are targeted by ERK and AMPK, respectively. To confirm this hypothesis, two newly GST-FoxO3A constructs were generated, one encoding for the N-terminal domain [GST-FoxO3A(1-148)] and the other for a region encompassing residues 385-525 [GST-FoxO3A(385-525)], which contains residues previously shown to be targeted by both AMPK (at S399 and S413, Calnan and Brunet, 2008) and ERK (S425, Yang et al., 2008). Moreover, the GST-FoxO3A (1-148) vector was mutagenized by Serine/alanine substitution at positions 12 and/or 30 to obtain the constructs GST-FoxO3A (1-148) S12A, GST-FoxO3A (1-148) S30A and GST-FoxO3A (1-148) S12A/S30A (Figure 4.15a). The indicated purified proteins were subjected to a kinase assay to test the ability of AMPK and ERK to phosphorylate their candidate residues in vitro directly. Data presented in Figure 4.15b show that ERK could efficiently phosphorylate GST-FoxO3A (1-148) as well as the positive control [GST-FoxO3A (385-525)] and that the S12A substitution is sufficient to decrease P32 incorporation in GST-FoxO3A (1-148) significantly. By in silico prediction, similar results were obtained with the S12A/S30A double mutant, indicating that ERK directly phosphorylates FoxO3Aat S12. To ascertain whether AMPK could phosphorylate S30, GST-FoxO3A (1-148) and GST-FoxO3A (385-525) were assayed with AMPK. The results demonstrated that AMPK efficiently phosphorylated the N-terminus of FoxO3Ain vitro (Figure 4.15b, right panel). Serine-to-Alanine substitution at position 30 impaired the radioactive labelling,

indicating that AMPK phosphorylates FoxO3Aat S30. Indeed, also, in this case, similar results were obtained with the S12A/S30A double mutant.

Furthermore, the alignment of the N-terminal region of human FoxO proteins obtained by using the CLUSTALW (1.83) tool revealed that S30 is evolutionarily conserved from humans to nematodes (Figure 4.16a), and this is located in a part of a highly conserved subdomain which is shared by other human FoxOs. Moreover, the phylogenetic analysis performed by using the T-Coffee tool for sequence alignment showed homology of FoxO3A sequences surrounding S30 from *Caenorhabditis elegans* to *Homo sapiens.* Interestingly, S12 is less conserved across species and is not present in the other members of the human FoxO family (Figure 4.16b).

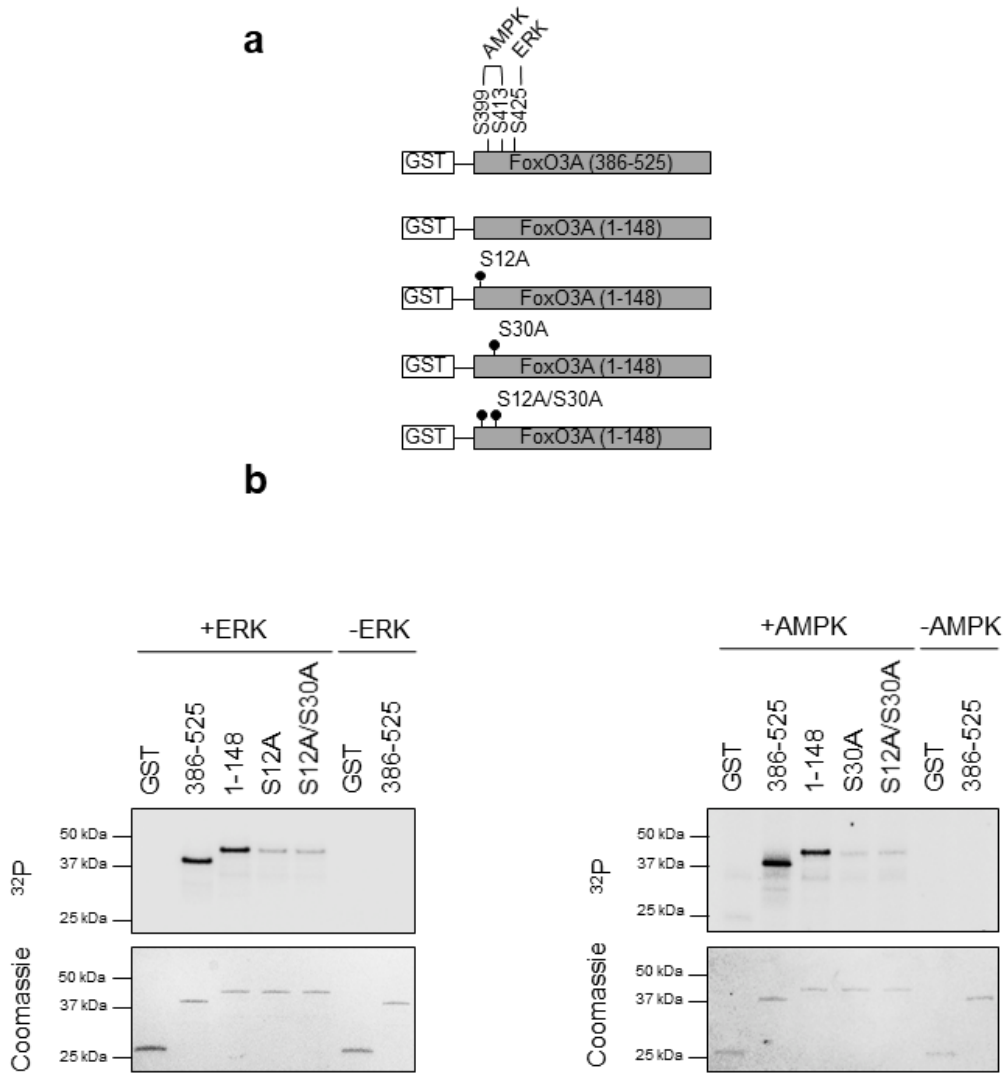


***Figure 4.15 -*** *The AMPK and MEK/ERK signalling pathways regulate mitochondrial FoxO3A*

*(a) Scheme of GST-FoxO3A recombinant constructs generated. In vitro kinase assays performed with the indicated GST-FoxO3A (1–148) and mutant recombinant proteins as substrates, in the presence of recombinant ERK (a) or recombinant AMPK (b). In both assays, GST-FoxO3A (386–525) was used as a positive control. GST-empty protein was used as a negative control. Coomassie gel staining (lower panels) was used as a loading control. fl. full-length FoxO3A, cl.*

*cleaved FoxO3A, N-term. N-terminal domain, FKH-DBD forkhead DNA-binding domain, NLS nuclear localization signal, TAD transactivation domain, C-term. C-terminal domain. The presented results are representative of at least three independent experiments (Celestini et al., 2018).*

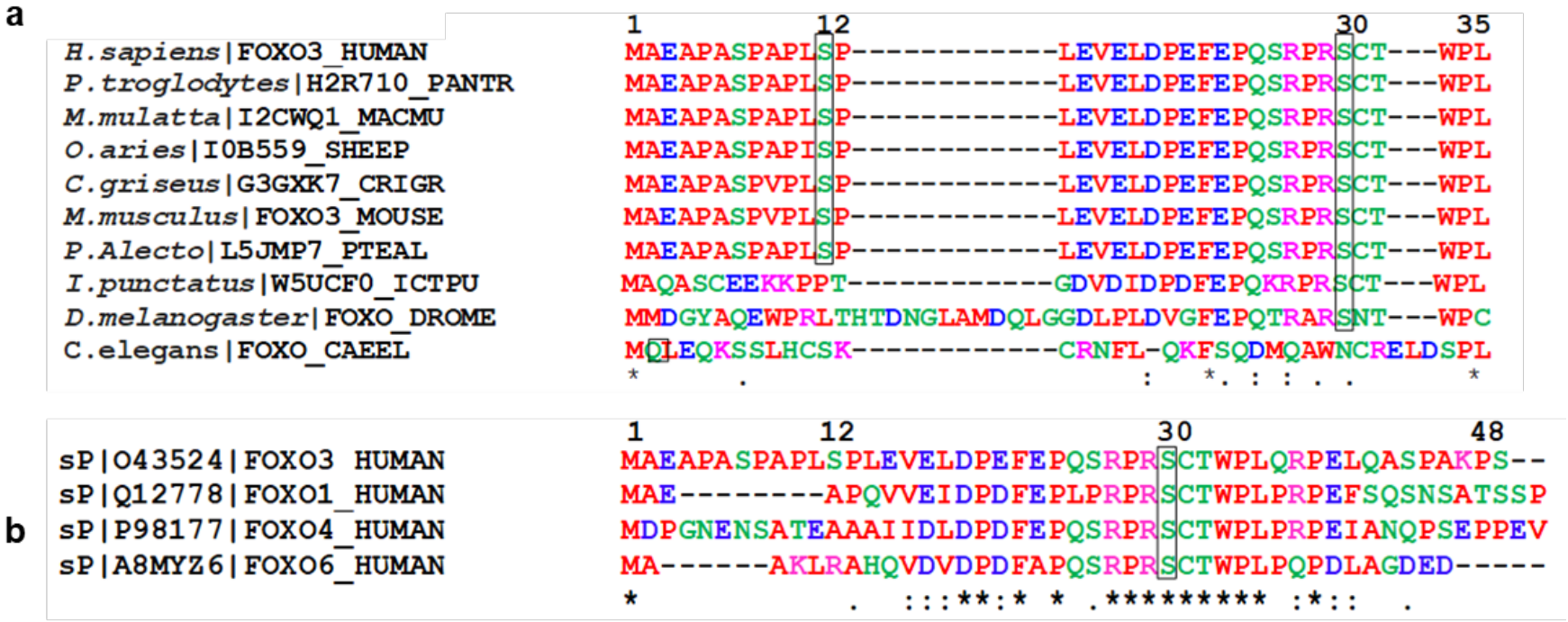


***Figure 4.16*** *– Analysis of the 1-30 region*

*(a) Alignment of the N-terminal region of human FoxO proteins performed by using the CLUSTALW (1.83). Human FoxO proteins were annotated with specific UniProtKB/Swiss-Prot accession numbers and entry names (http://www.uniprot.org). (b) Phylogenetic analysis*

*showing homology of the FoxO3A region encompassing residues S12 and S30. Sequences were aligned by using the T-Coffee tool available on the MSA (Multiple Sequence Alignment) server (http://www.ebi.ac.uk/Tools/msa/tcoffee/).*

### 4.2.5 FoxO3A mitochondrial accumulation requirements in normal cells and tissues upon nutrient shortage

In normal cells, glucose restriction induces only AMPK activation, while ERK is not phosphorylated (Figure 4.17a). To explore the "mitochondrial code" of FoxO3A in normal model, NIH-3T3 normal murine fibroblasts were transfected with FoxO3A-wt, FoxO3A-S12A and FoxO3A-S30A. Interestingly, our data showed that the replacement of S30 with a non-phosphorylatable Alanine is sufficient to prevent FoxO3A mitochondrial localisation under glucose restriction (Figure 4.17b). These data indicate that normal fibroblasts require only AMPK activation to induce FoxO3A mitochondrial accumulation, whereas MEK/ERK signalling pathway is not involved.

To get further insight into the mechanism observed in cell culture, two group of mice were subjected to overnight fasting (18 h), a procedure known to significantly lower plasma glucose levels (Andrikopoulos et al., 2008). Upon their sacrifice, mitochondria from kidney and liver, two tissues containing a significant amount of both FoxO3A-fl. and -cl. in the previous analysis (Figure 4.4), were isolated and purified. Immunoblot analysis revealed the accumulation of both forms of FoxO3A in fasted mice, suggesting that nutrient shortage caused localisation of the transcription factor at the outer mitochondrial membrane (FoxO3A-fl.) and its subsequent import, cleavage and translocation into the mitochondrial matrix (FoxO3A-cl.). Treatment of murine mitochondria with proteinase K confirmed that the cleaved form (FoxO3A-cl.) is detectable also *in vivo* into the mitochondrial matrix (Figure 4.18b-c). To get the full picture, the status of AMPK and ERK in

kidney and liver of mice upon fasting was analysed (Figure 4.18a). Consistent with results obtained in the NIH-3T3 cell line, only AMPK was found to be significantly activated in the animal tissue under nutrient shortage conditions, which supports its role in the signal transduction pathways leading to mitochondrial translocation of FoxO3A.

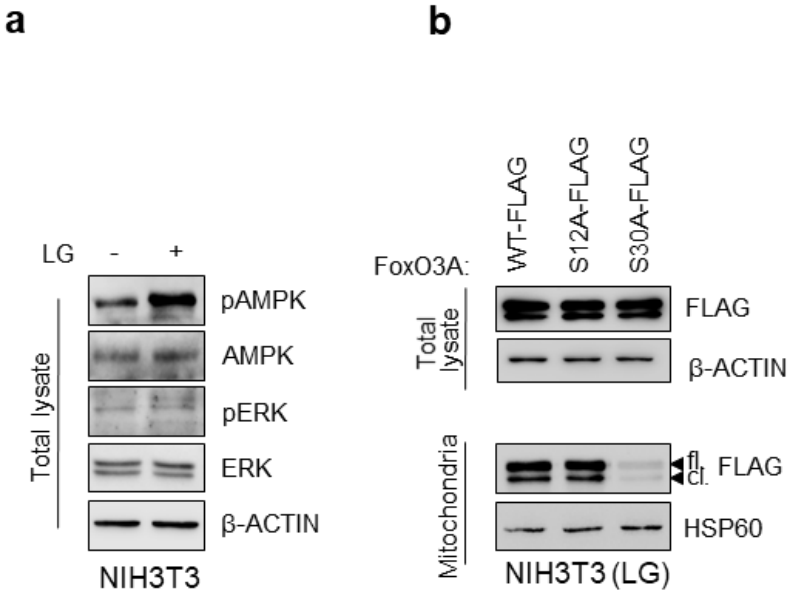


***Figure 4.17 -*** *FoxO3A accumulation into the mitochondria only requires the AMPK signal in normal cells*

*(a) Immunoblot analysis of total proteins isolated from murine NIH3T3 cells upon LG (0.75 mM glucose, 24 h). β-ACTIN: loading control. (b) Immunoblot analysis of total and mitochondrial proteins isolated from NIH3T3 cells transfected with the indicated plasmids for 48 h and subjected to LG (24 h). β-ACTIN and HSP60 were used as total lysate and mitochondria controls, respectively. fl. full-length FoxO3A, cl. cleaved FoxO3A. The presented results are representative of at least three independent experiments (Celestini et al., 2018).*

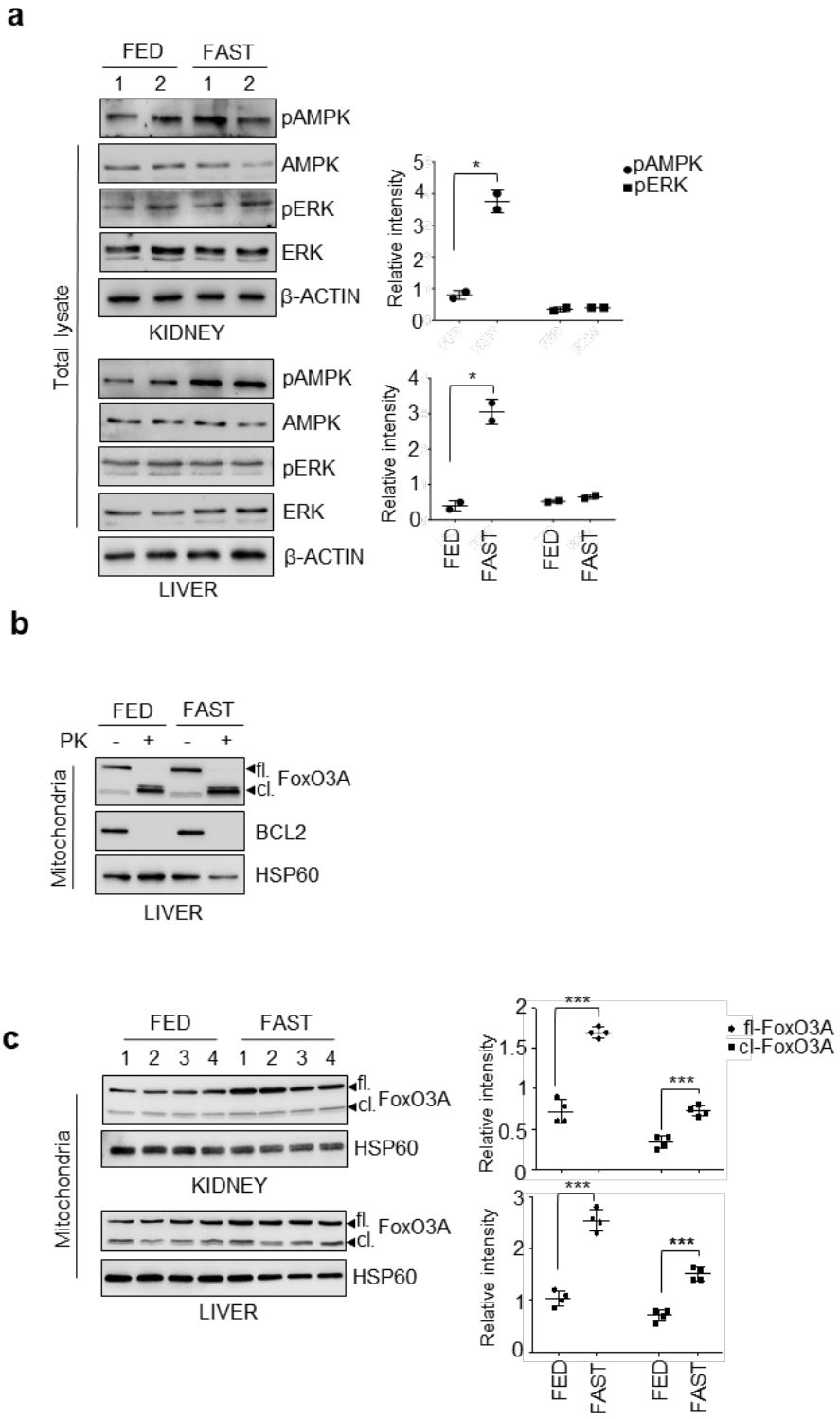


***Figure 4.18*** *-FoxO3A accumulation into the mitochondria only requires the AMPK signal in tissues under nutrient shortage*

*(a) Left panel: immunoblot analysis of total proteins isolated from kidney and liver of fed or fasted (18 h) mice (1 and 2). β-ACTIN: loading control. Right panel: densitometric analysis of the phosphorylated forms of AMPK and ERK normalized against total AMPK and ERK, respectively, and the loading control. (b) Immunoblot analysis of mitochondrial proteins isolated from the liver of fed or fasted (18 h) mice in the presence or absence of PK. BCL2: outer membrane control, HSP60: mitochondrial matrix control. (c) Left panel: immunoblot analysis of mitochondrial proteins isolated from kidney and liver of fed or fasted (18 h) mice. HSP60: loading control. Right panel: densitometric analysis of full-length and cleaved FoxO3A normalized against the mitochondrial fractionation loading control. fl. full-length FoxO3A, cl. cleaved FoxO3A. The presented results are representative of at least three independent experiments. Where applicable, data are presented as mean ± SEM and significance was calculated with Student's* t *test;* *p < *0.05,* **p < *0.01, and* ***p < *0.001 (Celestini et al., 2018).*

## 4.3 Role of mitochondrial FoxO3Ain stressed cancer cells

As a shorter form of FoxO3A originated by the cleavage of its N-terminus has never been described to date, in the light of data previously published by Peserico and colleagues, this novel FoxO3A form needs to be characterised in its ability to bind mtDNA and induce the expression of the mitochondrial genome in nutrient shortage conditions.

### 4.3.1 Mitochondrial FoxO3A regulates the mtDNA expression in metabolically stressed cancer cells

To characterise the ability of the cleaved form of FoxO3A to modulate the mitochondrial genome fate, an HA-FoxO3A-FLAG vector was expressed in HCT116 cancer cells, followed by chromatin immunoprecipitation (ChIP) analysis, performed on mitochondrial fraction by using an anti-HA antibody or an anti-FLAG. Only the latter was able to recognise the cleaved form, which could efficiently bind the D-loop of mtDNA at FRHE consensus sites (FHRE#1: bp 14,963–15,110; FHRE#2: bp 15,400–15,469) under metabolic stress conditions (Figure 4.19a). Further ChIP analyses performed on endogenous proteins from mitochondria purified from different cell lines (HCT116 and HT29 human colorectal cancer cells; HEK-293 immortalized human embryonic kidney epithelial cells) confirmed that endogenous FoxO3A-cl. is recruited at FHRE#1-2 sites together with SIRT3, TFAM and mtRNApol in glucose-restricted cells (Figure 4.19b, d, f, h). The specificity of immunoprecipitation was ensured by a parallel analysis carried out on mitochondria purified from mtDNA-depleted (rho0) HT-29 cells (Schubert et al., 2015) which served as a proper negative control (Figure 419d).

Importantly, FoxO3A-cl., SIRT3, TFAM and mtRNApol form a multiportion complex in the mitochondrial matrix (Figure 4.21a), that is enriched in nutrient shortage conditions. Interestingly, it is worth noting that the glucose deprivation does not influences SIRT3 expression in HCT116 cell lines (Fig 4.20a). On the other hand, SIRT3 phosphorylation is enriched upon low glucose (Fig 4.20b).

However, few data are available about the regulation of SIRT3 function by PMTs (Flick et al. 2012). Of note, the presence of FoxO3A-SIRT3-mtRNAPol-TFAM complex (Figure 4.21a) on mtDNA well correlates with increased expression of all mitochondrial transcripts, as shown by quantitative real-time analysis of mtRNA in cell lines subjected to glucose restriction (Figure 4.19c, e, g, i). These results are consistent with the previous reports (Peserico et al., 2013). Interestingly, upon nutrient shortage, the acetylation of FoxO3A decreases in HCT116 (Figure 4.21b). SIRT3 deacetylatesFoxO3A in the nucleus (Sundaresan et al., 2009), an *in vitro* deacetylation assay was performed on the mitochondrial fraction obtained from an HCT116 cell transfected with FoxO3A-FLAG, in the presence of a newly generated GST-SIRT3 purified protein. To modulate the activity of SIRT3, the Sirtuin inhibitor, Nicotinamide (NAM), was added to the reaction. The assay confirmed that SIRT3 is required for FoxO3A mitochondrial deacetylation (Figure 4.21c).

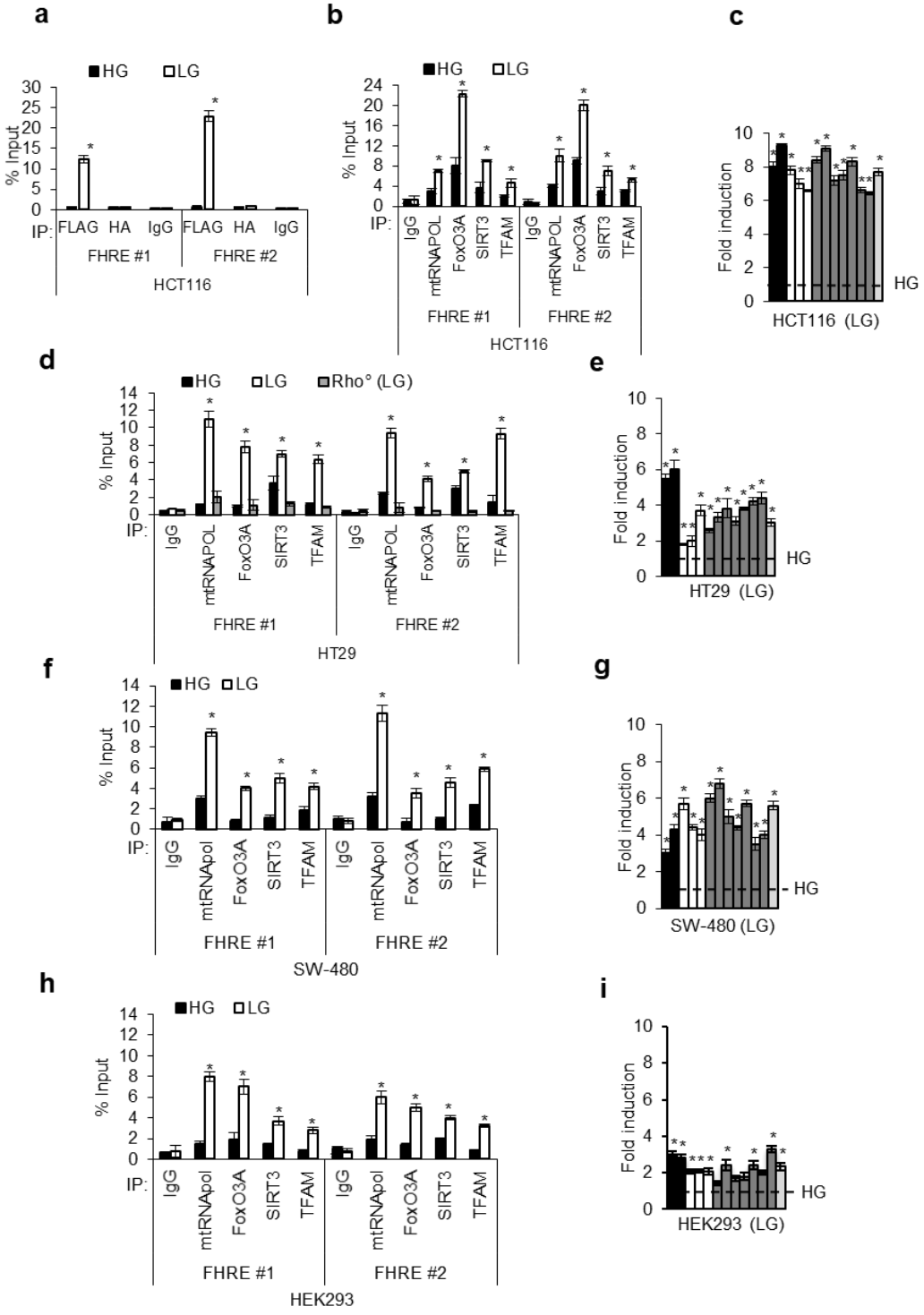


***Figure 4.19 -*** *GR-dependent FoxO3A mitochondrial import leads to increased mitochondrial gene expression.*

*(a) ChIP analysis of exogenous FoxO3A recruitment at FHRE #1–2 sites on mtDNA (FHRE #1: bp 14,963–15,110; FHRE #2: bp 15,400–15,469) upon LG (0.75 mM*

*glucose, 24 h) in HCT116 cells transfected with HA-FoxO3A-WT-FLAG. (b, d, f, h) ChIP analysis of endogenous FoxO3A recruitment at FHRE #1–2 sites on mtDNA in HCT116 (b), HT29 and Rho0 HT29 (negative control, d), SW480 (f) and HEK293 (h) cells upon LG (24 h). Anti-IgGs were used as controls. (c, e g, d) Mitochondrial gene regulation in HCT116 (c) HT29 and Rho0 HT29 (negative control, e), SW480 (g) and HEK293 (i) upon LG (0.75 mM glucose, 24 h) assessed by RT-PCR. Black bars: ATPase 6 and 8 genes; white bars: COX1, COX2, and COX3 genes; gray bars: ND1, ND2, ND3, ND4, ND4L, ND5, and ND6 genes; light gray bar: CYTOCHROME B gene. The dotted line corresponds to the expression levels detected in cells cultured in HG. The presented results are representative of at least three independent experiments. Where applicable, data are presented as mean ± SEM and significance was calculated with Student's* t *test;* *$p < 0.05$, **$p < 0.01$, *and* ***$p < 0.001$*(Celestini et al., 2018).*

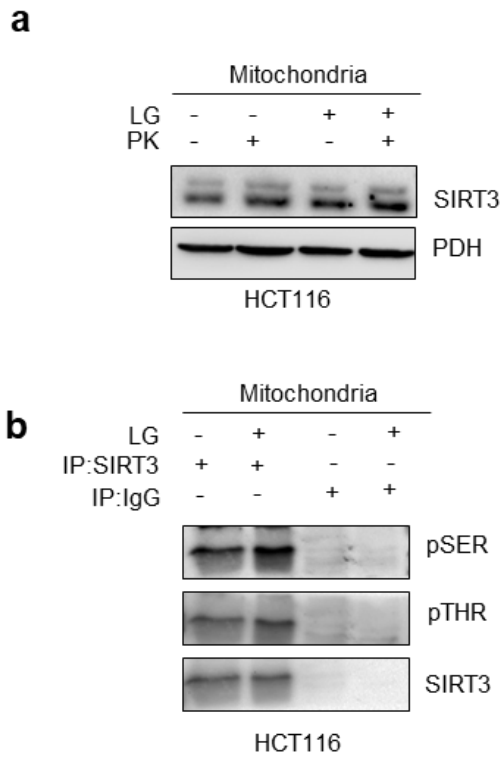


***Figure 4.20 -*** *SIRT3 phosphorylation increases upon glucose restriction*

*(a) Immunoblot analysis with the indicated antibodies of mitochondrial fraction isolated from HCT116 cells treated with low glucose (LG, 0.75mM glucose) for 24h. Mitochondrial fractions were treated with proteinase K (PK) to degrade outer mitochondrial membrane proteins. PDH: loading control. (b) Immunoprecipitation analysis with the indicated antibodies of HCT116 mitochondrial fractions upon LG (24h. The presented results are representative of at least three independent experiments.*

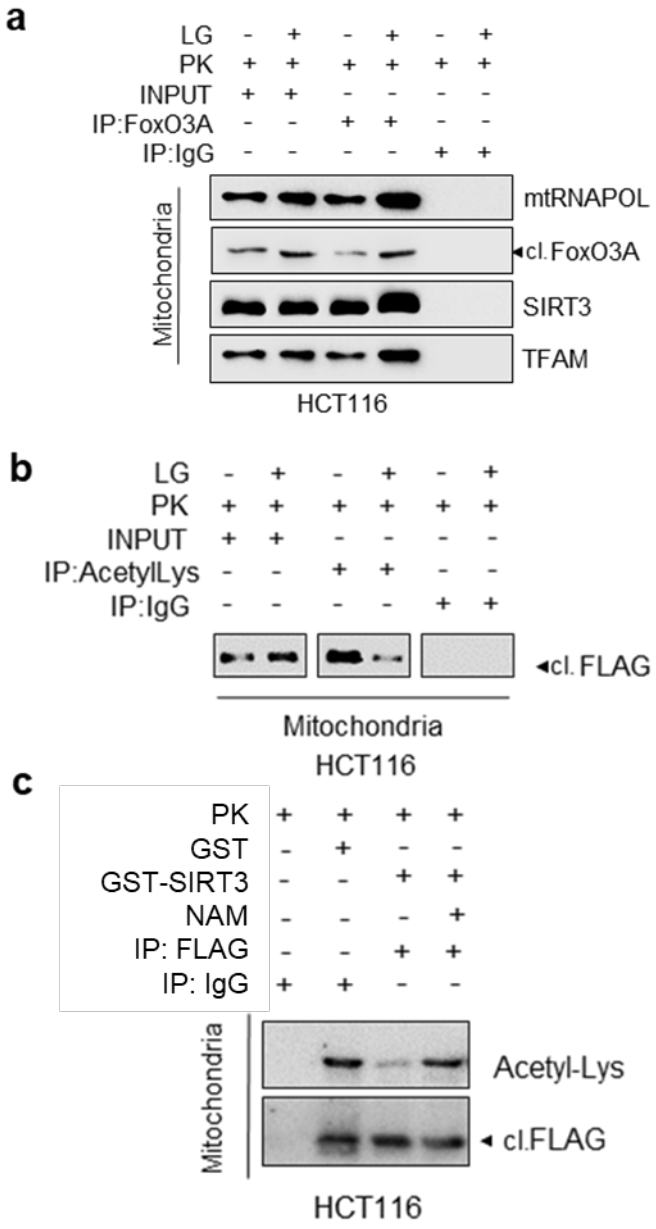


***Figure 4.21 -*** *SIRT3 deacetylates mtFoxO3A.*

*(a) Co-immunoprecipitation analysis with the indicated antibodies of PK-treated HCT116 mitochondrial fractions upon LG (0.75 mM glucose, 24 h). (b) Upon glucose restriction, HCT116 cells were transfected with FoxO3A-FLAG and mitochondrial fraction was isolated and analysed by immunoprecipitation with anti-acetylLysine antibody. (c) In vitro deacetylation assay. FoxO3A-WT-FLAG*

*was transfected in HCT116 cells. Upon LG (24h), the mitochondrial enriched-fraction was purified and treated with Proteinase K to degrade the outer membrane protein. Then it has been immunoprecipitated with anti-FLAG antibody and incubated with recombinant GST-SIRT3, in presence/absence of the Sirtuin inhibitor Nicotinamide (NAM). cl: cleaved FoxO3A-FLAG. The presented results are representative of at least three independent experiments.*

### 4.3.2 Characterization of FoxO3A localisation mutants in a FoxO3A$^{-/-}$ cancer cell line

To further explore FoxO3A function in cancer cells under metabolic stress, and, particularly, to dissect the role of mitochondrial FoxO3A and its possible contribution to nuclear FoxO3A activity, by using the CRISPR/Cas9 system for genome editing (Figure 4.22a), a FoxO3A knockout HCT116 cell line (HCT116 FoxO3A$^{-/-}$) was generated. To validate it, immunoblot analysis was performed on mitochondria isolated from metabolically stressed HCT116 FoxO3A$^{-/-}$cells, with two antibodies detecting the endogenous form of FoxO3A, one directed against the N-terminus, and the other targeting the C-terminal domain. None of them was able to recognize the 90kDa or the 70kDa bands in whole mitochondria of HCT116 FoxO3A$^{-/-}$cells (Figure 4.22b). Additionally, further confirmation was obtained by performing an RT-PCR with specific FoxO3A primers (data not shown).

After the validation of the FoxO3A knock-out model, FoxO3A expression was reconstituted in these cells by transfecting them with different plasmids: the FoxO3A-WT, the non-phosphorylatable mutant FoxO3A-S12A/S30A plasmid and with a newly generated mutant plasmid, FoxO3A-S12D/S30D, where Ser12 and

Ser30 were replaced with aspartic acid residues to mimic Phosphoserines (Figure 4.23a). As shown in Figure 4.23, the phospho-mimetic mutant (FoxO3A-S12D/S30D) is strongly accumulated in the mitochondria, also in the absence of stress (HG). This mutated FoxO3A bound to mtDNA and induced the expression of mitochondrial genes, while the unphosphorylatable mutant (FoxO3A-S12A/S30A) failed to do so (Figure 4.23b-f and 4.24). Importantly, both FoxO3A mutants were still able to enter in the nucleus and bound FHRE sites at the promoters of two well-known FoxO3A target genes, p21 and p27, under metabolic stress (Figure 4.23d).

In the same cellular system, another FoxO3A mutant, FoxO3A-Δ242/271, lacking the nuclear localisation signals (NLS, Tsai et al., 2007), was introduced. This protein was unable to enter in the nucleus (Figure 4.23c) to bind the FHRE sites of p21 and p27 (Figure 4.23e), but was still capable of entering into the mitochondria and bound the FHRE#1-2 sites at the D-loop of mtDNA in metabolically stressed cancer cells (Figure 4.23g).

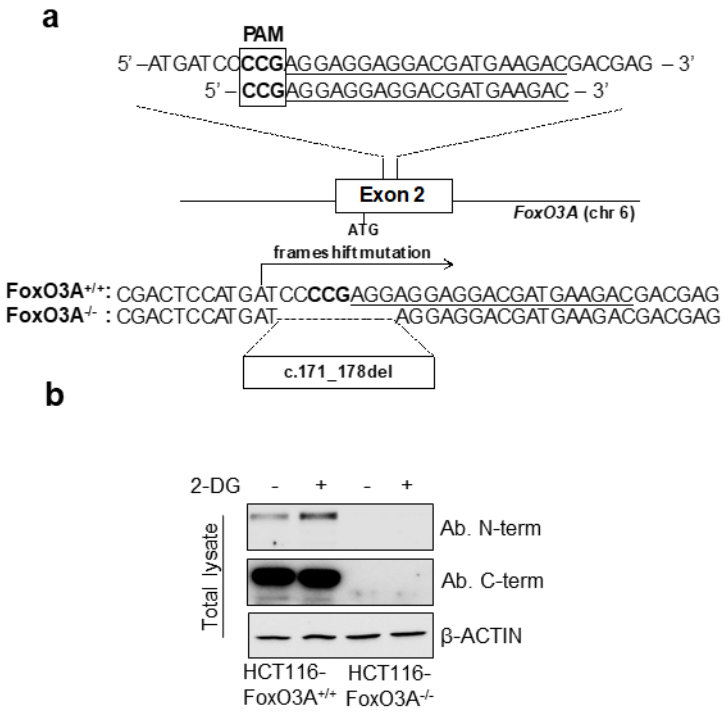


***Figure 4.22 -****Generation of HCT116 FoxO3A$^{-/-}$ by using Crispr-Cas9 system.*

*(a) Scheme of gRNA location in human FoxO3A locus. Targeting sites and proto-spacer adjacent motifs (PAMs) and the deleted region are indicated. (b) Immunoblot analysis of total lysate obtained from HCT116 FoxO3A$^{+/+}$ and HCT116 FoxO3A$^{-/-}$ cells with different anti-FoxO3A antibodies upon 2DG (1 mM, 6h) treatment (Celestini et al., 2018).*

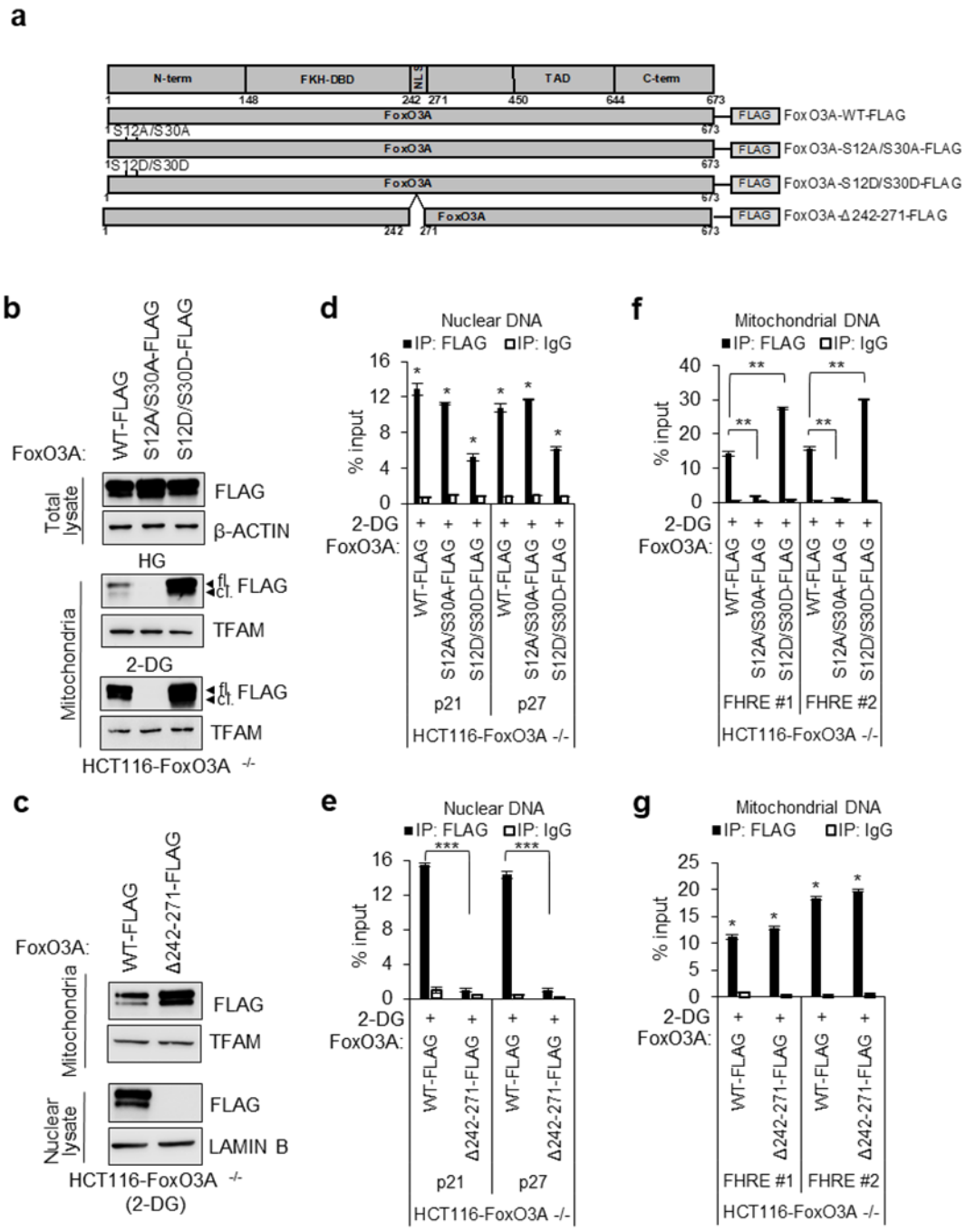


***Figure 4.23-****Mitochondrial-FoxO3A regulates mitochondrial gene expression in metabolically stressed cancer cells.*

*HCT116 FoxO3A$^{-/-}$ cells were transfected with the indicated FoxO3A plasmids for 48h and treated with 2DG (1 mM, 6h), to induce metabolic stress. (a) Immunoblot*

*analysis of total and mitochondrial proteins. (d-g) ChIP analysis of exogenous FoxO3A recruitment at FHRE p21-p27 sites on nuclear DNA (d,e) and FHRE #1-2 sites on mtDNA (f,g). (c) Immunoblot analysis of nuclear and mitochondrial proteins. (d-g) Anti-IgGs were used as controls. (b,c) β-ACTIN, TFAM and LAMIN B were used as total, mitochondrial and nuclear lysate controls, respectively, as appropriate. fl.: full-length FoxO3A; cl.: cleaved FoxO3A; N-term.: N-terminal domain; FKHDBD: forkhead DNA-binding domain; NLS: nuclear localisation signal; TAD: transactivation domain; C-term.: C-terminal domain. The presented results are representative of at least three independent experiments. Where applicable, data are presented as mean±SEM and significance was calculated with Student's t test; *p value < 0.05, **p < 0.01 and ***p < 0.001 (Celestini et al., 2018).*

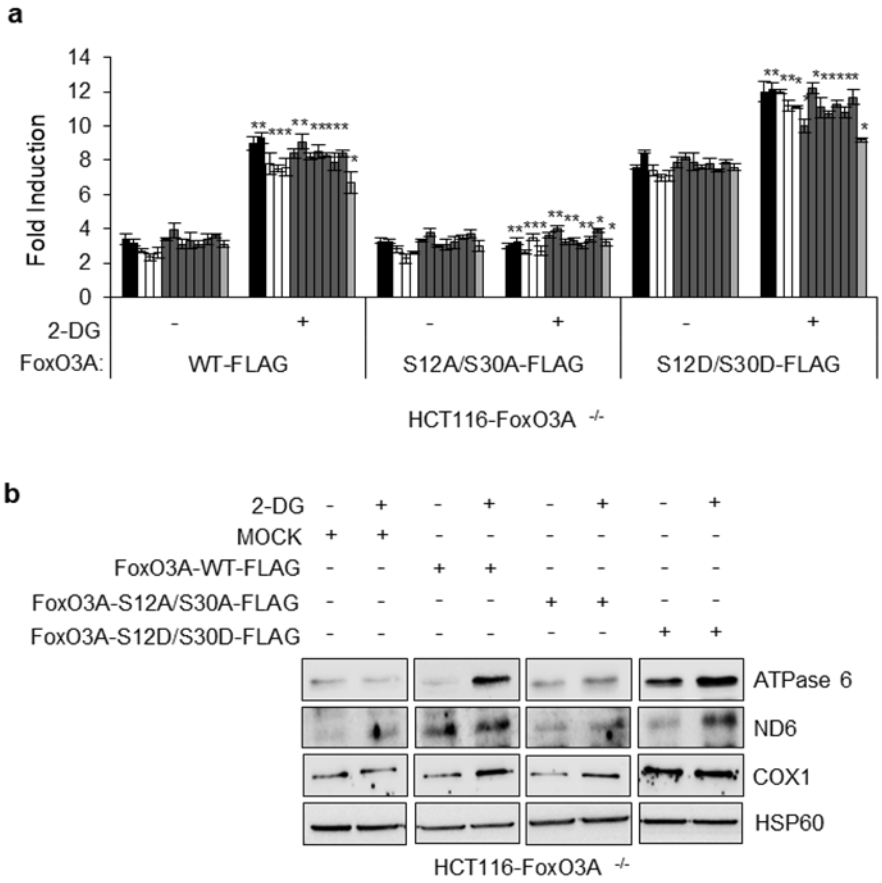


***Figure 4.24 –*** *Mitochondrial-FoxO3A regulates mitochondrial gene expression in metabolically stressed cancer cells (2)*

*(a, b) HCT116 FoxO3A$^{-/-}$ cells were transfected with the indicated plasmids for 48h and treated with 2-deoxy-glucose (2DG, 1 mM, 6h). (a) Mitochondrial gene regulation assessed by RT-PCR. Black bars: ATPase 6 and 8 genes; white bars: COX1, COX2 and COX3 genes; grey bars: ND1, ND2, ND3, ND4, ND4L, ND5, and ND6 genes; light grey bar: cytochrome b gene. (b) Immunoblot analysis of total proteins with the indicated antibodies. HSP60 was used as loading control. The presented results are representative of at least three independent experiments. Where applicable, data are presented as mean ± SEM and significance was*

*calculated with Student's t test. *p value < 0.05 was considered statistically significant (Celestini et al., 2018).*

### 4.3.3 Role of mtFoxO3A in cancer cell response to metabolic stress

As discussed above, a nuclear transcriptional programme of FoxO3A regulates a plethora of functions, such as triggering apoptosis through the expression of genes necessary for cell death. Moreover, its role as tumour suppressor has been widely discussed (Hu et al., 2004; Fei et al., 2009; Han et al., 2018; Jiang et al., 2013; Habashy et al., 2011; Yang et al., 2013; Yu et al., 2016; Liu et al., 2015).

In the effort to dissect FoxO3A nuclear and mitochondrial activities in cancer cells under metabolic stress and chemotherapy, HCT116 FoxO3A$^{+/+}$ and HCT116 FoxO3A$^{-/-}$ cells were cultured in glucose shortage conditions or the presence of drugs currently administered to colorectal cancer patients. The chemotherapic reagents were selected on the bases of the fact that their activity has been shown to involve FoxO3A in cellular models, such as Metformin, Cisplatin, Irinotecan, 5-Fluorouracil and Etoposide (Chiacchiera and Simone, 2010; Fernández de Mattos et al., 2008; Wang et al., 2015; Yu et al., 2016; Germani et al., 2014).

Surprisingly, relative cell viability and relative cell death evaluations revealed that HCT116 FoxO3A$^{-/-}$ cells were more sensitive to metabolic stress and chemotherapeutics than their wild-type isogenic counterparts were. This evidence suggested that the presence of FoxO3A in HCT116 cell line results in resistance and survival. Of note, treatment with Metformin showed opposite results, with HCT116 FoxO3A$^{+/+}$ cells being more sensitive to its administration than HCT116 FoxO3A$^{-/-}$ cells (Figure 4.25a). Moreover, several human cancer cell lines

(HCT116 and HT-29 colorectal cancer cells, DU145 prostate cancer cells, A549 lung cancer cells, MDA-MB-468 breast cancer cells and OVCAR-3 ovarian cancer cells) and HEK-293 cells have been cultured in low glucose conditions to assay their resistance under metabolic stress. Collected results showed that the higher the amount of mtFoxO3A they accumulated, the more they resisted and survived in LG cultures (Figure 4.25b), and supporting the hypothesis that mtFoxO3A could represent a survival factor in cancer cells under metabolic stress. Therefore, FoxO3A expression in HCT116 FoxO3A$^{-/-}$ cells were reconstituted by transfecting them with various FLAG-tagged vectors, encoding for FoxO3A-WT or non-phosphorylatable double mutant FoxO3A-S12A/S30A (impaired in its mitochondrial localisation, but still able to localise into the nucleus and bind target genes, see Figure 4.23), or FoxO3A-Δ242/271 which lacks the NLS (but still able to enter the mitochondria and bind FHRE sites at the mtDNA, see Figure 4.23). Upon transfection, cells were cultured in LG conditions.

Interestingly, the obtained results showed that reconstitution of FoxO3A-WT expression increased cell survival (Figure 4.26a), by results obtained in HCT116 FoxO3A$^{+/+}$ (Figure 4.25a). Of note, FoxO3A-Δ242/271 was still able to rescue metabolic stress-dependent cell death, while the mutant impaired in mitochondrial localisation failed to do so (Figure 4.26a). Furthermore, the analysis of FoxO3A mitochondrial target genes expression (ND6, Cox1) revealed that both the wild-type form and the Δ242/271 mutant were able to activate mitochondrial transcription in surviving cells. Moreover, the FoxO3A-S12A/S30A mutant possibly contributed to apoptosis induction in metabolically stressed cancer cells by promoting the transcription of Bim and the PARP cleavage (Figure 4.26a-b).

This scenario, strongly suggested that the mitochondrial form of FoxO3A in HCT116 cell line is linked to survival.

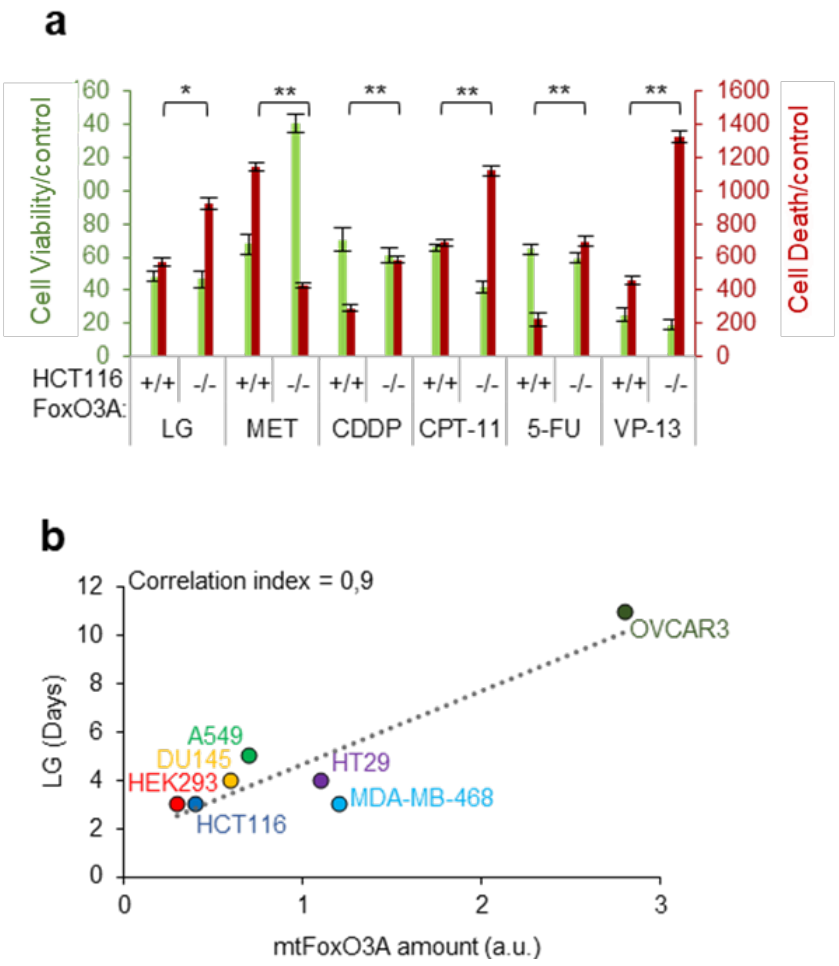


***Figure 4.25 -*** *mtFoxO3A is involved in cancer cell response to metabolic stress.*

*(a) HCT116 FoxO3A$^{+/+}$ and HCT116 FoxO3A$^{-/-}$ cells were subjected to different treatments: glucose restriction (LG, 0.75 mM glucose, 24 h), Metformin (MET, 10 µM, 72 h), Cisplatin (CDDP, 30 µM, 48 h), Irinotecan (CPT-11, 30 µM, 24 h), 5-fluorouracil (5-FU, 2 µM, 24 h) and etoposide (VP-16, 40 µM, 24 h). Chemoterapeutic drugs selected are commonly used in CRC. The selected drug dose have been previously defined by performing dose-response curves and defining the IC50 for each drug. Cell viability/control and cell death/control were*

*calculated as described in Material and Methods. (b) Correlation between LG-resistance (days) and mitochondrial FoxO3A (mtFoxO3A) protein levels in different human cell lines (HCT116 and HT29 colorectal cancer cells, HEK293 embryonic kidney cell, DU145 prostate cancer cells, A549 lung cancer cells, MDA-MB-468 breast cancer cells and OVCAR3 ovarian cancer cells). a.u. arbitrary units. The presented results are representative of at least three independent experiments. Where applicable, data are presented as mean ± SEM and significance was calculated with Student's* t *test;* *$p < 0.05$, **$p < 0.01$, and ***$p < 0.001$ *(Celestini et al., 2018).*

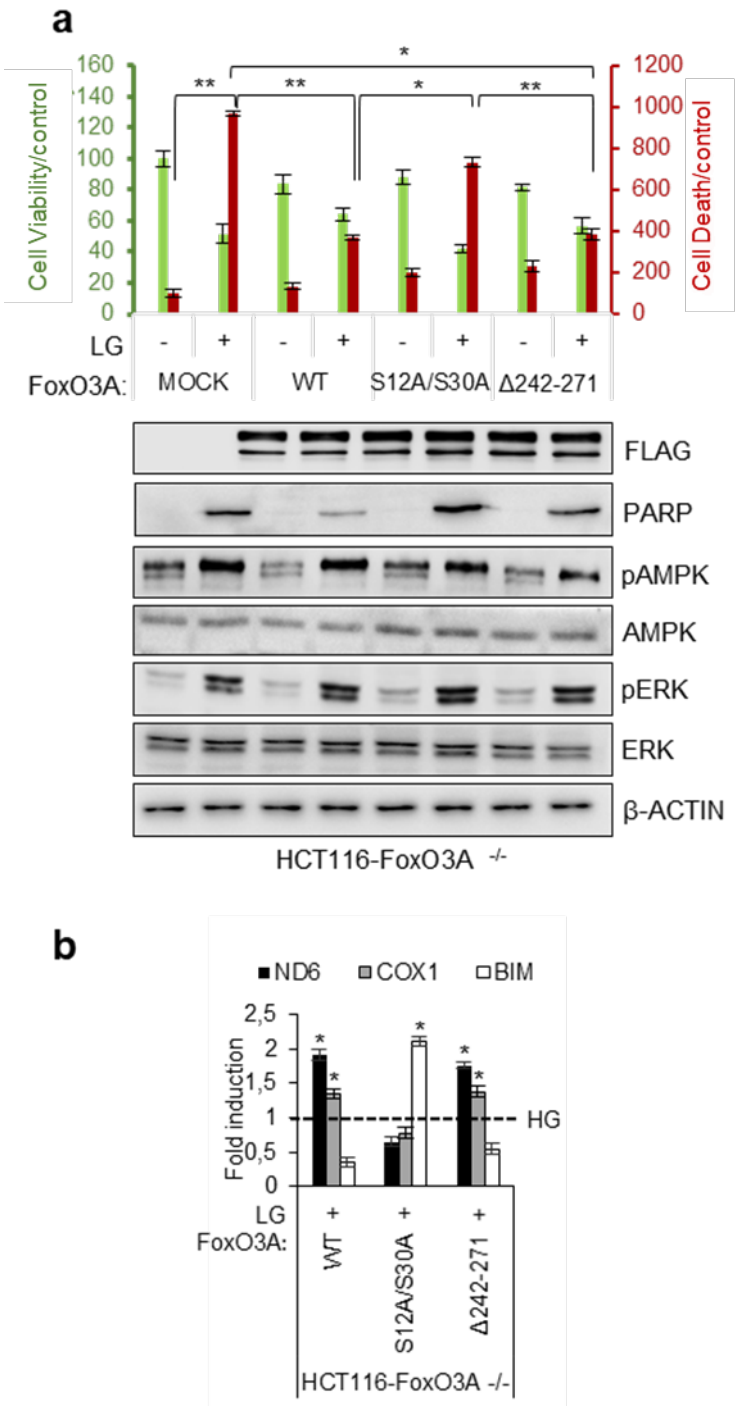


***Figure 4.26 -*** *mtFoxO3A as a survival factor in cancer cells under metabolic stress*

***(****a) HCT116 FoxO3A$^{-/-}$ cells were transfected with the indicated plasmids (48 h) and subjected to LG (24 h). Upper panel: cell viability/control and cell death/control calculated as described in Material and Methods. Lower panel:*

*immunoblot analysis of total proteins. β-ACTIN: loading control. (b) Transcription analysis of selected mitochondrial (ND6 and COX1) and nuclear (BIM) genes by RT-PCR in HCT116 FoxO3A$^{-/-}$ cells transfected with the indicated plasmids (48 h) and subjected to LG (24 h). The presented results are representative of at least three independent experiments. Where applicable, data* are presented as mean ± SEM and significance was calculated with Student's *t* test; $*p < 0.05$, $**p < 0.01$, and $***p < 0.001$ (Celestini et al., 2018).

Subsequently, to confirm these experimental observations, FoxO3A knockout cells were transfected with GFP-tagged vectors encoding for FoxO3A-WT, FoxO3A-S12A/S30A and FoxO3A-Δ242/271, and then subjected to metabolic stress by treating them with the calorie mimetic 2DG. Then, TIME staining was performed to visualise the polarisation status of mitochondrial membranes in GFP-positive cells. TMRE failed to stain mitochondria of HCT116 FoxO3A$^{-/-}$ cells transfected with the FoxO3A-S12A/S30A mutant (Figure 4.27a), as they were undergoing apoptosis (Figure 4.27a). The maintenance of polarised membrane potential, together with functional electron chain transportation, demonstrate that the healthy and functionally active state of mitochondria in metabolically stressed cancer cells is sustained. These results highlighted the functional importance of FoxO3A S12 and S30 residues and of the activation of pathways dictating their phosphorylation (see Figure 4.26a), in cancer cell resistance to metabolic stress. This evidence suggested to assess the effect of the inhibition of the MEK/ERK and/or the AMPK pathway in HCT116 FoxO3A$^{+/+}$ cells cultured in LG conditions. Of note, Trametinib (a MEK inhibitor approved by the FDA for clinical use) and compound C (an AMPK inhibitor) co-treatment was tested on the wild-type HCT116, by using

a citotoxicity assay. Increasing concentrations of both drugs showed a cytotoxic effect in metabolically stressed cancer cells (Figure 4.27b).

To confirm these results *in vivo,* HCT116 FoxO3A$^{+/+}$ cells were injected in nude mice. Then, growing tumours were treated with 2DG (100 mg/kg) intra-peritoneally to induce metabolic stress. At the end of the treatment, mice were sacrificed, and tumours were explanted for immunoblot analysis. The results obtained (shown in Figure 4.28) reveal that the metabolic stress induced the activation of both the MEK/ERK and the AMPK pathways in tumour tissues. Moreover, the stress stimuli induced also the mitochondrial localisation of FoxO3A, similar to what was observed in cancer cells in culture.

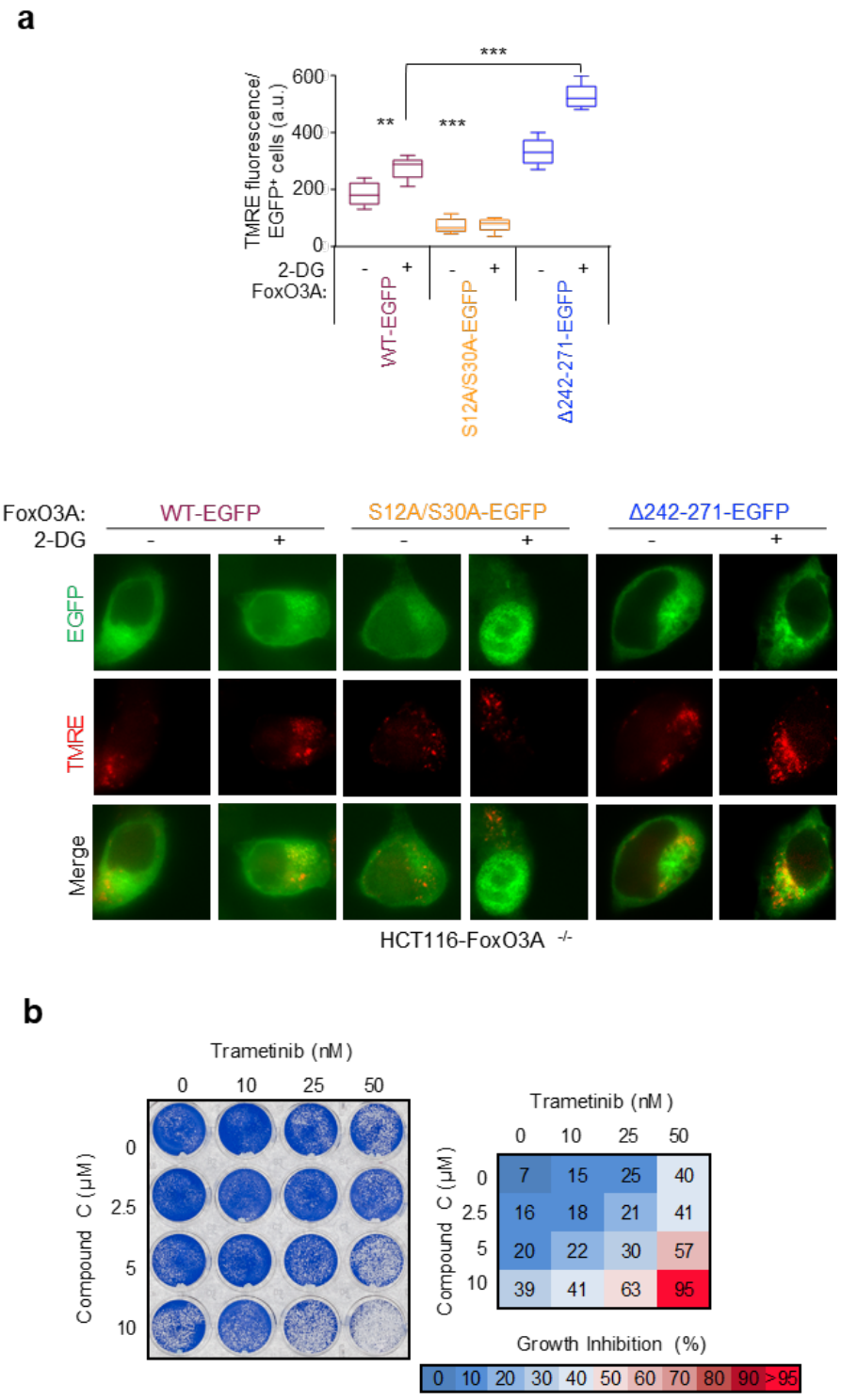


***Figure 4.27–*** *mtFoxO3A as a survival factor in cancer cells under metabolic stress (2)*

*(a) HCT116 FoxO3A$^{-/-}$ cells, transfected with the indicated plasmids (48 h), were subjected to metabolic stress with 2DG (1 mM, 6 h). The graph reflects the quantification of tetramethylrhodamine ethyl ester (TMRE) fluorescence of active mitochondria in transfected cells. (b) Citotoxicity assay on HCT116 FoxO3A$^{+/+}$ cells cultured in LG (24 h) and treated with increasing concentrations of Trametinib and/or compound C, as indicated, for 24 h. Cell growth percent inhibition at each drug concentration is shown. The presented results are representative of at least three independent experiments. Where applicable, data are presented as mean ± SEM and significance was calculated with Student's* t *test;* *p < *0.05,* **p < *0.01, and* ***p < *0.001 (Celestini et al., 2018).*

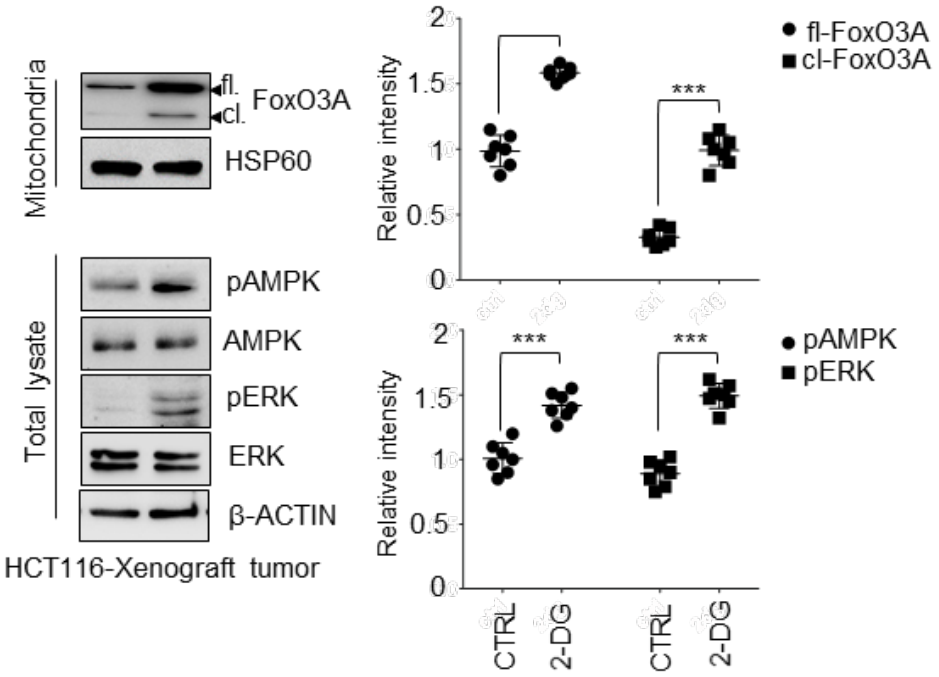


***Figure 4.28-****mtFoxO3A accumulation in vivo under metabolic stress*

*Left panel: immunoblot analysis of total and mitochondrial proteins isolated from tumours (*$n \geq 7$ *for each group) derived from HCT116-xenografted nude mice subjected to 2DG treatment (100 mg/kg, 6 days). β-ACTIN and HSP60 were used as total and mitochondrial loading control, respectively. fl. full-length FoxO3A, cl. cleaved FoxO3A. Right panel: densitometric analysis of full-length and cleaved FoxO3A normalized against the mitochondrial loading control and the results of the densitometric analysis of the phosphorylated-AMPK and ERK normalized against total AMPK and ERK, respectively, and the loading control. The results are representative of at least three independent experiments. Data are presented as mean* $\pm$ *SEM and significance was calculated with Student's* t *test;* *$p < 0.05$, **$p < 0.01$, *and* ***$p < 0.001$*(Celestini et al., 2018).*

### 4.3.4 Role of mtFoxO3A in cancer cell response to chemotherapeutic agents

The results gathered in metabolically stressed cancer cells, the role of FoxO3A-WT, FoxO3A-S12A/S30A and FoxO3A-Δ242/271 in the response of reconstituted HCT116 FoxO3A$^{-/-}$ cells to chemotherapeutic agents was evaluated. Specifically, FoxO3A knockout HCT116 cells were transfected with the relevant FLAG-tagged vectors and then cultured in the absence or the presence of Irinotecan (CTP-11), Cisplatin (CDDP), 5-Fluorouracil (5-FU) or Etoposide (VP-16). Consistent with data obtained in the multi-drug screening performed in HCT116 FoxO3A$^{-/-}$ vs HCT116 FoxO3A$^{+/+}$ cells (see Figure 4.25a), reconstitution of FoxO3A-WT expression resulted in increased survival (Figure 4.29). Moreover, in line with what was observed in metabolically stressed cells, the evaluation of the mitochondrial localisation-impaired non-phosphorylatable mutant (FoxO3A-S12A/S30A) revealed that it was unable to rescue chemotherapy-induced apoptosis (4.29a-b, 4.30). On the other hand, the mutant could activate Bim transcription to contribute to the apoptotic response (Figure 4.29b). Of note, the ΔNLS mutant (FoxO3A-Δ242/271) behaved similar to FoxO3A-WT, and both were able to activate mitochondrial gene expression in chemotherapy-induced cellular stress (4.29b). Importantly, the molecular analysis of transfected HCT116 FoxO3A$^{-/-}$ cells showed activation of the MEK/ERK, but not the AMPK pathway, in response to chemotherapy (Figure 4.29a, lower panel). Indeed, only Serine 12 of FoxO3A is required to elicit chemoresistance in these conditions (Figure 4.29c). Of note, the FDA-approved MEK inhibitor Trametinib and CPT-11 co-treatment was tested on

the wild-type HCT116. Results obtained showed a additive cytotoxic effect in HCT116 FoxO3A$^{+/+}$ cancer cells (Figure 4.31b).

To validate the obtained experimental observation *in vivo*, HCT116 FoxO3A$^{+/+}$ cells were injected in nude mice to generate HCT116-xenograft tumour model. The mice were treated with Cisplatin (2 mg/kg) that was given intra-peritoneally once every three days. At the end of the treatment, mice were sacrificed and tumours explanted for immunoblot analysis. Consistently with the observation made in cell culture, the analysis revealed that chemotherapy-induced the accumulation of FoxO3A into the mitochondria and, at the same time, the activation of the MEK/ERK. On the other hand, the AMPK pathway is not activated (Figure 4.31a).

Briefly, the data collected show that, in metabolically stressed cancer cells, the activation of MEK/ERK and AMPK - which phosphorylate Serine 12 and 30 respectively- induces the recruitment and import of FoxO3A to the mitochondria. Here, the protein is cleaved to reach mitochondrial DNA and activate its expression to support mitochondrial metabolism and cell survival.

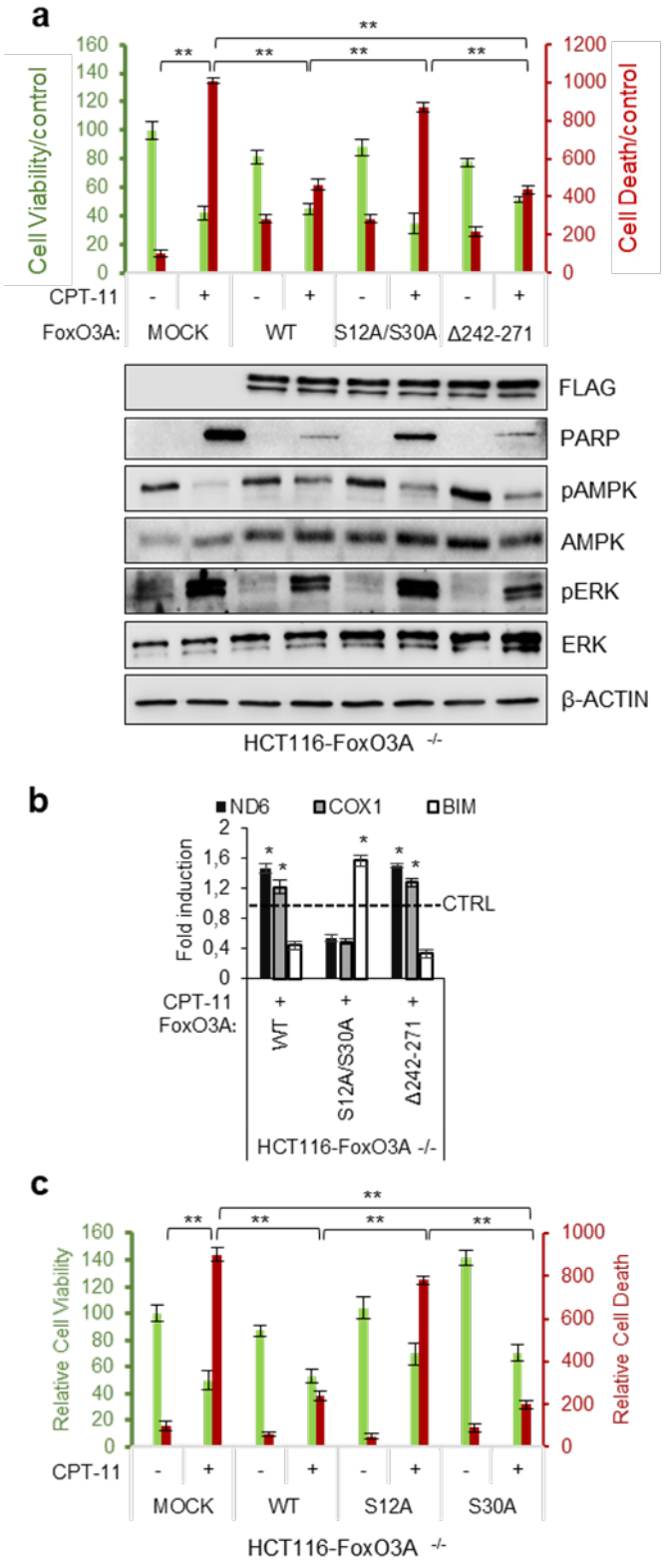


***Figure 4.29 -*** *mtFoxO3A is involved in chemoresistance.*

*HCT116 FoxO3A$^{-/-}$ cells were transfected with the indicated plasmids for 48 h and then treated with Irinotecan (CPT-11, 30 μM, 24 h). (a) Upper panel: r Cell*

*viability/control and cell death/control calculated as described in Material and Methods. Lower panel: immunoblot analysis of total proteins. β-ACTIN: loading control. (b) Transcription analysis of selected mitochondrial (ND6 and COX1) and nuclear (Bim) genes by RT-PCR. (c) HCT116 FoxO3A$^{-/-}$ cells were transfected with the indicated plasmids for 48 h and then treated with Irinotecan (CPT-11, 30 μM, 24 h). (c) HCT116 FoxO3A$^{-/-}$ cells were transfected with the indicated plasmids for 48h and then treated with Irinotecan (CPT-11, 30 μM, 24h). Cell viability/control and cell death/control were calculated as described in Material and Methods. The presented results are representative of at least three independent experiments. Data are presented as mean ± SEM and significance was calculated with Student's t test. *p value < 0.05 and **p < 0.01 were considered statistically significant (Celestini et al., 2018).*

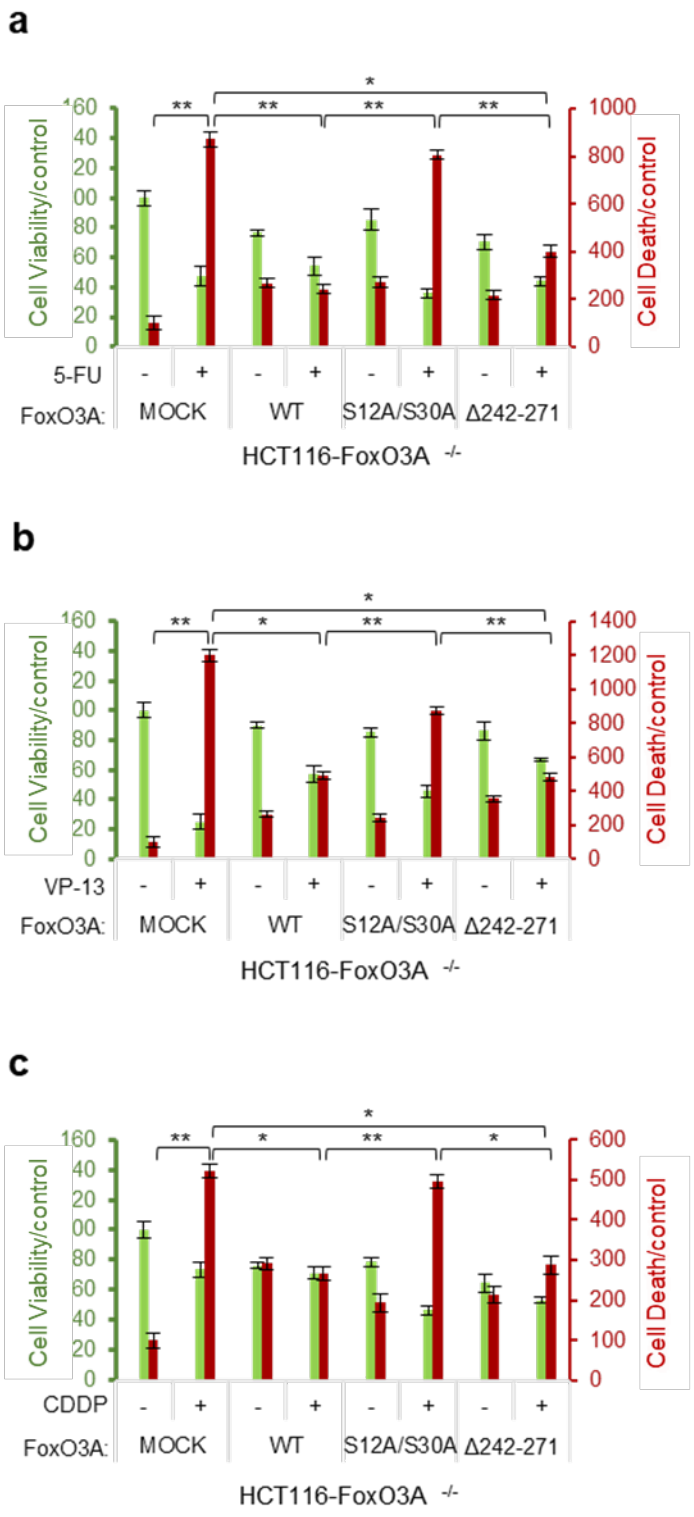


***Figure 4.30 -*** *mtFoxO3A is involved in cancer cell response to chemotherapeutic agents.*

*HCT116 FoxO3A$^{-/-}$ cells were transfected with the indicated plasmids for 48h. Upon treatment with 5-Fluorouracil (5-FU, 2 μM, 24h) (A), Etoposide (VP-16, 40 μM, 24h) (B) or Cisplatin (CDDP, 30 μM, 48h) (C), Cell viability/control and cell death/control were calculated as described in Material and Methods. The drugs concentrations selected have been previously defined by using dose-response curves. The presented results are representative of at least 3 independent experiments. Data are presented as mean ± SEM and significance was calculated with Student's t test. *p value < 0.05 and **p < 0.01 were considered statistically significant (Celestini et al., 2018).*

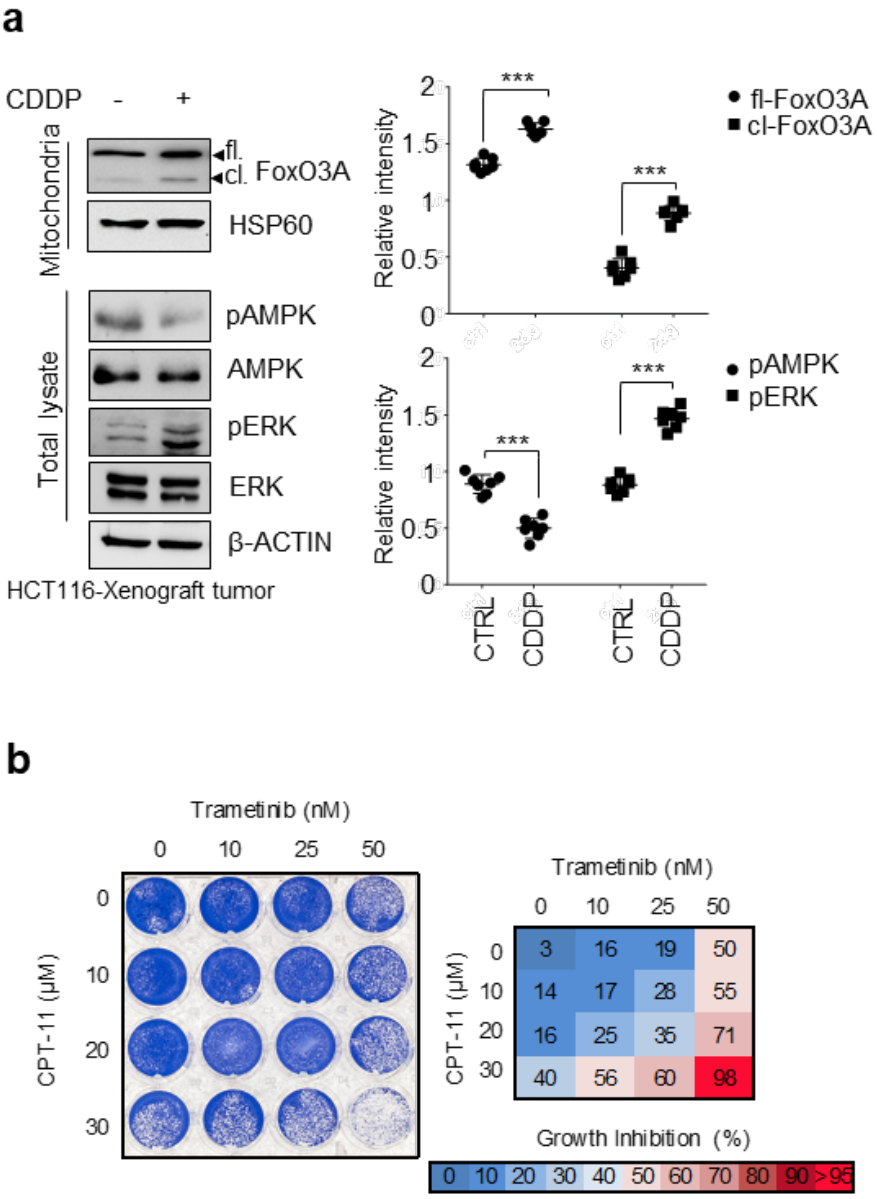


***Figure 4.31-*** *mtFoxO3A is involved in cancer cell response to chemotherapeutic agents (2)*

*(a) Left panel: immunoblot analysis of total and mitochondrial proteins isolated from tumours (n ≥ 7 for each group) derived from HCT116-xenografted nude mice subjected to Cisplatin treatment (CDDP, 2 mg/kg, 6 days). β-ACTIN and HSP60 were used as total lysate and mitochondrial fraction controls, respectively. Right panel: densitometric analysis of full-length and cleaved FoxO3A normalized*

*against the mitochondrial fractionation loading control and the results of the densitometric analysis of the phosphorylated forms of AMPK and ERK normalized against total AMPK and ERK, respectively, and the loading control. (b) Citotoxicity assay on HCT116 FoxO3A$^{+/+}$ cells treated with increasing concentrations of Trametinib (24 h) and/or Irinotecan (24 h), as indicated. The drug concentrations used have been previously defined by using a dose-response curve. Cell growth percent inhibition at each drug concentration is presented. The presented results are representative of at least three independent experiments. Data are presented as mean ± SEM and significance was calculated with Student's t test. *p value < 0.05 and **p < 0.01 were considered statistically significant (Celestini et al., 2018).*

### 4.3.5 Role of mtFoxO3A in cancer cell response to chemotherapeutic agents: the response to Metformin

The characterisation of HCT116 FoxO3A$^{+/+}$ and HCT116 FoxO3A$^{-/-}$ cells revealed an opposite behaviour for Metformin treatment compared with metabolic stress and chemotherapeutic agents (4.25a). Moreover, molecular analysis of HCT116 FoxO3A$^{+/+}$ cells indicated that Metformin only activates AMPK and induces cells to undergo apoptosis (Figure 4.32a). Therefore, further investigation was required. As prevoiusly, in HCT116 FoxO3A$^{-/-}$ cells were transfected with various FLAG-tagged vectors: FoxO3A-WT, the non-phosphorylatable double mutant FoxO3A-S12A/S30A and FoxO3A-ΔNLS (Figure 4.23).

Interestingly, the reconstitution of FoxO3A expression with the wild-type form or the ΔNLS mutant significantly increased cell death (Figure 4.32b), supporting the

preliminary observations and suggesting that mtFoxO3A is required for the Metformin-induced apoptosis. Indeed, reconstitution with a vector encoding for the FoxO3A-S30A mutant was sufficient to reduce cell death to the levels of mock-transfected cells. These results indicate that Metformin can induce apoptosis via the AMPK-mtFoxO3A axis. Furthermore, the co-treatment of Metformin with a chemotherapeutic drug (Irinotecan) was assessed by performing a citotoxicity assay. Consistently with data obtained in FoxO3A knockout cells transfected with FoxO3A mutants, results obtained showed a additive cytotoxic effect of Metformin with Irinotecan in HCT116 FoxO3A$^{+/+}$ cells (Figure 4.32c).

To summerize, in cancer cells treated with chemotherapeutic agents, accumulation of FoxO3A into the mitochondria promoted survival and chemo-resistance in a MEK/ERK-dependent manner. Moreover, mitochondrial FoxO3A seems to be required for apoptosis induction by Metformin.

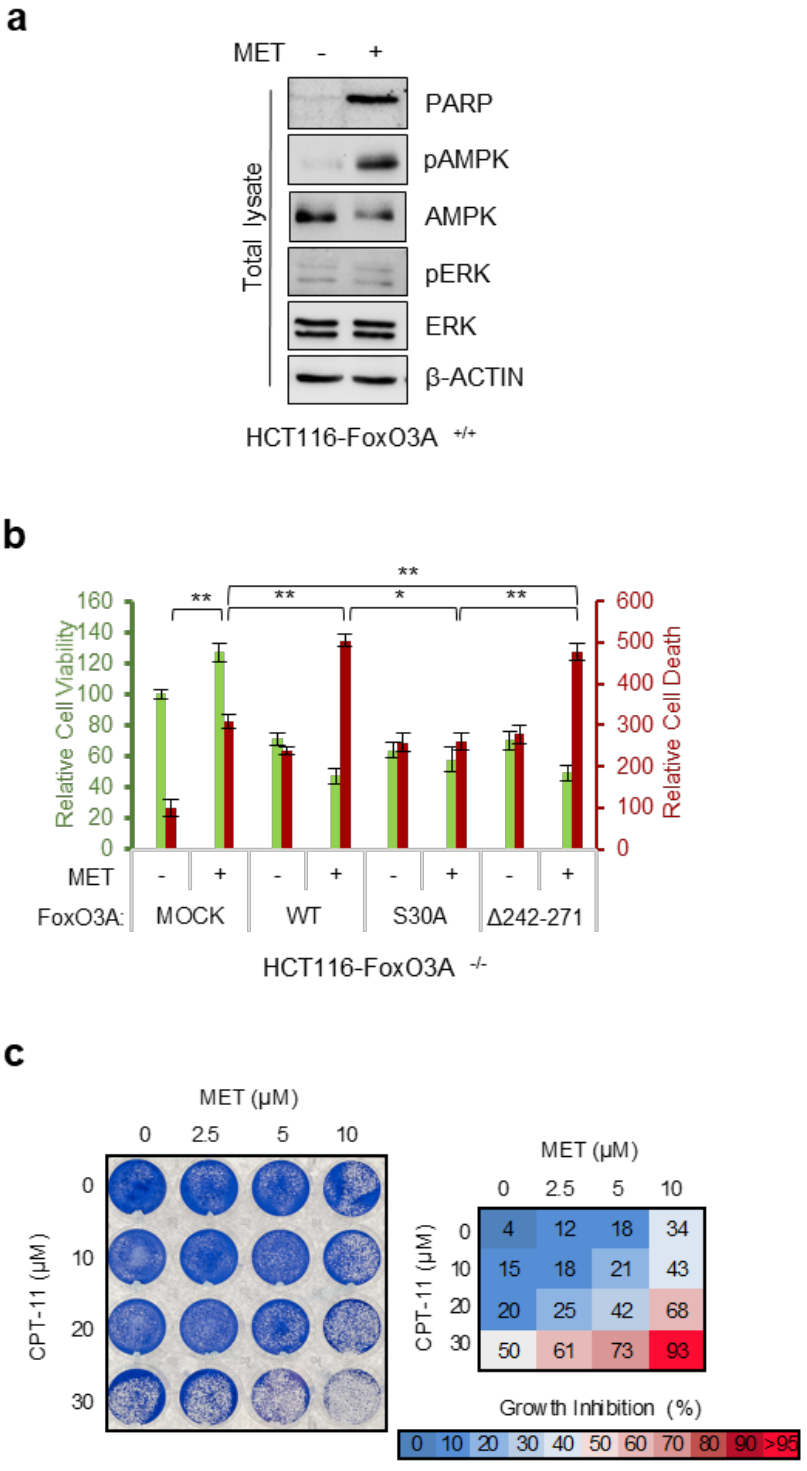


***Figure 4.32-****mtFoxO3Ais required for Metformin-induced apoptosis*

*(a) Immunoblot analysis of total proteins isolated from HCT116 FoxO3A$^{+/+}$ cells upon Metformin treatment (MET, 10 μM, 72 h). β-ACTIN: loading control. (b)*

*HCT116 FoxO3A$^{-/-}$ cells were transfected with the indicated plasmids for 48 h and then treated with Metformin (MET, 10 μM, 72 h). Cell viability/control and cell death/control were calculated as described in Material and Methods. (C) Citotoxicity assay on HCT116 FoxO3A$^{+/+}$ cells treated with increasing concentrations of Metformin (24 h) and/or Irinotecan (24 h), as indicated. Cell growth percent inhibition at each drug concentration is presented. The data presented are the mean of at least three independent experiments. Where applicable, data are presented as mean ± SEM and significance was calculated with Student's t test; *p < 0.05, **p < 0.01, and ***p < 0.001 (Celestini et al., 2018)*

# Chapter 5 - Discussion

.

# 5 Discussion

FoxO transcription factors activity plays a major role in several biological processes, including cell cycle progression, proliferation, DNA damage-repair, oxidative stress resistance, metabolism and cell death. Therefore, as a key element of the molecular machinery driving cells towards survival or death, the regulation of FoxOs activity in response to extracellular cues is fundamental in lifespan, aging and cancer. A wide range of external stimuli controls FoxOs, including insulin, growth factors, nutrients, cytokines and oxidative stress, which affect FoxO protein amount, subcellular localisation, binding to the DNA and transcriptional efficiency. These regulation mechanisms are mediated by signalling pathways that eventually induce changes in PTMs on FoxO proteins, which, in turn, result in changes in subcellular localisation. In 2008, Calnan and Brunet proposed a fascinating model which interprets the combinations of the PTMs acting on FoxOs as a functional "FoxO code", modulating their functions. Among multiple PTMs, the main one is phosphorylation, which is an evolutionarily conserved mechanism from invertebrates to humans. Specifically, it is often considered as the most critical one for FoxO and cell fate. For instance, AKT, SGK, Casein kinase-1 (CK1), Dual-specificity Tyrosine (Y)-phosphorylation-regulated kinase (DYRK1A) and IKKα directly phosphorylate FoxOs thus promoting their binding to the 14-3-3 nuclear export protein. On the other hand, JNK1 phosphorylates the 14-3-3 protein thereby inhibiting its binding to FoxOs and promoting their nuclear localisation (Calnan and Brunet, 2008).

Interestingly, novel subcellular localisation of one of the four members of the human FoxO family, FoxO3A, is described (Peserico et al., 2013). Glucose restriction triggers the AMPK-dependent mitochondrial accumulation of FoxO3A. Once into the mitochondria, FoxO3A can form a transcriptionally active complex with mtRNAPol and SIRT3, the latter of which is the primary mitochondrial protein deacetylase and can efficiently deacetylate FoxO3A (Sundaresan et al., 2009). This event finally leads to increased mitochondrial respiration to sustain energy metabolism upon nutrient shortage. Importantly, SIRT3 activity, even if it is not required for FoxO3a mitochondrial accumulation, is needed for FoxO3A binding to mtDNA and the expression of the mitochondrial-encoded core or catalytic subunits of the OXPHOS machinery. These findings uncovered an unprecedented mechanism and raised the interest in the existence of a mitochondrial tale of the "FoxO3A code", which would imply fine-tuned regulation processes through specific post-translational modifications.

In the last decade, due to their cytostatic and apoptotic abilities, FOXOs have been widely investigated as tumour suppressors. Among the FoxOs, the best characterised in several human cancers is FoxO3A (Fei et al., 2009; Jiang et al., 2013; Habashy et al., 2011; Yang et al., 2013; Liu et al., 2015), while FOXO1 inactivation has been associated with human cervical cancer (Zhang et al., 2015). Fascinatingly, recent experimental evidences also showed that overexpression of FoxO3A promotes cancer cell growth and tumour progression in different human cancer such as hepatocellular carcinoma, breast cancer, blood cancer and glioblastoma (Han et al., 2018; Yu et al., 2016, Storz et al., 2009; Scisci et al., 2013; Ahn et al., 2018; Liang et al., 2013; Qian et al., 2017; Rehman et al., 2018). Taken

together, these studies support the idea of a more complex role of FoxO3A in cancer progression, which requires further investigations. Data collected in this project contribute to the interpretation of the dichotomic role of FoxO3A in cancer. On one hand, data elucidated the contribution of mtFoxO3A in cancer cell survival and chemo-resistance. On the other hand, nuclear FoxO3A has been confirmed as a master regulator of the expression of fundamental genes required for cell cycle arrest and cell death. Specifically, when the mitochondrial rescue mechanism is impaired, FoxO3A accumulates into the nucleus and induces the expression of genes involved in cell cycle control (p21, p27) and apoptosis (Bim) upon metabolic or therapy-dependent stress induction.

Recent advances in cancer understanding suggest reconsidering the "Warburg effect" in its interpretation of the mitochondrial role in tumorigenesis. Indeed, several pieces of evidence indicate that, while aberrant tumour cell growth is frequently associated with alterations of biochemical metabolism, mitochondrial function is not usually impaired (Cairns, Harris, Mak 2011; DeBernardinis and Chandel, 2016). Even if there is not any positive selection for mitochondrial respiration defects during tumour evolution, aerobic glycolysis is not generally caused by impairment of respiratory functions in mitochondria (Ju et al., 2014, Stewart et al., 2015). On the contrary, increased energy production, sufficient macromolecular biosynthesis and maintenance of redox balance are often observed in human cancers (Wallace CD, 2012; Weinberg and Chandel, 2015; Zong, Rabinowitz, White, 2016). In addition to respiration, mitochondria are the powerhouse for bioenergetics and biosynthetic pathways, being responsible for various molecular processes that are critical in the tumorigenesis process, which

requires a high level of flexibility to adapt to cellular and environmental alterations. Thus, understanding the role of mitochondrial function in cancer might reveal novel approaches to targeted cancer therapy. Indeed, recent reports suggested that cancer cells are highly susceptible to the inhibition of oxidative phosphorylation, induced by biguanides and other complex I-targeting drugs. Of note, this kind of agent can act as sensitisers to cancer therapeutics and chemotherapy, as discussed above in section 1.1.5 (Kuntz et al., 2017; Tan et al., 2017).

On light of these considerations, the identification of a novel mitochondrial arm of the AMPK-FoxO3A axis aimed to sustain cellular metabolism upon nutrient shortage in normal cells (Peserico et al., 2013) represents an attractive incentive to investigate the existence of a similar pathway also in cancer cells. Thus, in this study, the mitochondrial form of Foxo3A, together with relevant signalling cascades, has been explored in tumour cells subjected to metabolic stress, and cancer therapeutics. The investigation revealed the involvement of the MEK/ERK pathway, as well as the AMPK one, in the mitochondrial signalling of FoxO3A, which results in support of the healthy and functionally active state of mitochondria in metabolically stressed cancer cells. These results might have important implications from a pharmacological point of view. As discussed above (see paragraph 1.3), in humans AMPK phosphorylates FoxO3A at least at six known residues (Greer et al., 2007a-b, Greer et al., 2009). Data presented here show a novel AMPK phosphorylation site, the Serine 30, on the N-terminal domain of FoxO3A, evolutionarily conserved from humans to fruit flies (*D. melanogaster*). The newly identified Serine is required in cancer cells for FoxO3A recruitment at the mitochondrial surface before undergoing translocation and processing, upon

nutrient shortage. The investigation also revealed a novel target site of ERK, the Serine 12, which is specific to human FoxO3A.

Interestingly, in line with previous findings showing that genetic silencing of AMPK was sufficient to prevent mtFoxO3A accumulation in normal cells subjected to nutrient deprivation (Peserico et al., 2013), here it has been show that normal cells and tissues under metabolic stress required only the AMPK signal on S30 to direct FoxO3A into the mitochondria. However, ERK involvement in FoxO3A mitochondrial localisation is an exclusive requirement of tumour cells. This critical difference between normal and cancer cells suggests an attractive strategy to be explored for cancer therapy.

Moreover, in colorectal cancer cells treated with selected chemotherapeutic agents, mtFoxO3A is responsible for mitochondrial function preservation, chemotherapy resistance and cell survival in a MEK/ERK-dependent manner (Figure 5.1). Chemotherapeutic agents do not activate AMPK (see Figure 4.29). Keeping in mind that several MEK inhibitors -such as PD0325901, Selumetinib and Trametinib- are currently under active development for different kind of cancers (Liu et al., 2018), it worth underling that MEK inhibition by Trametinib enhances cell death when combined with chemotherapeutics in CRC cells (see Figure 4.31). Combination therapy with MEK inhibitors and chemotherapeutic agents is predicted to overcome resistance mechanisms and potentiates the antitumour activity of each agent, and various phase II/III trials based on such approaches are currently ongoing (Zhaoa and Adjei, 2014). Addittionally, ERK1/2 selective inhibitors are gaining increasing interest, especially to overcome the acquired drug resistance induced by upstream kinases -MEK- inhibitors (Liu et al., 2018). The

potential of the combined therapy with MEK or ERK inhibitors with chemotherapy in CRC therapy to overcome drug resistance should be further deepened.

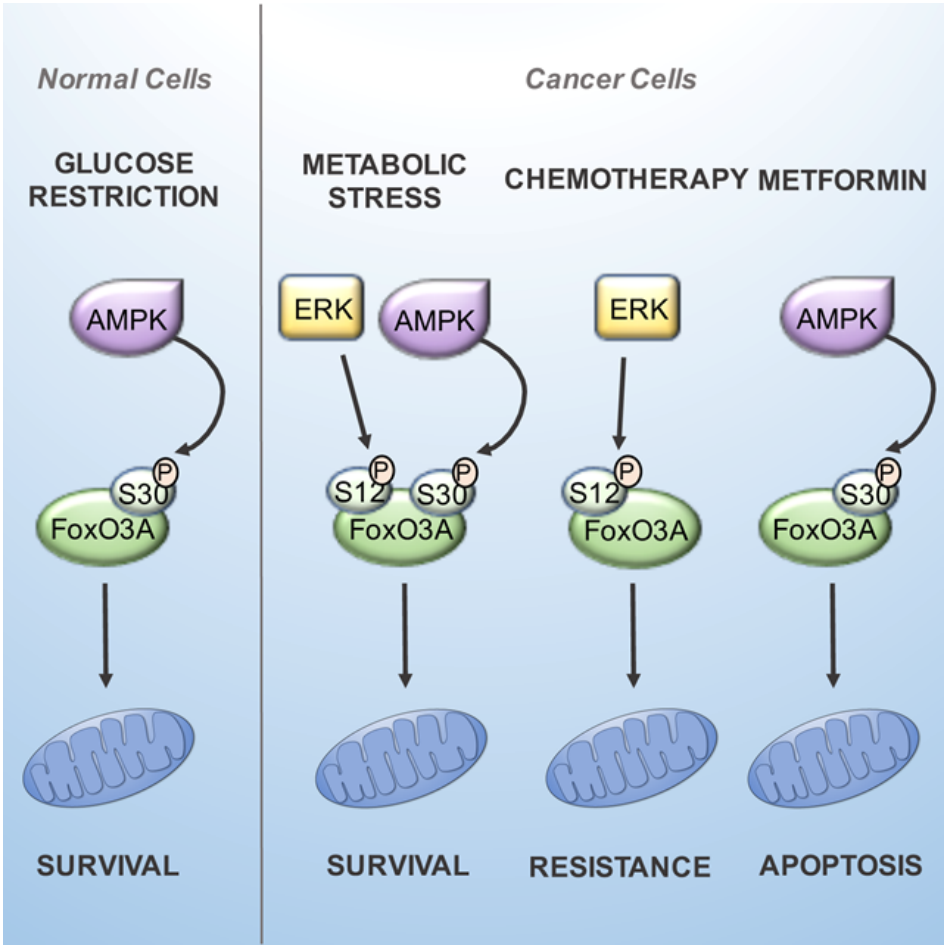


***Figure 5.1 -*** *FoxO3A as a survival factor in metabolically stressed cancer cells.*

*Normal cells and tissues under metabolic stress require only the AMPK signal on S30 to direct FoxO3A into the mitochondria. It seems that ERK involvement in FoxO3A mitochondrial localization is exclusive to tumour cells, which reveals a critical difference between normal and cancer cells that could be exploited for cancer therapeutics. In metabolically stressed cancer cells, FoxO3A is recruited to the mitochondria through activation of MEK/ERK and AMPK, which phosphorylate Serine 12 and 30, respectively, on FoxO3A N-terminal domain.*

*Subsequently, FoxO3A is imported and cleaved to reach mitochondrial DNA, where it activates expression of the mitochondrial genome to support mitochondrial metabolism. In cancer cells treated with chemotherapeutic agents, accumulation of FoxO3A into the mitochondria promoted survival in a MEK/ERK-dependent manner, while mitochondrial FoxO3A was required for apoptosis induction by Metformin. Image from Celestini et al., 2018.*

As AMPK is a well-established tumour suppressor through LKB1/AMPK pathway ability to restrain tumour growth, it may appear not straightforward to reconcile this biological activity with its involvement in the promotion of cancer cell survival. However, the evidence collected in this project can reinforce recent studies showing AMPK ability to act also as a "tumour promoter", depending on metabolic conditions and surrounding microenvironment of cancer cells (Zadra et al., 2015). Moreover, the dual role of AMPK in cancer is supported by the results of the use of AMPK modulators in cancer therapy, such as Metformin. The analysis of HCT116 FoxO3A$^{+/+}$ versus HCT116 FoxO3A$^{-/-}$ cells suggests that AMPK-mtFoxO3A axis may be required for Metformin to extensively induce apoptosis in cancer cells. Metformin is a biguanide drug commonly used in the treatment of diabetes, which has been proven to have anticancer activity in diabetic patients (Evans et al., 2005; Chae et al., 2016; Wheaton et al., 2014). Clinical studies showed that Metformin could reduce the risk of recurrence and cancer-specific mortality in patients with CRC and concurrent diabetes (Lee et al., 2012a; Lee et al., 2012b). The various direct and indirect mechanisms for the anti-tumour effect of Metformin are still under strong debate, as briefly mentioned before (Paragraph 1.1.5). Specifically, it has been proposed that the anti-proliferative effect of

Metformin is due to a specific action of the biguanide on cancer stem cells (Kim et al., 2017). Other studies are aimed to ascertain if Metformin anticancer properties are linked to its systemic effect on glucose and insulin levels or are mediated by mitochondrial electron transport chain (ETC) targeting, as Metformin inhibits the activity of Complex I of the mitochondrial machinery responsible for oxidative phosphorylation. With a similar mechanism, Metformin induces AMPK activation in cultured cells (Wheaton et al., 2014). Importantly, several phases II/III clinical trials are currently evaluating the Metformin efficacy in association with chemotherapeutic agents as well as its chemoprevention activity as a single agent (Evans et al., 2005; Chae et al., 2016). Experimental evidence collected in this study showed that in CRC cells Metformin activity is mediated by AMPK and requires mt-FoxO3A to elicit its pro-apoptotic effect in cancer cells. In FoxO3A$^{-/-}$ cell model, Metformin treatment combined with Irinotecan lead to an enhanced cytotoxic effect (see Figure 4.32). Our data described a kind of "vicious circle" in which Metformin activates AMPK, which in turn triggers FoxO3A translocation to the mitochondria resulting in increased oxidative phosphorylation (OXPHOS), which is blocked by Metformin inhibition of Complex I. Therefore, Metformin could be useful to circumvent mtFoxO3A-dependent chemo-resistance and sensitise cancer cells to chemotherapy, by enforcing the accumulation of FoxO3A into the mitochondria. Consequentially, this event induces an increase in mitochondrially encoded protein levels, in mitochondria in which oxidative phosphorylation is blocked by complex I inhibition. Thus, OXPHOS inhibitors could be adopted as a pharmacological attempt to sensitize cells to chemotherapy.

Addittionally, *in vivo* Metformin-mediated suppression of tumour growth may be due on AMPK down-regulation. Cells characterised by defective LKB1/AMPK pathway, upon metabolic stress induced by Metformin treatment, show impaired ability to restore ATP levels. Consequently, these cells are more susceptible to cell death. In cancer therapy, the chemotherapeutic drug Sunitinib inhibits AMPK. The combinatorial treatment of Sunitinib and Metformin and, in general, the combined use of Metformin with agents that inhibit AMPK could be clinically relevant (Laderoute et al., 2010).

Taken together, data from literature and data collected in this thesis encourage to deepen the potential relevance in cancer therapy of the combination of chemotherapic agents that can inhibit AMPK with other AMPK-activating drugs (Metformin, salicylate etc...), to sensitise cancer cells to chemotherapy and overcome the drug-resistance.

# Chapter 6–Concluding remarks

# 6 Concluding remarks

The findings presented in this thesis shed light on the role of some major players involved in the mitochondrial signalling of FoxO3A in cancer cells. Through data collected in this project, we identified new players and mechanism of action, with the aim to propose and test new cancer therapy strategy.

A therapeutic combination involving inhibitors targeting the MAPK pathway (MEK and/or ERK), and/or OXPHOS modulators represent an opportunity to overcome acquired resistance to current treatments.

From the perspective of the molecular biology of mtFoxO3A, many aspects may be elucidated yet to determine the hierarchy between the identified signalling pathways them and/or their possible tissue-specificity. Moreover, there could be other potential key proteins actively involved in signalling pathways targeting FoxO3A N-terminus and eventually modulating its mitochondrial localisation and function. Pharmacologically, these investigations will be instrumental in devising personalised therapeutic strategies – employing molecularly targeted drugs – aimed at manipulating cellular metabolism to counteract cancer initiation and progression.

# Chapter 7 - Bibliography

# 7 Bibliography


- Ahn B.H., Kim H.S., Song S., Lee I.H., Liu J., Vassilopoulos A., et al. (2008). A role for the mitochondrial deacetylase Sirt3 in regulating energy homeostasis. Proc Natl Acad Sci U S A. 105(38), 14447-52.
- Ahn H., Kim H., Abdul R., Kim Y., Sim J., Choi D., Paik S.S.,et al. (2018). Overexpression of Forkhead Box O3a and Its Association With Aggressive Phenotypes and Poor Prognosis in Human Hepatocellular Carcinoma, American Journal of Clinical Pathology, 149(29), 117–127
- Alberts B., Johnson A., Lewis J., et al. (1994). Molecular Biology of the Cell. New York: Garland Publishing Inc. 32-36.
- Alexeyev M.F. (2009). Is there more to aging than mitochondrial DNA and reactive oxygen species? FEBS J, 276(20): 5768–5787.
- Alhazzazi T.Y., Kamarajan P., Verdin E., Kapila Y.L. (2011). SIRT3 and cancer: tumor promoter or suppressor? Biochim Biophys Acta. 1816(1), 80-8.
- Alhazzazi T.Y., Kamarajan P., Verdin E., Kapila Y.L. (2013) Sirtuin-3 (SIRT3) and the Hallmarks of Cancer. Genes Cancer. 4(3-4), 164-71.
- Allison S.J., Milner J. (2007) SIRT3 is pro-apoptotic and participates in distinct basal apoptotic pathways. Cell Cycle 6, 2669–2677.
- Andrade B.M., Pires de Carvalho D. (2014). Perspectives of the AMP-activated kinase (AMPK) signalling pathway in thyroid cancer. Bioscience Reports 34 (2).

- Andrikopoulos S., Blair A.R., Deluca N., Fam B.C., Proietto J. (2008). Evaluating the glucose tolerance test in mice. Am J Physiol Endocrinol Metab 295: E1323-1332.
- Anselmi, C.V., Malovini, A., Roncarati, R., Novelli, V., Villa F., Condorelli, G., Bellazzi, R., et al., (2009). Association of the FOXO3A locus with extreme longevity in a southern Italian centenarian study. Rejuvenation Res 12(2), 95-104.
- Arden K.C, (2004). FoxO: linking new signaling pathways. Mol Cell 14, 416-418.
- Arden, K. C. (2006). Multiple roles of FOXO transcription factors in mammalian cells point to multiple roles in cancer. Exp. Gerontol. 41(8), 709-17.
- Birch-Machin M. (2006). The role of mitochondria in ageing and carcinogenesis. Clin Exp Dermatol, 31: 548-552.
- Birsoy K., Possemato R., Lorbeer F.K., Bayraktar E.C., Thiru P., Yucel B., Wang T., (2014). Metabolic determinants of cancer cell sensitivity to glucose limitation and biguanides. Nature. 508, 108–112.
- Blom N., Gammeltoft S., and Brunak S. (1999). Sequence- and structure-based prediction of eukaryotic protein phosphorylation sites. Journal of Molecular Biology: 294(5), 1351-1362.
- Bonnet S., Archer S.L., Allalunis-Turner J., Haromy A., Beaulieu C., Thompson R., Lee C.T., Lopaschuk G.D., Puttagunta L, et al. (2007). A mitochondria-K+ channel axis is suppressed in cancer and its normalization promotes apoptosis and inhibits cancer growth. Cancer Cell 11, 37–51.

- Brandon M,. Baldi P., Wallace D.C. (2006). Mitochondrial mutations in cancer. Oncogene. 25, 4647–4662.
- Brownawell A.M., Kops G.J., Macara I.G., Burgering B.M.gre (2001). Inhibition of nuclear import by protein kinase B (Akt) regulates the subcellular distribution and activity of the forkhead transcription factor AFX. Mol Cell Biol 21, 3534-3546.
- Brunet A., Bonni A., Zigmond M.J., Lin M.Z., Juo P., Hu L.S. et al (1999). Akt promotes cell survival by phosphorylating and inhibiting a Forkhead transcription factor. Cell 96, 857-868.
- Brunet A., Park J., Tran H., Hu L.S., Hemmings B.A., Greenberg M.E. (2001). Protein kinase SGK mediates survival signals by phosphorylating the forkhead transcription factor FKHRL1 (FOXO3a). Mol Cell Biol 21, 952-965.
- Brunet A., Sweeney L.B., Sturgill J.F., Chua K.F., Greer P.L., Lin Y., et al. (2004). Stress-dependent regulation of FOXO transcription factors by the SIRT1 deacetylase. Science 303:2011-5.
- Caballero-Caballero A., Engel T., Martinez-Villarreal J., Sanz-Rodriguez A., Chang P., Dunleavy M., Mooney C.M., et al. (2013) Mitochondrial localization of the forkhead box class O transcription factor FOXO3a in brain. J Neurochem 124(6), 749–756.
- Cairns, R.A., Harris, I.S. and Mak, T.W. (2011). Regulation of cancer cell metabolism. Nat Rev Cancer 11, 85–95.
- Calnan D.R., Brunet A. (2008). The FoxO code. Oncogene. 27, 2276–88.

- Calnan D.R., Webb A.E., White J.L., Stowe T.R., Goswami T., Shi X., et al. (2012). Methylation by Set9 modulates FoxO3 stability and transcriptional activity. Aging 4(7), 462–79.
- Canto C., Auwerx J. (2010). AMP-activated protein kinase and its downstream transcriptional pathways. Cell Mol Life Sci. 67, 3407–3423.
- Cantó C., Auwerx J., (2011). Calorie restriction: is AMPK a key sensor and effector? Physiology 26, 214-224
- Canto C., Gerhart-Hines Z., Feige J.N., Lagouge M., Noriega L., Milne J.C., et al. (2009). AMPK regulates energy expenditure by modulating NAD+ metabolism and SIRT1 activity. Nature 458:1056-60. 37.
- Cantor R. and Sabatini D. M. (2012).Cancer cell metabolism: One hallmark, many faces. Cancer Discov. 2, 881–898.
- Cardaci S., Zheng L., MacKay G., van den Broek N.J., MacKenzie E.D., Nixon C., Stevenson D., et al. (2015). Pyruvate carboxylation enables growth of SDH-deficient cells by supporting aspartate biosynthesis. Nature cell biology. 17:1317–1326.
- Carlsson, P., Mahlapuu, M. (2002). Forkhead Transcription Factors: Key Players in Development and Metabolism. Dev. Biol. 250, 1–23.
- Castrillon D.H., Miao L., Kollipara R., Horner J.W., De Pinho R.A. (2003). Suppression of ovarian follicle activation in mice by the transcription factor Foxo3a. Science 301(5630), 215-8.
- Celestini V., Tezil T., Russo L., Fasano C., Sanese P., Forte G., Peserico A., et al. (2018). Uncoupling FoxO3A mitochondrial and nuclear functions in cancer

cells undergoing metabolic stress and chemotherapy, Cell Death and Disease 9, 231

- Chacinska A., Koehler C.M., Milenkovic D., Lithgow T., Pfanner N., et al. (2009). Importing Mitochondrial Proteins: Machineries and Mechanisms. Cell 138, 628–644.
- Chae Y.K., Arya A., Malecek M.K., Shin D.S., Carneiro B., Chandra S. , Kaplan J. et al. (2016). Repurposing Metformin for cancer treatment: current clinical studies. Oncotarget 7, 40767–40780.
- Chen Y., Fu L.L., Wen X., Wang X.Y., Liu J., Cheng Y., et al. (2014). Sirtuin-3 (SIRT3), a therapeutic target with oncogenic and tumor-suppressive function in cancer. Cell Death Dis. 5:e1047.
- Chiacchiera F., Matrone A., Ferrari E., Ingravallo G., Lo Sasso G., Murzilli S., et al (2009). p38α blockade inhibits colorectal cancer growth in vivo by inducing a switch from HIF1α- to FoxO-dependent transcription. Cell Death Differ. 16(9), 1203-14.
- Chiacchiera F., Simone C. (2009). Inhibition of p38alpha unveils an AMPK-FoxO3A axis linking autophagy to cancer-specific metabolism. Autophagy 5, 1030-3.
- Chiacchiera, F. and Simone, C. (2010). The AMPK-FoxO3A axis as a target for cancer treatment. Cell Cycle 9, 1091–1096.
- Clark, K. L., Halay, E. D., Lai, E., Burley, S. K. (1993). Co-crystal structure of the HNF-3/fork head DNA-recognition motif resembles histone H5. Nature 364(6436), 412-20.

- Colman R.J., Anderson R.M., Johnson S.C., Kastman E.K., Kosmatka K.J., Beasley T.M., et al. (2009). Caloric restriction delays disease onset and mortality in rhesus monkeys. Science 325, 201–4.
- Colombo S.L., Moncada S. (2009). AMPKalpha1 regulates the antioxidant status of vascular endothelial cells. Biochem J 421:163-9.
- Comes F., Matrone A., Lastella P., Nico B., Susca F.C., Bagnulo R. et al. (2007). A novel cell type-specific role of p38alpha in the control of autophagy and cell death in colorectal cancer cells. Cell Death Differ. 14, 693–702.
- Commisso C., Davidson S.M., Soydaner-Azeloglu R.G., Parker S.J., Kamphorst J.J., Hackett S., Grabocka E., Nofal M., et al. (2013). Macropinocytosis of protein is an amino acid supply route in Ras-transformed cells. Nature 497, 633–637.
- Coomans de Brachène, A. & Demoulin, J.B. (2016). FOXO transcription factors in cancer development and therapy. Cell. Mol. Life Sci. 73: 1159
- Costantini, P. Belzacq A.S., Vieira H.L., Larochette N., de Pablo M.A., Zamzami N., Susin S.A., Brenner C., Kroemer G. (2000). Oxidation of a critical thiol residue of the adenine nucleotide translocator enforce sBcl-2-independent permeability transition pore opening and apoptosis. Oncogene 19, 307–314.
- Daitoku H., Sakamaki J., Fukamizu A. (2011). Regulation of FoxO transcription factors by acetylation and protein–protein interactions, In Biochimica et Biophysica Acta (BBA) - Molecular Cell Research, 1813 (11):1954-1960.
- Dansen T.B., Burgering B.M. (2008). Unravelling the tumor-suppressive functions of FOXO proteins. Trends Cell Biol 18, 421-429.

- DeBerardinis, R.J. and Chandel, N.S. (2016). Fundamentals of cancer metabolism. Sci Adv 27;2(5).
- Desouki M.M., Doubinskaia I., Gius D., Abdulkadir S.A. (2014). Decreased mitochondrial SIRT3 expression is a potential molecular biomarker associated with poor outcome in breast cancer. Hum Pathol. 45(5),1071-7.
- Dijkers P.F., Medema R.H, Lammers J.W., Koenderman L., Coffer P.J. (2000). Expression of the proapoptotic Bcl-2 family member Bim is regulated by the forkhead transcription factor FKHR-L1. Curr Biol 10, 1201-1204.
- Dragovich, T. Gordon M., Mendelson D., Wong L., Modiano M., Chow H.H., Samulitis B., et al. (2007). Phase I trial of imexon in patients with advanced malignancy. J. Clin. Oncol. 25, 1779–1784.
- Eales K.L, Hollinshead K.E.R. & Tennant D.A. (2016). Hypoxia and metabolic adaptation of cancer cells. Oncogenesis 25;5:e190.
- Eijkelenboom A & Burgering B.M.T. (2013). FOXOs: signalling integrators for homeostasis maintenanceNature Reviews Molecular Cell Biology 14, 83-97.
- Elstrom, R.L. Bauer D.E., Buzzai M., Karnauskas R., Harris M.H., Plas D.R., Zhuang H., et al. (2004). Akt stimulates aerobic glycolysis in cancer cells. Cancer Res. 64, 3892–3899.
- Essafi A., Fernandez de Mattos S., Hassen Y.A., Soeiro I., Mufti G.J., Thomas N.S. Medema R.H., et al (2005). Direct transcriptional regulation of Bim by FoxO3a mediates STI571-induced apoptosis in Bcr-Ablexpressing cells. Oncogene 24, 2317-2329.

- Evans J.M., Donnelly L.A., Emslie-Smith A.M., Alessi D.R., Morris A.D. (2005). Metformin and reduced risk of cancer in diabetic patients. BMJ 330, 1304-1305.
- Falkenberg M., Gaspari M., Rantanen A., Trifunovic A., Larsson N.G., Gustafsson C.M. (2002). Mitochondrial transcription factors B1 and B2 activate transcription of human mtDNA. Nat Genet 31: 289–294.
- Farhan M., Wang H., Gaur U., Little P.J., Xu J., Zheng W. (2017). FOXO Signaling Pathways as Therapeutic Targets in Cancer. Int J Biol Sci.13(7),815–27.
- Fei M., Zhao Y., Wang Y., Lu M., Cheng C., Huang X., Zhang D. et al. (2009). Low expression of Foxo3a is associated with poor prognosis in ovarian cancer patients. Cancer Invest. 27, 52-59.
- Ferber E.C., Peck B., Delpuech O., Bell G.P., East P. and Schulze A., (2012). FoxO3A regulates reactive oxygen metabolism by inhibiting mitochondrial gene expression, Cell Death and Differentiation 19, 968–979.
- Fernández de Mattos, S., Villalonga, P., Clardy, J. and Lam, E.W.F. (2008). FOXO3a mediates the cytotoxic effects of Cisplatin in colon cancer cells. Mol Cancer Ther 7, 3237–3246.
- Fernandez de Mattos, S., Essafi, A., Soeiro, I., Pietersen, A.M., Birkenkamp, K. U., Edwards, C. S., et al. (2004). FoxO3a and BCR-ABL regulate cyclin D2 transcription through a STAT5/BCL6-dependent mechanism. Mol Cell Biol 24, 10058–71

- Finley L.W., Carracedo A., Lee J., Souza A., Egia A., Zhang J., Teruya-Feldstein J., et al. (2011). SIRT3 opposes reprogramming of cancer cell metabolism through HIF1α destabilization. Cancer Cell. 19(3), 416-28.
- Flachsbart, F., Caliebe, A., Kleindorp, R., Blanché, H , von Eller-Eberstein, H., Nikolaus, S., Schreiber, S., Nebel, A. (2009). Association of FOXO3A variation with human longevity confirmed in German centenarians. Proc Natl Acad Sci USA 106(8), 2700-5.
- Flick F., Luscher B. (2012). Regulation of sirtuin function by posttranslational modifications. Front Pharmacol. 3:29
- Fontana L., Klein S. (2007) Aging, adiposity, and calorie restriction. JAMA 297, 986–94.
- Frezza C., Cipolat S., Scorrano L. (2007). Organelle isolation: functional mitochondria from mouse liver, muscle and cultured fibroblasts. Nat Protoc 2, 287–295.
- Fu, Z., Tindall, D. J. (2008). FOXOs, cancer and regulation of apoptosis. Oncogene 27 (2312).
- Fukasawa Y., Tsuji J., Fu s., Tomii K., Horton P. and Imai K. (2015). MitoFates: Improved Prediction of Mitochondrial Targeting Sequences and Their Cleavage Sites.Molecular & Cellular Proteomics, 14(4), 1113-1126.
- Furukawa-Hibi Y., Yoshida-Araki K., Ohta T., Ikeda K., Motoyama N. (2002). FOXO Forkhead Transcription Factors Induce G2-M Checkpoint in Response to Oxidative Stress. JBC, 277(30), 26729–26732.
- Fulda, S., Galluzzi, L. & Kroemer, G. (2010). Targeting mitochondria for cancer therapy. Nature Rev. Drug Discov. 9, 447–464.

- Gakh O., Cavadini P., Isaya G. (2002). Mitochondrial processing peptidases. Biochimica et Biophysica Acta - Molecular Cell Research 1592, 63–77.
- Galluzzi, L. & Kroemer, G. (2008). Necroptosis: a specialized pathway of programmed necrosis. Cell 135, 1161–1163.
- Gao P., Tchernyshyov I., Chang T.C., Lee Y.S., Kita K., Ochi T., Zeller K.I., et al. (2009). c-Myc suppression of miR-23a/b enhances mitochondrial glutaminase expression and glutamine metabolism. Nature 458, 762–765.
- Gaude E., Frezza C. (2014).Defects in mitochondrial metabolism and cancer. Cancer & metabolism 2:10.
- Germani, A., Matrone, A., Grossi, V., Peserico, A., Sanese, P., Liuzzi, M., Palermo, R., Murzilli, S.,Campese, A.F., Ingravallo, G., et al. (2014). Targeted therapy against chemoresistant colorectal cancers: Inhibition of p38α modulates the effect of Cisplatin in vitro and in vivo through the tumor suppressor FoxO3A. Cancer Lett 344, 110–118.
- Gill K.S., Fernandes P., O'Donovan T.R., McKenna S.L., Doddakula K.K., Power D.G., Soden D.M., Forde P.F. (2016) Glycolysis inhibition as a cancer treatment and its role in an anti-tumour immune response. Biochim Biophys Acta 1866(2016), 87–105.
- Gillies, R.J. and Gatenby, R.A. (2007). Adaptive landscapes and emergent phenotypes: why do cancers have high glycolysis? J. Bioenerg. Biomembr. 39, 251–257.
- Gomes, A.R., Brosens, J.J. & Lam, E.W.F. (2008). Resist or die: FOXO transcription factors determine the cellular response to chemotherapy. Cell Cycle 7, 3133–3136.

- Gottlieb, E. and Tomlinson, I.P. (2005). Mitochondrial tumour suppressors: a genetic and biochemical update. Nat. Rev. Cancer 5, 857–866.
- Greer E.L., Banko M.R., Brunet A. (2009). AMP-activated protein kinase and FoxO transcription factors in dietary restriction-induced longevity. Ann N Y Acad Sci. 1170, 688-92.
- Greer E.L., Brunet A. (2005). FOXO transcription factors at the interface between longevity and tumor suppression. Oncogene 24, 7410–7425.
- Greer E.L., Oskoui P.R., Banko M.R., Maniar J.M., Gygi M.P., Gygi S.P., et al. (2007a). The energy sensor AMP-activated protein kinase directly regulates the mammalian FOXO3 transcription factor. J Biol Chem 282:30107-19.
- Greer, E.L., Dowlatshahi, D., Banko, M.R., Villen, J., Hoang, K., Blanchard, D., Gygi, S.P., and Brunet, A. (2007b). An AMPK-FOXO pathway mediates longevity induced by a novel method of dietary restriction in C. elegans. Curr. Biol. 17, 1646–1656.
- Greijer, A.E. and van der Wall, E. (2004). The role of hypoxia inducible factor 1 (HIF-1) in hypoxia induced apoptosis. J. Clin. Pathol. 57, 1009–101415.
- Grossi V., Liuzzi M., Murzilli S., Martelli N., Napoli A., Ingravallo G., Del Rio A, Simone C. (2012). Sorafenib inhibits p38alpha activity in colorectal cancer cells and synergizes with the DFG-in inhibitor SB202190 to increase apoptotic response. Cancer Biology & Therapy, 13, 1471-81.
- Gwinn D.M., Shackelford D.B., Egan D.F., Mihaylova M.M., Mery A., Vasquez D.S., Turk B.E., Shaw R.J. (2008). AMPK phosphorylation of raptor mediates a metabolic checkpoint. Mol Cell. 30, 214–226.

- Habashy H.O., Rakha E.A., Aleskandarany M., Ahmed M.A., Green A.R., Ellis I.O., Powe D.G. (2011). FOXO3A nuclear localisation is associated with good prognosis in luminal- like breast cancer. Breast Cancer Res Treat. 129, 11-21.
- Haigis M.C, Sinclair D.A. (2010) Mammalian sirtuins: biological insights and disease relevance. Annu Rev Pathol.5, 253-95.
- Hanahan D, Weinberg RA (2000). The hallmarks of cancer. Cell 100, 57-70.
- Hanahan D, Weinberg RA (2011). Hallmarks of cancer: the next generation. Cell 144, 646-674.
- Hardie D.G., Ross F.A., Hawley S.A. (2012). AMPK: a nutrient and energy sensor that maintains energy homeostasis. Nat Rev Mol Cell Biol. 13, 251–262.
- Herzig S., Shaw R.J. (2018). AMPK: guardian of metabolism and mitochondrial homeostasis. Nat Rev Mol Cell Biol. 19(2), 121-135.
- Hirschey M.D., Shima t., Huang J.Y., Verdin E., (2009). Acetylation of Mitochondrial Proteins, Methods in Enzymology, Academic Press, 457, 137-147
- Ho K.K., McGuire V.A., Koo C.Y., Muir K.W., de Olano N., Maifoshie E., Kelly D.J., et al., (2012). Phosphorylation of FOXO3a on Ser-7 by p38 promotes its nuclear localization in response to doxorubicin. J Biol Chem. 287(2):1545-55.
- Hochberg Y. (1988). A sharper Bonferroni procedure for multiple tests of significance. Biometrika. 75, 800–803.

- Hu M.C., Lee D.F., Xia W., Golfman L.S., Ou-Yang F., Yang J.Y., Zou Y., et al. (2004). IkappaB kinase promotes tumorigenesis through inhibition of forkhead FOXO3a. Cell.; 117,225–237.
- Huang J.Y., Hirschey M.D., Shimazu T., Ho L., Verdin E. (2010) Mitochondrial sirtuins. Biochim Biophys Acta. 1804(8),1645-5.
- Huang, P., Feng, L., Oldham, E. A., Keating, M. J. & Plunkett, W. Superoxide dismutase as a target for the selective killing of cancer cells. Nature 407, 390–395 (2000).
- Hui R.C., Francis R.E., Guest S.K., Costa J.R., Gomes A.R., Myatt S.S., Brosens J.J., Lam E.W. (2008). Doxorubicin activates FOXO3a to induce the expression of multidrug resistance gene ABCB1 (MDR1) in K562 leukemic cells. Mol Cancer Ther. 7, 670–678.
- Iakoucheva L.M., Radivojac P., Brown C.J., O'Connor T.R., Sikes J.G., Obradovic Z., Dunker A.K. (2004). Intrinsic disorder and protein phosphorylation. Nucleic Acids Research, 32 (3), 1037-1049.
- Jacobs, K.M., Pennington J.D., Bisht K.S., Aykin-Burns N., Kim H.S., Mishra M., Sun L., et al. (2008). SIRT3 interacts with the daf-16 homolog FOXO3a in the mitochondria, as well as increases FOXO3a dependent gene expression. Int J Biol Sci, 4(5), 291-9.
- Jiang Y., Zou L., Lu W.Q., Zhang Y., Shen A.G. (2013). Foxo3a expression is a prognostic marker in breast cancer. PLoS ONE 8(8).
- Ju Y.S., Alexandrov L.B., Gerstung M., Martincorena I., Nik-Zainal S., Ramakrishna M., Davies H.R., et al., (2014). Origins and functional

consequences of somatic mitochondrial DNA mutations in human cancer. eLife. 1;3.

- Kenyon, C., Chang, J., Gensch, E., Rudner, A., Tabtiang, R. (1993). A C. elegans mutant that lives twice as long as wild type. Nature 366(6454), 461-4.
- Kim H.S., Patel K., Muldoon-Jacobs K., Bisht K.S., Aykin-Burns N., Pennington J.D., van der Meer R., et al. (2010). SIRT3 is a mitochondria-localized tumor suppressor required for maintenance of mitochondrial integrity and metabolism during stress. Cancer Cell 17, 41-52.
- Kim J. and Chi V. D. (2006). Cancer's Molecular Sweet Tooth and the Warburg Effect. Cancer Research 66(18).
- Kim J., Yang G., Kim Y., Kim J., Ha J. (2016). AMPK activators: mechanisms of action and physiological activities. Exp Mol Med. 48:e224.
- Kim J.H., Lee K.J., Seo Y., Kwon J.H., Yoon J.P., Kang J.Y., Lee H.J., et al. (2018) Effects of Metformin on colorectal cancer stem cells depend on alterations in glutamine metabolism. Sci Rep. 11;8(1):409
- Kiyotsugu Y., Yi T., Zhai B., Yu Y., Raschle T., Etzkorn M., et al. (2014). Quantitative phosphoproteomic analysis reveals system-wide signaling pathways downstream of SDF-1/CXCR4 in breast cancer stem cells. Proc Natl Acad Sci USA 111, E2182-190.
- Klammer M., Kaminski M., Zedler A., Oppermann F., Blencke S., Marx S., et al. (2012). Phosphosignature Predicts Dasatinib Response in Non-small Cell Lung Cancer. Mol Cell Proteomics 11, 651–668.
- Kobayashi Y., Furukawa-Hibi Y., Chen C., Horio Y., Isobe K., Ikeda K., Motoyama N. (2005). SIRT1 is critical regulator of FOXO-mediated

transcription in response to oxidative stress International Journal Of Molecular Medicine 16: 237-243.

- Koppenol W.H., Bounds P.L., Dang C.V. (2011). Otto Warburg's contributions to current concepts of cancer metabolism. Nat. Rev. Cancer 11, 325–337.
- Kops G.J., Dansen T.B., Polderman P.E., Saarloos I., Wirtz K.W., Coffer P.J., Huang T.T., (2002). Forkhead transcription factor FOXO3a protects quiescent cells from oxidative stress. Nature, 419(6904), 316-21.
- Kuntz E.M., Baquero P., Michie A.M., Dunn K., Tardito S., Holyoake T.L., Helgason G.V. et al. (2017). Targeting mitochondrial oxidative phosphorylation eradicates therapy-resistant chronic myeloid leukemia stem cells. Nat Med 23, 1234-1240.
- Laderoute K.R., Calaoagan J.M., Madrid P.B., Klon A.E., Ehrlich P.J. (2010). SU11248 (sunitinib) directly inhibits the activity of mammalian 5′-AMP-activated protein kinase (AMPK) Cancer Biology & Therapy. 10:68–76.
- Lang M., Vocke C.D., Merino M.J., Schmidt L.S., Linehan W.M. (2015). Mitochondrial DNA mutations distinguish bilateral multifocal renal oncocytomas from familial Birt-Hogg-Dube tumors. Mod Pathol. 28:1458–1469.
- Larsson N.G., Wang J., Wilhelmsson H., Oldfors A., Rustin P., Lewandoski M., Barsh G.S., Clayton D.A. (1998). Mitochondrial transcription factor A is necessary for mtDNA maintenance and embryogenesis in mice. Nat. Genet. 18:231–236.
- Lee J. H., Jeon S.M., Hong S.P., Cheon J.H., Kim T.I., Kim W.H. (2012a). Metformin use is associated with a decreased incidence of colorectal adenomas

in diabetic patients with previous colorectal cancer. Dig. Liver Dis. 44, 1042–1047

- Lee, J. H., Kim T.I., Jeon S.M., Hong S.P., Cheon J.H., Kim W.H. (2012b).The effects of Metformin on the survival of colorectal cancer patients with diabetes mellitus. Int. J. Cancer. 131,752–759
- Lehtinen M.K., Yuan Z., Boag P.R., Yang Y., Villen J., Becker E.B. et al (2006). A conserved MST-FOXO signalling pathway mediates oxidative-stress responses and extends life span. Cell 125: 987-1001.
- Li Y., Liu L., Tollefsbol T.O. (2010). Glucose restriction can extend normal cell lifespan and impair precancerous cell growth through epigenetic control of hTERT and p16 expression. FASEB J. 24,1442–53.
- Liang C., Chen W., Zhi X., Ma T., Xia X., Liu H., Zhang Q., (2013). Serotonin promotes the proliferation of serum-deprived hepatocellular carcinoma cells via upregulation of FOXO3A. Mol Cancer. 12(14).
- Liang J., Xu Z.X., Ding Z,, Lu Y,, Yu Q,, Werle K.D., Zhou G., et al. (2015). Myristoylation confers noncanonical AMPK functions in autophagy selectivity and mitochondrial surveillance. Nat. Commun. 6, 7926.
- Liu F., Yang X., Geng M., Huang M., (2018). Targeting ERK, an Achilles' Heel of the MAPK pathway, in cancer therapy,Acta Pharmaceutica Sinica B,
- Liu H.B., Gao X.X., Zhang Q., Liu J., Cui Y., Zhu Y., Liu Y.F. (2015). Expression and prognostic implications of FOXO3A and Ki67 in lung adenocarcinomas. Asian Pac J Cancer Prev. 16,1443-1448.

- Lombard D.B., Alt F.W., Cheng H.L., Bunkenborg J., Streeper R.S., Mostoslavsky R., et al. (2007). Mammalian Sir2 homolog SIRT3 regulates global mitochondrial lysine acetylation. Mol Cell Biol. 27(24), 8807-14.
- Maeda, H. Hori S., Ohizumi H., Segawa T., Kakehi Y., Ogawa O., Kakizuka A. (2004). Effective treatment of advanced solid tumors by the combination of arsenic trioxide and l-buthionine-sulfoximine. Cell Death Differ. 11, 737–746.
- Magda, D. & Miller, R. A. (2006).Motexafin gadolinium: a novel redox active drug for cancer therapy. Semin. Cancer Biol. 16, 466–476.
- Marin T.L., Gongol B., Martin M., King S.J., Smith L., Johnson D.A., (2015). Subramaniam S, Chien S, Shyy JY. Identification of AMP-activated protein kinase targets by a consensus sequence search of the proteome. BMC Syst Biol. 9(13).
- Maschek G., Savaraj N., Priebe W., Braunschweiger P., Hamilton K., Tidmarsh G.F. De Young L.R., Lampidis T.J. (2004). 2-deoxy-D-glucose increases the efficacy of adriamycin and paclitaxel in human osteosarcoma and non-small cell lung cancers in vivo. Cancer Res 64, 31–34.
- Masoro E.J. (2005). Overview of caloric restriction and ageing Mech. Ageing Dev. 126, 913-922
- McCay C.M., Crowell M.F., Maynard L.A. (1989). The effect of retarded growth upon the length of life span and upon the ultimate body size. Nutrition. 5(3), 155–71
- Medema R.H., Kops G.J., Bos J.L., Burgering B.M. (2000). AFX-like Forkhead transcription factors mediate cell-cycle regulation by Ras and PKB through p27kip1. Nature 404, 782-787.

- Mertins P., Mani D.R., Ruggles K.V., Gillette M.A., Clauser K.R., Wang P., et al. (2016). Proteogenomics connects somatic mutations to signalling in breast cancer. Nature 534, 55–62.
- Mertins P., Yang F., Liu T., Mani D.R., Petyuk V.A., Gillette M.A., et al. (2014). Ischemia in tumors induces early and sustained phosphorylation changes in stress kinase pathways but does not affect global protein levels. Mol Cell Proteomics 13, 1690–1704.
- Mihaylova M.M., Shaw R.J. (2011). The AMPK signalling pathway coordinates cell growth, autophagy and metabolism. Nat Cell Biol.13, 1016–1023.
- Miyamoto K., Araki K.Y., Naka K., Arai F., Takubo K., Yamazaki S., Matsuoka S., et al. (2007). Foxo3a is essential for maintenance of the hematopoietic stem cell pool. Cell Stem Cell. 1(1), 101-12.
- Modur V., Nagarajan R., Evers B.M., Milbrandt J. (2002). FOXO proteins regulate tumor necrosis factor-related apoptosis inducing ligand expression. Implications for PTEN mutation in prostate cancer. J Biol Chem 277, 47928-47937
- Moll, U.M. and Schramm, L.M. (1998). p53 – an acrobat intumorigenesis. Crit. Rev. Oral Biol. Med. 9, 23–37.
- Mossmann D., Meisinger C., and Vögtle F.N. (2012). Processing of mitochondrial presequences. Biochim. Biophys. Acta 1819, 1098–1106.
- Motta, M.C., Divecha N., Lemieux M., Kamel C., Chen D., Gu W., Bultsma Y., et al. (2004). Mammalian SIRT1 represses forkhead transcription factors. Cell, 116(4): 551-63.

- Myatt S.S., Lam E.W. (2007). The emerging roles of forkhead box (Fox) proteins in cancer. Nat Rev Cancer. 7(11):847-59.
- Nakatani Y., Ogryzko V. (2003). Immunoaffinity Purification of Mammalian Protein Complexes. Methods Enzymol 370, 430–444.
- Nakayama, K.I. and Nakayama K., (2006). Ubiquitin ligases: cell-cycle control and cancer. Nat Rev Cancer, 6(5), 369-81.
- Neupert W., Herrmann J.M. (2007). Translocation of proteins into mitochondria. Annu Rev Biochem. 76, 723-49.
- Nishida, N., Yano H., Nishida T., Kamura T., and Kojiro M. (2006). Angiogenesis in Cancer. Vascular Health and Risk Management, 2, 213-219.
- Olsen J.V., Vermeulen M., Santamaria A., Kumar C., Miller M.L., Jensen L.J., et al. (2010). Quantitative phosphoproteomics reveals widespread full phosphorylation site occupancy during mitosis. Sci Signal 8, rs12.
- Paik, J. H., Kollipara, R., Chu, G., Ji, H., Xiao, Y., Ding, Z., Miao, L., et al. (2007). FoxOs are lineage-restricted redundant tumor suppressors and regulate endothelial cell homeostasis. Cell 128(2), 309-23.
- Pan C., Olsen J.V., Daub H. Mann M. (2009) .Global effects of kinase inhibitors on signaling networks revealed by quantitative phosphoproteomics. Mol Cell Proteomics 8, 2796–2808.
- Park S., Mori R., Shimokawa I. (2013). Do sirtuins promote mammalian longevity? A critical review on its relevance to the longevity effect induced by calorie restriction. Mol Cells 35(6), 474-80.
- Pelicano, H. Xu R., Du M., Feng L., Sasaki R., Carew J.S., Latha Ramdas H. et al. (2006). Mitochondrial respiration defects in cancer cells cause activation of

Akt survival pathway through a redox-mediated mechanism. J. Cell Biol. 175, 913–923.

- Peserico A., Germani A., Sanese P., Barbosa A.J., Di Virgilio V., Fittipaldi R., et al. (2015) A SMYD3 Small-Molecule Inhibitor Impairing Cancer Cell Growth. J Cell Physiol 230, 2447–2460.
- Peserico, A., Chiacchiera, F., Grossi, V., Matrone, A., Latorre, D., Simonatto, M., Fusella, A., Ryall, J.G., Finley, L.W., Haigis, M.C., et al. (2013). A novel AMPK-dependent FoxO3A-SIRT3 intramitochondrial complex sensing glucose levels. Cell. Mol Life Sci 70, 2015–2029.
- Potente M., Urbich C., Sasaki K., Hofmann W.K., Heeschen C., Aicher A., Kollipara R. et al. (2005). Involvement of Foxo transcription factors in angiogenesis and postnatal neovascularization. J Clin Invest. 115, 2382–2392.
- Qian, Z., Ren, L., Wu, D., Yang, X., Zhou, Z., Nie, Q., Jiang, G., et al. (2017). Overexpression of FoxO3a is associated with glioblastoma progression and predicts poor patient prognosis. Int. J. Cancer, 140, 2792–2804.
- Ramaswamy S., Nakamura N., Sansal I., Bergeron L., Sellers W.R. (2002). A novel mechanism of gene regulation and tumor suppression by the transcription factor FKHR. Cancer Cell 2, 81-91.
- Real P.J., Benito A., Cuevas J., Berciano M.T., de Juan A., Coffer P., Gomez-Roman J. et al. (2005). Blockade of epidermal growth factor receptors chemosensitizes breast cancer cells through up-regulation of Bnip3L. Cancer Res. 65, 8151–8157.

- Rehman A., Kim Y., Kim H., Sim J., Ahn H., Chung M.S., Shin S.J., Jang K. (2018). FOXO3a expression is associated with lymph node metastasis and poor disease-free survival in triple-negative breast cancer. J Clin Pathol. Mar 27.
- Rena G., Guo S., Cichy S.C., Unterman T.G., Cohen P. (1999). Phosphorylation of the transcription factor forkhead family member FKHR by protein kinase B. J Biol Chem 274, 17179-17183.
- Reznick, R. M. & Shulman, G. I. (2006). The role of AMP-activated protein kinase in mitochondrial biogenesis. J. Physiol. 574, 33–39.
- Rohle D., Popovici-Muller J., Palaskas N., Turcan S., Grommes C., Campos C., Tsoi J., et al. (2013). An inhibitor of mutant IDH1 delays growth and promotes differentiation of glioma cells. Science. 340, 626–630.
- Rokudai S., Fujita N., Kitahara O., Nakamura Y., Tsuruo T. (2002). Involvement of FKHR-dependent TRADD expression in chemotherapeutic drug-induced apoptosis. Mol Cell Biol 22, 8695-8708.
- Roth D.B., Gellert M. (2000). New guardians of the genome. Nature 404, 823-825.
- Ryan M.T., Voos W., Pfanner N. (2001). Assaying protein import into mitochondria. Methods Cell Biol 65, 189–215.
- Sanchez A.M., Candau R.B., Bernardi H. (2014). FoxO transcription factors: their roles in the maintenance of skeletal muscle homeostasis. Cell Mol Life Sci. 71(9), 1657-71.
- Santo E.E., Paik J. (2018). A splice junction-targeted CRISPR approach (spJCRISPR) reveals human FOXO3B to be a protein-coding gene. Gene. 2018 Jun 17. pii: S0378-1119(18)30704-2

- Scher M.B., Vaquero A., Reinberg D. (2007). SIRT3 is a nuclear NAD+-dependent histone deacetylase that translocates to the mitochondria upon cellular stress. Genes Dev. 21(8):920-8.
- Schmidt M., Fernandez de Mattos S., van der Horst A., Klompmaker R., Kops G. J. P. L., Lam E. W.-F., et al. (2002). Cell Cycle Inhibition by FoxO Forkhead Transcription Factors Involves Downregulation of Cyclin D. Mol Cell Biol. 22(22): 7842–7852.
- Schubert S., Heller S., Löffler B., Schäfer I., Seibel M., Villani G., and Seibel P. (2015). Generation of Rho Zero Cells: Visualization and Quantification of the mtDNA Depletion Process. Int J Mol Sci. 16(5):9850-65.
- Schwer B., North B.J., Frye R.A, Ott M., and Eric Verdin, (2002). The human silent information regulator (Sir)2 homologue hSIRT3 is a mitochondrial nicotinamide adenine dinucleotide–dependent deacetylase. JBC 158 (4), 647-657.
- Schwer B., Verdin E. (2008). Conserved metabolic regulatory functions of sirtuins. Cell Metab. 7(2),104-12.
- Semenza, G.L. (2007). Oxygen-dependent regulation of mitochondrial respiration by hypoxia-inducible factor 1. Biochem. J. 405, 1–9.
- Seoane J., Le H.V., Shen L., Anderson S.A., Massague J. (2004). Integration of Smad and forkhead pathways in the control of neuroepithelial and glioblastoma cell proliferation. Cell 117, 211-223.
- Sharma K., D'Souza R.C., Tyanova S., Schaab C., Wiśniewski J.R., Cox J., et al. (2014). Ultradeep Human Phosphoproteome Reveals a Distinct Regulatory Nature of Tyr and Ser/Thr-Based Signaling. Cell Rep 8, 1583–1594.

- Shroff E.H., Eberlin L.S., Dang V.M., Gouw A.M., Gabay M., Adam S.J., Bellovin D.I., et al. (2015). MYC oncogene overexpression drives renal cell carcinoma in a mouse model through glutamine metabolism. Proceedings of the National Academy of Sciences of the United States of America. 112, 6539–6544.
- Simons, A. L., Ahmad, I. M., Mattson, D. M., Dornfeld, K. J. & Spitz, D. R. (2007). 2-Deoxy-D-glucose combined with Cisplatin enhances cytotoxicity via metabolic oxidative stress in human head and neck cancer cells. Cancer Res. 67, 3364–3370.
- Sisci D., Maris P., Cesario M.G., Anselmo W., Coroniti R., Trombino G.E., Romeo F., et al. (2013). The estrogen receptor α is the key regulator of the bifunctional role of FoxO3a transcription factor in breast cancer motility and invasiveness. Cell Cycle. 12, 3405-3420.
- Smith A.C. and Robinson A.J. (2016). MitoMiner v3.1, an update on the mitochondrial proteomics database. Nucleic Acids Res. 44(1), 1258-61.
- Stewart J.B., Alaei-Mahabadi B., Sabarinathan R., Samuelsson T., Gorodkin J., Gustafsson C.M., Larsson E. (2015). Simultaneous DNA and RNA Mapping of Somatic Mitochondrial Mutations across Diverse Human Cancers. PLoS Genet. 11(6).
- Storz P., Döppler H., Copland J.A., Simpson K.J., Toker A. (2009) FOXO3A promotes tumor cell invasion through the induction of matrix metalloproteinases. Mol Cell Biol. 29, 4906-4917
- Sundaresan N.R., Gupta M., Kim G., Rajamohan S.B., Isbatan A., Gupta M.P. (2009). Sirt3 blocks the cardiac hypertrophic response by augmenting Foxo3a-

dependent antioxidant defense mechanisms in mice. J Clin Invest. 119(9): p. 2758-71

- Sundaresan N.R., Samant S.A., Pillai V.B., Rajamohan S.B., Gupta M.P. (2008). SIRT3 is a stress responsive deacetylase in cardiomyocytes that protects cells from stress-mediated cell death by deacetylation of Ku-70.Mol Cell Biol. 28, 6384–6401.
- Sunters A., Fernández de Mattos S., Stahl M., Brosens J.J., Zoumpoulidou G., Saunders C.A., Coffer P.J., et al. (2003). FoxO3a transcriptional regulation of Bim controls apoptosis in paclitaxel-treated breast cancer cell lines. J Biol Chem. 278, 49795–49805
- Sunters A., Madureira P.A., Pomeranz K.M., Aubert M., Brosens J.J., Cook S.J., Burgering B.M., et al. (2006). Paclitaxel-induced nuclear translocation of FOXO3a in breast cancer cells is mediated by c-Jun NH2-terminal kinase and Akt. Cancer Res. 66:212–220.
- Tan J., Song M., Zhou M., Hu Y. (2017). Antibiotic tigecycline enhances Cisplatin activity against human hepatocellular carcinoma through inducing mitochondrial dysfunction and oxidative damage. Biochem Biophys Res Commun 483, 17-23.
- Tezil, T., Bodur, C., Kutuk, O., and Basaga, H. (2012). IKK-β mediates chemoresistance by sequestering FOXO3; A critical factor for cell survival and death. Cell. Signal. 24, 1361–1368.
- Tissenbaum H.A., Guarente L. (2001). Increased dosage of a sir-2 gene extends lifespan in Caenorhabditis elegans. Nature 410: 227-230.

- Torrens-Mas M., Oliver J., Roca P. and Sastre-Serra J. (2017), SIRT3: Oncogene and Tumor Suppressor in Cancer, Cancers 9, 90.
- Tran H., Brunet A., Grenier J.M., Datta S.R., Fornace A.J., Jr., Di Stefano P.S. et al. (2002). DNA repair pathway stimulated by the forkhead transcription factor FOXO3a through the Gadd45 protein. Science 296, 530-534.
- Tsai K.L., Sun Y.J., Huang C.Y., Yang J.Y., Hung M.C., and Hsiao C.D. et al. (2007). Crystal structure of the human FOXO3A-DBD/DNA complex suggests the effects of post-translational modification. Nucleic Acids Res 35: 6984–6994.
- Tseng A.H.H., Shieh S.S., Wang D.L. (2013). SIRT3 deacetylates FOXO3 to protect mitochondria against oxidative damage. Free Radic Biol Med. 63, 222-34.
- Tzivion G., Dobson M., Ramakrishnan G. (2011). FoxO transcription factors; Regulation by AKT and 14-3-3 proteins. Biochim Biophys Acta. 1813(11),1938-45.
- Van der Horst A., Burgering B.M. (2007). Stressing the role of FoxO proteins in lifespan and disease. Nat Rev Mol Cell Biol. 8, 440-450.
- Van Goethem G., Dermaut B., Lofgren A., Martin J.J., Van Broeckhoven C. (2001). Mutation of POLG is associated with progressive external ophthalmoplegia characterized by mtDNA deletions. Nat Genet. 28:211–2.
- Verma M., Shulga N., Pastorino J.G. (2013). Sirtuin-3 modulates Bak- and Bax-dependent apoptosis. J Cell Sci. 126(1), 274-88
- Wallace, D.C. (2012). Mitochondrial function and cancer. Nat Rev Cancer 12, 695–698.

- Wang F., Travins J., De La Barre B., Penard-Lacronique V., Schalm S., Hansen E., Straley K., et al. (2013). Targeted inhibition of mutant IDH2 in leukemia cells induces cellular differentiation. Science. 340, 622–626.
- Wang H., Zhang L., Yang X., Jin Y., Pei S., Zhang D., et al. (2015). PUMA mediates the combinational therapy of 5-FU and NVP-BEZ235 in colon cancer. Oncotarget 6: 14385–14398.
- Wang, H., Zhang, L., Yang, X., Jin, Y., Pei, S., Zhang, D., Zhang, H., Zhou, B., Zhang, Y., and Lin D. (2015). PUMA mediates the combinational therapy of 5-FU and NVP-BEZ235 in colon cancer. Oncotarget 6, 14385–98.
- Warburg O. (1956). On the origin of cancer cells. Science 123(3191), 309-14.
- Weigel, D., Jackle, H. (1990). The fork head domain: a novel DNA binding motif of eukaryotic transcription factors? Cell 63, 455–456.
- Weigel, D., Jurgens, G., Kuttner, F., Seifert, E. and Jackle, H. (1989). The homeotic gene fork head encodes a nuclear protein and is expressed in the terminal regions of the Drosophila embryo. Cell 57, 645–658.
- Weinberg, S.E. and Chandel, N.S. (2015). Targeting mitochondria metabolism for cancer therapy. Nat Chem Biol 11, 9–15.
- Weir H. J., Yao P., Huynh F.K., Escoubas C.C., Goncalves R.L., Burkewitz K., Laboy R. et al. (2017). Dietary Restriction and AMPK Increase Lifespan via Mitochondrial Network and Peroxisome Remodeling. Cell Metabolism 26(6), 884-896.
- Weng S.C., Kashida Y., Kulp S.K., Wang D., Brueggemeier R.W., Shapiro C.L., Chen C.S. (2008). Sensitizing estrogen receptor-negative breast cancer cells totamoxifen with OSU-03012, a novel celecoxib-derived

phosphoinositide-dependent protein kinase-1/Akt signaling inhibitor. Mol Cancer Ther. 7, 800–808.

- Wheaton W.W., Weinberg S.E., Hamanaka R.B., Soberanes S., Sullivan L.B., Anso E., Glasauer A. et al. (2014). Metformin inhibits mitochondrial complex I of cancer cells to reduce tumorigenesis. Elife 3: e02242.
- Willcox, B. J., Donlon, T. A., He, Q., Chen, R., Grove, J. S., Yano, K., Masaki, K. H., (2008). FOXO3A genotype is strongly associated with human longevity. Proc Natl Acad Sci USA 105(37), 13987-92
- Wilson, M.S., Brosens, J.J., Schwenen, H.D. & Lam, E.W. (2011). FOXO and FOXM1 in cancer: the FOXO-FOXM1 axis shapes the outcome of cancer chemotherapy. Curr. Drug Targets 12, 1256–1266
- Wong Y.H., Lee T.Y., Liang H.K., Huang C.M., Yang Y.H., Chu C.H., et al. (2007). "KinasePhos 2.0: a web server for identifying protein kinase-specific phosphorylation sites based on sequences and coupling patterns" Nucleic Acids Research, 35, W588-594.
- Xuan Z., Zhang M.Q. (2005). From worm to human: bioinformatics approaches to identify FOXO target genes. Mech Ageing Dev. 126, 209–215.
- Yang J.Y., Xia W., Hu M.C. (2006). Ionizing radiation activates expression of FOXO3a, Fas ligand, and Bim, and induces cell apoptosis. Int J Oncol. 29, 643–648.
- Yang X.B., Zhao J.J., Huang C.Y., Wang Q.J., Pan K., Wang D.D., Pan Q.Z., et al. (2013). Decreased expression of the FOXO3A gene is associated with poor prognosis in primary gastric adenocarcinoma patients. PLoS ONE. 8(10).

- Yang, J.Y., Zong, C.S., Xia, W., Yamaguchi, H., Ding, Q., Xie, X., Lang, J.Y., Lai, C.C., Chang, C.J., Huang, W.C., (2008). ERK promotes tumorigenesis by inhibiting FOXO3a via MDM2-mediated degradation. Nat Cell Biol 10, 138–148.
- Yao S.., Fan L.Y., Lam E.L. (2017). The FOXO3-FOXM1 axis: A key cancer drug target and a modulator of cancer drug resistance. Seminars in Cancer Biology,S1044-579X(17)30042-1.
- Yu S., Yu Y., Zhang W., Yuan W., Zhao N., Li Q., Cui Y., (2016). FOXO3a promotes gastric cancer cell migration and invasion through the induction of cathepsin L. Oncotarget 7,34773–34784.
- Yu Y., Guo M., Wei Y., Yu S., Li H., Wang Y., et al. (2016). FoxO3A confers cetuximab resistance in RAS wild-type metastatic colorectal cancer through c-Myc. Oncotarget 7: 80888-80900.
- Yun, J., & Finkel, T. (2014). Mitohormesis. Cell Metab. 19(5):757-66.
- Yuneva M., Zamboni N., Oefner P., Sachidanandam R., Lazebnik Y. (2007). Deficiency in glutamine but not glucose induces MYC-dependent apoptosis in human cells. J Cell Biol. 178, 93–105.
- Zadra G., Batista J.L., Loda M. (2015). Dissecting the dual role of AMPK in cancer: from experimental to human studies. Mol Cancer Res. 13: 1059–1072.
- Zamzami N., Susin S.A., Marchetti P., Hirsch T., Gomez-Monterrey I., Castedo M., et al. Mitochondrial control of nuclear apoptosis. J Exp Med (1996) 183:1533-44.

- Zeviar, D.D., Gonzalez, M.J., Massari, J.R.M., Duconge, J., and Mikirova, N. (2014). The role of mitochondria in cancer and other chronic diseases. JOM. 29: 157.
- Zhang B., Gui L.S., Zhao X.L., Zhu L.L., Li Q.W. (2015). FOXO1 is a tumor suppressor in cervical cancer. Genet Mol Res. 14(2):6605-16
- Zhang F, Aft R.L. (2009). Chemosensitizing and cytotoxic effects of 2-deoxy-D-glucose on breast cancer cells. J Can Res Ther 5, 41-3.
- Zhang, Y., Gan, B., Liu, D. & Paik, J. H. (2011). FoxO family members in cancer. Cancer Biol. Ther. 12, 253 –259.
- Zhao Y., Adjei A. (2014). The clinical development of MEK inhibitors. Nat Publ Gr 11: 385–400.
- Zhou L., Li R., Liu C., Sun T., Htet Aung L.H., Chen C., Gao J., Zhao Y., Wang K. (2017). Foxo3a inhibits mitochondrial fission and protects against doxorubicin-induced cardiotoxicity by suppressing MIEF2, Free Radical Biology and Medicine, 104, 360-370
- Zong, W., Rabinowitz, J.D. and White, E. (2016). Review Mitochondria and Cancer. Mol Cell 61, 667–676

# Appendixes

# Appendix Table 1 - List of constructs used in this study

| Expressed protein | Vector | Plasmid | Figure(s) |
|---|---|---|---|
| 3x-FLAG | Mammalian | p3xFLAGCMV14 | 4.6, 4.7-8, 4.11, 4.24, 4.26, 4.29-30, 4.32 |
| 3x-FLAG-FoxO3A | Mammalian | p3xFLAGCMV14 | 4.6, 4.7-8, 4.11-13, 4.17, 4.19, 4.23-24, 4.26-27, 4.29-30, 4.32 |
| 3x-HA-FoxO3A-FLAG | Mammalian | p3xFLAGCMV14 | 4.6, 4.19 |
| 3x-FLAG-FoxO3A-(Δ1-148) | Mammalian | p3xFLAGCMV14 | 4.7 |
| 3x-FLAG-FoxO3A-(Δ80-108) | Mammalian | p3xFLAGCMV14 | 4.8 |
| 3x-FLAG-FoxO3A-S12A | Mammalian | p3xFLAGCMV14 | 4.11-12, 4.17, 4.29 |
| 3x-FLAG-FoxO3A-S26A | Mammalian | p3xFLAGCMV14 | 4.11 |
| 3x-FLAG-FoxO3A-S30A | Mammalian | p3xFLAGCMV14 | 4.11-12, 4.17, 4.29, 4.32 |
| 3x-FLAG-FoxO3A-S43A | Mammalian | p3xFLAGCMV14 | 4.11 |
| 3x-FLAG-FoxO3A-S48A | Mammalian | p3xFLAGCMV14 | 4.11 |
| 3x-FLAG-FoxO3A-S55A | Mammalian | p3xFLAGCMV14 | 4.11 |
| 3x-FLAG-FoxO3A-S12A/S30A | Mammalian | p3xFLAGCMV14 | 4.12-4.23-24, 4.26, 4.29, 4.30 |
| 3x-FLAG-FoxO3A-(Δ1-30) | Mammalian | p3xFLAGCMV14 | 4.12 |
| 3x-FLAG-FoxO3A-S12D/S30D | Mammalian | p3xFLAGCMV14 | 4.23-24 |
| 3xFLAG-FoxO3A-(Δ242-271) | Mammalian | p3xFLAGCMV14 | 4.23-24, 4.26, 4.29, 4.30, 4.32 |
| GST-4T-3 | Bacterial | pGEX-4T-3 | 4.15 |
| GST-FoxO3A(1-148) | Bacterial | pGEX-4T-3 | 4.15 |
| GST-FoxO3A(1-148)S12A | Bacterial | pGEX-4T-3 | 4.15 |
| GST-FoxO3A(1-148)S30A | Bacterial | pGEX-4T-3 | 4.15 |
| GST-FoxO3A(1-148)S12A/S30A | Bacterial | pGEX-4T-3 | 4.15 |
| GST-FoxO3A(386-525) | Bacterial | pGEX-4T-3 | 4.15 |
| FoxO3A EGFP – wt | Mammalian | pEGFP-N3 | 4.27 |
| FoxO3A EGFP – S12A/S30A | Mammalian | pEGFP-N3 | 4.27 |
| FoxO3A EGFP – (Δ242-271) | Mammalian | pEGFP-N3 | 4.27 |

# Appendix Table 2 - List of human cloning and site-directed mutagenesis primer sequences

| Plasmid(s) | Primers sequence (5'-3') |
|---|---|
| FoxO3A-FLAG*<br>EGFP-FoxO3A | Fw GCTCAAGCTTATGGCAGAGGCACCG |
| | Rv CATGGATCCGCCTGGCACCCAGC |
| HA-FoxO3A-FLAG** | Fw AAGCTTAGCTCTGCTTATATAGACC |
| | Rv CATGGATCCGCCTGGCACCCAGC |
| FoxO3A(Δ1-148)-FLAG*** | Fw GATATCGGATCCATGAAATGTTCGTCGCGGCGG |
| | Rv GATATCCTCGAGTAAGCCTGGCACCCAGCTCTG |
| FoxO3A(1-148)-GST^ | Fw GATATCGGATCCATGGCAGAGGCACCGGCTT |
| | Rv GATATCCTCGAGTAACCTCGGCTGCCCGGAG |
| FoxO3A(386-525)-GST^ | Fw GGATCCATGCTCATGGACGACCTGCTGGATAAC |
| | Rv GATATCCTCGAGTAAGCCTGGCACCCAGCTCTG |
| FoxO3A-S12A-FLAG***<br>FoxO3A-(1-148)S12A-GST^^ | Fw GGCCCCGCTCGCTCCGCTCGA |
| | Rv GGGGAAGCCGGTGCCTCTG |
| FoxO3A-S26A-FLAG*** | Fw CGAGCCCCAGGCCCGTCCGCGA |
| | Rv AACTCCGGGTCCAGCTCC |
| FoxO3A-S30A-FLAG***<br>FoxO3A-(1-148)S30A-GST^^<br>FoxO3A-S12/S30A-FLAG***<br>EGFP-FoxO3A-S12/S30A<br>FoxO3A-(1-148)S12A/S30A-GST^^ | Fw CCGTCCGCGAGCCTGTACGTG |
| | Rv CTCTGGGGCTCGAACTCCG |
| FoxO3A-S43A-FLAG*** | Fw GCTCCAAGCGGCCCCTGCCAAGCC |
| | Rv TCCGGCCTTTGCAGGGGC |
| FoxO3A-S48A-FLAG*** | Fw TGCCAAGCCCGCGGGGGAGAC |
| | Rv GGGCTCGCTTGGAGCTCC |
| FoxO3A-S55A-FLAG*** | Fw GGCCGCTGACGCCATGATCCC |
| | Rv GTCTCCCCCGAGGGCTTG |
| FoxO3A(Δ1-30)-FLAG*** | Fw TGTACGTGGCCCCTGCAAAGG |
| | Rv TGAACCGTCAGAATTAAGCTT |

| | |
|---|---|
| FoxO3A(Δ80-108)-FLAG*** | Fw GGGTCTGGGCCAGCCACC |
| | Rv GATCGCCATGGCCGAGCCG |
| FoxO3A-S12-FLAG*** | Fw GGCCCCGCTCgaTCCGCTCGAAG |
| | Rv GGGGAAGCCGGTGCCTCT |
| FoxO3A-S30D-FLAG***<br>FoxO3A-S12/S30D-FLAG*** | Fw CCGTCCGCGAgaCTGTACGTGG |
| | Rv CTCTGGGGCTCGAACTCC |
| FoxO3A(Δ242-271) –FLAG***<br>EGFP-FoxO3A(Δ242-271) | Fw GCAGCCCTGCAGACAGCCCC |
| | Rv CCCCCCATCAGGGTTGATGATCC |

* Construct obtained starting from pECE-HA- FoxO3A (kindly provided from Dr. M. Greenberg).

** Construct obtained starting from pECE-HA- FoxO3A (kindly provided from Dr. M. Greenberg), followed by HA-FoxO3A fragment insertion into pCMV-14-3xFLAG backbone.

*** Construct obtained starting from 3x-FLAG-FoxO3A.

^ Construct obtained starting from 3x-FLAG-FoxO3A, followed by FoxO3A(1-148) insertion into and pGEX-4T-3 empty vector.

^^Construct obtained starting from pGEX-4T-3-FoxO3A(1-148).

pEGFP-N3 plasmids were obtained through HindIII/BamHI digestion of the corresponding p3xFLAG plasmids, followed by fragment insertion into pEGFPN3 backbone.

# Appendix Table 3 - List of primary and secondary antibodies used

| **Antibody name** | **Source** | **Identifier** |
|---|---|---|
| Monoclonal mouse anti- FoxO3A | CST | #99199 |
| Monoclonal rabbit anti- FoxO3A | CST | #2497 |
| Monoclonal anti-rabbit COX4 | CST | #4850 |
| Monoclonal anti-rabbit BCL2 | CST | #2870 |
| Monoclonal anti-rabbit PDH | CST | #3205 |
| Mouse monoclonal FLAG M2 | SIGMA | #F1804 |
| Rabbit anti-HA-TAG | CST | #3724 |
| Mouse monoclonal anti-βACTIN | CST | #3700 |
| Rabbit polyclonal anti-pAMPK-α Thr 172 | CST | #2531 |
| Rabbit polyclonal anti-pAMPK1-α | CST | #2532 |
| Mouse monoclonal anti- p44/42 MAP2K1- ERK1/2 Thr202/Tyr204 | CST | #9106 |
| Rabbit polyclonal anti- 44/42 MA2PK1- ERK1/2 | CST | #9102 |
| Rabbit polyclonal anti-p-Acetyl-CoA Ser 79 | CST | #3661 |
| Rabbit monoclonal anti-TFAM | CST | #8076 |
| Polyclonal rabbit anti-HSP60 D307 | CST | #4870 |
| Rabbit anti- IgG | CST | #2729S |
| Rabbit polyclonal anti-mtRNAPOL H300 | Santa Cruz | #67350 |
| Rabbit monoclonal anti- SIRT3 | CST | #5490 |
| Rabbit monoclonal anti-LAMIN B1 | CST | #12586S |
| Rabbit polyclonal anti- PARP1 p85 fragment | PROMEGA | #G7341 |
| Amersham ECL Rabbit IgG, HRP-linked whole Ab (from donkey) | GE | NA934 |
| Amersham ECL Mouse IgG, HRP-linked whole Ab (from sheep) | GE | NA931 |

# Appendix Table 4 -List of human mRNA primer sequences

| Primer | Sequence (5'-3') |
|---|---|
| Atp6 | Fw GCCGCAGTACTGATCATTCTATTTC |
| | Rv TCGGTTGTTGATGAGATATTTGGA |
| Atp8 | Fw CCCTCACCAAAGCCCATAAA |
| | Rv GAATGAAGCGAACAGATTTTCGT |
| Cox1 | Fw CCCCGCATAAACAACATAAGC |
| | Rv CAGATGCGAGCAGGAGTAGGA |
| Cox2 | Fw ATGGCACATGCAGCGCAAGTAGG |
| | Rv GGCATACAGGACTAGGAAGCAG |
| Cox3 | Fw TTCCACGGACTTCACGTCATT |
| | Rv TGGCGGATGAAGCAGATAGTG |
| Cyt B | Fw TCGGCATTATCCTCCTGCTT |
| | Rv CTCACGGGAGGACATAGCCTCT |
| ND1 | Fw CCCGCCACATCTACCATCA |
| | Rv GAGCGATGGTGAGAGCTAAGGT |
| ND2 | Fw AAACCCTCGTTCCACAGAAGC |
| | Rv GGATTATGGATGCGGTTGCT |
| ND3 | Fw CCTACCATGAGCCCTACAAACAAC |
| | Rv GGATGATGATTAATAAGAGGGATGACA |
| ND4 | Fw ACAAGCTCCATCTGCCTACGA |
| | Rv GGCTGATTGAAGAGTATGCAATGA |
| ND4L | Fw TCAACACCCACTCCCTCTTAGC |
| | Rv CGCAGGCGGCAAAGACT |
| ND5 | Fw GCAGCCATTCAAGCAATCCTA |
| | Rv AGGCGAGGATGAAACCGATA |
| ND6 | Fw ACCCCCATGCCTCAGGAT |
| | Rv GGAATGATGGTTGTCTTTGGATATACT |
| D-Loop | Fw GCGTCTCGCAATGCTATCG |
| | Rv GAGCTCTCCATGCATTTGGTATT |
| Bim | Fw CACAAACCCCAAGTCCTCCTT |
| | Rv TGGAAGCCATTGCACTGAGA |

# Appendix Table 5 - List of human DNA primer sequences

| Primer name | Sequence (5'-3') |
|---|---|
| FHRE#1 | Fw CCGGAGCACCCTATGTCG |
| | Rv GCCTGTAATATTGAACGTAGGTGCC |
| FHRE#2 | Fw CATTACTGCCAGCCACCATGA |
| | Rv GGAGGGGGTTTTGATGTGGAT |
| p21 | Fw ATGTCCGTCAGAACCCATGC |
| | RvAGTGGTGTCTCGGTGACAAAGTC |
| p27 | Fw ACCTTCGCGGTCCTCTGG |
| | RvAACTAGCCAAACGGCCGG |

# Published Material by the candidate

Forte G., Grossi V., **Celestini V.**, Lucisano G., Scardapane M., Varvara D., Patruno M., Bagnulo R., Loconte D., Giunti L., Petracca A., Giglio S., Genuardi M., Pellegrini F., Resta N., Simone C. (2014).Characterization of the rs2802292 SNP identifies FOXO3A as a modifier locus predicting cancer risk in patients with PJS and PHTS hamartomatous polyposis syndromes, BMC Cancer. 14: 661.

**Celestini V**., Tezil T., Russo L., Fasano C., Sanese P., Forte G., Peserico A., Lepore Signorile M., Longo G., De Rasmo D., Signorile A., Gadaleta R., Scialpi N., Cocco T.M., Terao M., Garattini E., Moschetta A., Villani G., Grossi V. and Simone C. (2018) Uncoupling FoxO3A mitochondrial and nuclear functions in cancer cells undergoing metabolic stress and chemotherapy. Cell Death & Disease. 9: 231.